USE OF NANO-SILICA TO INCREASE EARLY STRENGTH AND REDUCE SETTING TIME OF CONCRETES WITH HIGH VOLUMES OF SLAG OR FLY ASH

JAHIDUL ISLAM

NATIONAL UNIVERSITY OF SINGAPORE

2011

USE OF NANO-SILICA TO INCREASE EARLY STRENGTH AND REDUCE SETTING TIME OF CONCRETES WITH HIGH VOLUMES OF SLAG OR FLY ASH

JAHIDUL ISLAM
(B.Sc. Engg., BUET)

A THESIS SUBMITTED
FOR THE DEGREE OF MASTER OF ENGINEERING

DEPARTMENT OF CIVIL ENGINEERING

NATIONAL UNIVERSITY OF SINGAPORE

2011

Acknowledgements

The author would like to express his sincere appreciation and deep gratitude to his supervisor, Associate Professor Zhang Min-Hong for her invaluable guidance, patience, constructive discussion, kind encouragement and full support throughout this research.

Appreciation is made to Ms. Li Wei, past undergraduate student Mr. Huynh Thanh Binh, and Structure Laboratory Technologist Mr. Ang Beng Oon for their kind assistance to conduct some of the experimental work.

The author is really thankful for the constant thoughtfulness and unending support from his wife and friends throughout the education period in the university.

Finally, the author gratefully acknowledges the National University of Singapore for providing partial scholarship to pursue this study.

January, 2011

Jahidul Islam

Table of Contents

Acknowledgements i
Table of Contents ii
Summery vi
List of Notations ix
List of Acronyms x
List of Tables xi
List of Figures xiii
Chapter 1 Introduction 1
1.1 Background 1
1.2 Objectives 3
1.3 Scope 4
1.4 Organization of the Thesis 5
Chapter 2 Literature Review 6
2.1 Hydration of Portland Cement 6
2.2 Hydration and Reaction of Slag and Early Strength Development of Concrete with High Volume of Slag 9
2.3 Pozzolanic Reaction of Fly Ash and Early Strength Development of Concrete with High Volume of Fly Ash 10
2.4 Effect of Silica Fume on Early Strength of Concrete Made with Slag or Fly Ash 12
2.4.1 Characteristics of Silica Fume 12
2.4.2 Mechanisms by which Silica Fume Improve Concrete Strength 13
2.4.3 Effect of Silica Fume on Early Strength of Concrete Containing Slag 14
2.4.4 Effect of Silica Fume on Early Strength of Concrete Containing Fly Ash 14
2.5 Nano-Silica to Improve Compressive Strength 16
2.5.1 Characteristics of Nano-Silica 16
2.5.2 Effect of Nano-Silica on Cement Paste, Mortar and Concrete 16
2.5.3 Effect of Nano-Silica on Early Strength of Concrete Containing Fly Ash 17
2.6 Nano-Particle Dispersion 19
Chapter 3 Experimental Details 26

3.1 Introduction 26
3.2 Materials 27
3.2.1 Cement 27
3.2.2 Ground Granulated Blast Furnace Slag and Fly Ash 27
3.2.3 Nano-Silica and Silica Fume 28
3.2.4 Water 28
3.2.5 Superplasticizer 28
3.2.6 Fine and Coarse Aggregates 28
3.3 Mix Proportions of Mortars, Concretes, and Cement Pastes 29
3.3.1 Mix Proportions of Mortars 29
3.3.2 Mix Proportions of Concretes 29
3.3.3 Mix Proportions of Cement Pastes 29
3.4 Mixing and Preparation of Mortar, Concrete, Cement Paste and Specimens 30
3.4.1 Mixing and Preparation of Mortar Specimens 30
3.4.2 Mixing and Preparation of Concrete Specimens 30
3.4.3 Mixing and Preparation of Cement Paste and Specimens 31
3.5 Test Methods and Analyses 32
3.5.1 Compressive Strength of Mortars and Concretes 32
3.5.2 Rate of Heat Generation and Cement Hydration of Cement Pastes 32
3.5.3 Porosity and Pore Size Distribution of the Cement Pastes 33
3.5.4 Resistance to Chloride-Ion Penetration of Concretes 33
Chapter 4 Results and Discussion 43
4.1 High-Volume Slag Pastes, Mortars, and Concretes 43
4.1.1 Compressive Strength Development 43
4.1.1.1 Effect of Nano-Silica Dosage on Strength Development of Mortars 43
4.1.1.2 Effect of Particle Size of Nano-Silica on Strength Development of Mortars 44
4.1.1.3 Effect of Mixing and Dispersion Method on Strength Development of Mortars 44
4.1.1.4 Strength Development of Slag Concrete with Nano-Silica 45
4.1.1.5 Discussion on Strength Development 45
4.1.1.5.1 Physical Effect 46
4.1.1.5.2 Chemical Effect 46
4.1.1.5.3 Microstructure Modification 46

4.1.2 Effect of Nano-Silica on Setting Time of Concrete 47
4.1.3 Rate of Heat Development of Pastes 47
4.1.3.1 Effect of Nano-Silica Dosage 47
4.1.3.2 Effect of Particle Size of Nano-Silica 49
4.1.3.3 Effect of Mixing and Dispersion Method 50
4.1.4 Porosity and Pore-Size Distribution of Pastes 51
4.1.4.1 Effect of Nano-Silica Dosage 51
4.1.4.2 Effect of Particle Size of Nano-Silica 52
4.1.4.3 Effect of Mixing and Dispersion Method 53
4.1.5 Resistance to Chloride-Ion Penetration of Concretes 53
4.2 High-Volume Fly Ash Pastes, Mortars, and Concretes 53
4.2.1 Compressive Strength Development 53
4.2.1.1 Effect of Nano-Silica Dosage on Strength Development of Mortars 53
4.2.1.2 Effect of Particle Size of Nano-Silica on Strength Development of Mortars 54
4.2.1.3 Effect of Mixing and Dispersion Method on Strength Development of Mortars 54
4.2.1.4 Strength Development of Fly Ash Concrete with Nano-Silica 55
4.2.2 Effect of Nano-Silica on Setting Time of Concrete 55
4.2.3 Rate of Heat Development of Pastes 56
4.2.3.1 Effect of Nano-Silica Dosage 56
4.2.3.2 Effect of Particle Size of Nano-Silica 57
4.2.3.3 Effect of Mixing and Dispersion Method 58
4.2.4 Resistance to Chloride-Ion Penetration of Concretes 58
4.3 Comparison between High-Volume Slag and Fly Ash Pastes, Mortars, and Concretes with Nano-Silica 59
4.3.1 Effect of Nano-Silica on Rate of Heat Development at Early Age 59
4.3.2 Compressive Strength Development 60
4.3.2.1 Effect of Nano-Silica on Strength Development Mortars 60
4.3.2.2 Effect of Mixing and Dispersion Method on Strength Development of Mortars 61
4.3.2.3 Effect of Nano-Silica on Strength Development of Concretes 61
Chapter 5 Conclusions and Recommendations 77
5.1 Conclusions 77

5.2 Recommendations 79
References 80
Appendix 89

Summery

Ground granulated blast-furnace slag and fly ash have been used in concrete for many years as mineral admixtures to replace Portland cement. Concretes with high volumes of slag or fly ash (>50%) have been used for applications where durability is of prime concern. These high-volume slag or fly ash concretes can develop good strengths over time if properly cured, exceeding those of similar concretes without slag or fly ash. However, early strengths of such concretes are often lower than Portland cement concrete without slag or fly ash which may affect construction progress.

The objectives of this research project are to study (1) Effects of nano-silica (NS) dosages, particle sizes, and dispersion methods on rate of heat development in cement pastes at early age, porosity and pore size distribution of cement pastes and compressive strength development of mortars; and (2) Effect of NS on setting time, compressive strength development and chloride-ion penetrability of concretes in comparison to those of silica fume. Most cement pastes, mortars, and concretes contained high volumes of slag or fly ash of about 50%. Control Portland cement paste and mortar without any mineral admixture were also included for comparison.

Two types of NS with specific surfaces of 200.1 and 321.6 m^2/g (mean particle size 12 and 7 nm, respectively) were included in the study in comparison to silica fume with a specific surface of 21.3 m^2/g. A constant water-to-cementitious materials ratio (w/cm) 0.45 was used for all mixtures. A superplasticizer was used to achieve targeted workability. Dosages of the NS varied from 0.5, 1.0 to 2% of the total cementitious material. The NS were dispersed by two different methods. In one method, NS was premixed with water using ultrasonic mixer before being mixed with

other materials. In the second method, NS was dispersed using conventional mechanical mixing. Compressive strengths of mortars at 1, 3, 7, 28, and 91 days, concrete setting times and strengths at 3, 7, 28, and 91 days, heat development of cement pastes up to 30 hrs, pore structure of pastes cured for 28 days, and concrete resistance to chloride-ion penetration at 28 days were determined.

The results indicate that length of dormant period was shortened, and rate of cement and slag hydration were accelerated with the incorporation of the NS in the high-volume slag or fly ash cement pastes. The incorporation of a small amount of NS reduced setting times, and increased 3- and 7-day compressive strengths of high-volume slag or fly ash concrete, significantly, in comparison to the corresponding reference concrete with 50% slag or fly ash. Compressive strength of the slag or fly ash mortars were increased with the increase in NS dosages from 0.5 to 2.0% by mass of cementitious material at various ages up to 91 days. The strengths of the slag or fly ash mortars were generally increased with the decrease in the particles size of silica inclusions at early age. Ultra-sonication of nano-silica with water is probably a better method for proper dispersion of nano-silica than mechanical mixing method.

With the increasing dosage of NS, large capillary porosity was decreased, whereas medium capillary porosity was increased in the slag cement pastes at 28 days. However, the total capillary porosity of the slag pastes was not affected significantly by the incorporation of the NS. Threshold and critical pore diameters in slag cement pastes were not affected by the incorporation of 1% NS, but were decreased with the inclusion of 2% NS. No significant difference in large, medium, and total capillary porosities and threshold and critical diameters was observed among the slag pastes with different particle sizes of silica, and among those prepared by ultrasonicated NS with water and by mechanical mixing method. The 28-day charge passed through the

slag or fly ash concrete with NS was lower than that of corresponding reference concrete.

Nano-silica with mean particle sizes of 7 and 12 nm appears to be more effective in increasing the rate of cement hydration and reaction compared with silica fume. The NS reduced the setting times and increased early strengths of the high-volume slag or fly ash concrete. However, the setting times and early strength of the high-volume slag or fly ash concrete were not affected by the silica fume significantly. The charge passed through the high-volume slag or fly ash concrete with NS was similar to that of corresponding concrete with silica fume.

Keywords: compressive strength, chloride-ion penetration, fly ash, nano-silica, pore size distribution, rate of cement hydration, setting times, silica fume, slag.

List of Notations

C_2S	di-calcium silicate, $2Cao.SiO_2$
C_3A	tri-calcium aluminate, $3CaO.Al_2O_3$
C_3S	tri-calcium silicate, $3CaO.SiO_2$
C_4AF	tetra-calcium aluminoferrite, $4CaO.Al_2O_3.Fe_2O_3$
AF_m, $C_4A\bar{S}H_{12}$	Monosulfoaluminate, $3CaO.Al_2O_3.CaSO_4.12H_2O$
AF_t, $C_6A\bar{S}_3H_{32}$	ettringite, $3CaO.Al_2O_3.3CaSO_4.32H_2O$
CH	calcium hydroxide, $Ca(OH)_2$
C-S-H or $C_3S_2H_8$	calcium silicate hydrates, $3CaO.2SiO_2.8H_2O$
$C\bar{S}H_2$	gypsum, $CaSO_4.2H_2O$
H	H_2O
P	pressure
r	pore radius
S	silica, silicon di-oxide, SiO_2
w/cm	water-to-cementitious material ratio
γ	surface tension
θ	contact angle

List of Acronyms

ACI	the American Concrete Institute
ASTM	the American Society for Testing and Materials
BS EN	the British Standard European Norm
ITZ	interfacial transition zone
LOI	loss on ignitation
MIP	mercury intrusion porosimetry
NS	nano-silica
OPC	ordinary Portland cement
XRF	X-ray fluorescence

List of Tables

Chapter 2

Table 2.1 - Comparison of chemical and physical characteristics of Portland cement, fly ash, slag cement, and silica fume (Holland 2005) 21

Chapter 3

Table 3.1 - Physical properties and chemical compositions of materials 35

Table 3.2 - Mix proportions and flow values of mortars with different dosages of Type 1 nano-silica with specific surface area of 200 m^2/g (w/cm = 0.45) 35

Table 3.3 - Mix proportions of mortars for evaluating the effect of nano-silica size in comparison to that of silica fume (w/cm = 0.45) 36

Table 3.4 - Mix proportions of mortars for evaluating mixing and dispersion methods of nano-silica (w/cm = 0.45) 36

Table 3.5 - Mix proportions of concretes for evaluating the effect of nano-silica in comparison to that of silica fume (w/cm = 0.45) 37

Chapter 4

Table 4.1 - Strength increases of the high-volume slag mortars and concretes with NS and silica fume compared with reference mortar and concrete with 50% slag 63

Table 4.2 – Strength increases of the high-volume fly ash mortars and concretes with NS and silica fume compared with reference mortar and concrete with 50% fly ash . 63

Table 4.3 – Porosity of high-volume slag cement pastes with NS or silica fume compared with reference slag paste and control cement paste 64

Table 4.4 – Compressive strength increased for different type of nano-inclusions compared to reference slag or fly ash mortar/concrete 64

Appendix

Table A.1 - Compressive strength of control Portland cement mortar (Control) 89

Table A.2 - Compressive strength of reference slag mortar (SL0) 90

Table A.3 - Compressive strength of slag mortar with 0.5% type 1 NS (SL0.51) 91

Table A.4 - Compressive strength of slag mortar with 1% type 1 NS (SL11) 92

Table A.5 - Compressive strength of slag mortar with 2% type 1 NS (SL21) 93

Table A.6 - Compressive strength of slag mortar with 1% type 2 NS (SL12) 94

Table A.7 - Compressive strength of slag mortar with 1% silica fume (SL1SF) 95

Table A.8 - Compressive strength of slag mortar with 1% type 1 NS and mixed with mechanical mixing method (SL11(M)) 96

Table A.9 - Compressive strength of reference fly ash mortar (FA0) 97

Table A.10 - Compressive strength of fly ash mortar with 0.5% type 1 NS (FA0.51) 98

Table A.11 - Compressive strength of fly ash mortar with 1% type 1 NS (FA11) 99

Table A.12 - Compressive strength of fly ash mortar with 2% type 1 NS (FA21) ... 100

Table A.13 - Compressive strength of fly ash mortar with 1% type 2 NS (FA12) ... 101

Table A.14 - Compressive strength of fly ash mortar with 1% silica fume (FA1SF) 102

Table A.15 - Compressive strength of fly ash mortar with 1% type 1 NS and mixed with mechanical mixing method (FA11(M)) 103

Table A.16 - Compressive strength of reference slag concrete (CSL0) 104

Table A.17 - Compressive strength of slag concrete with 2% type 1 NS (CSL21) ... 105

Table A.18 - Compressive strength of slag concrete with 2% silica fume (CSL2SF) 106

Table A.19 - Compressive strength of reference fly ash concrete (CFA0) 107

Table A.20 - Compressive strength of fly ash concrete with 2% type 1 NS (CFA21) 108

Table A.21 - Compressive strength of fly ash concrete with 2% silica fume (CFA2SF) 109

Table A.22 - Charge passed in slag concretes at 28 days 110

Table A.23 - Charge passed in fly ash concretes at 28 days 110

List of Figures

Chapter 2

Figure 2.1 - Rate of heat evolution during hydration of Portland cement (Mindess et al. 2003). 22

Figure 2.2 - Compressive strength development in blast furnace slag replaced concrete and effect of silica fume (Malhotra et al. 1985)..... 22

Figure 2.3 - Compressive strength development in fly ash replaced concrete and effect of silica fume (Carette and Malhotra 1983)..... 23

Figure 2.4 - Particle size and specific surface area related to concrete materials (Sobolev and Gutierrez 2005; Sanchez and Sobolev 2010)..... 23

Figure 2.5 - Development of compressive strength for cement pastes with NS or silica fume (SF) as cement replacement (Data taken from Qing et al. 2007) 24

Figure 2.6 - Development of compressive strength of fly ash concrete with a small dosage of NS as cement replacement (Li 2004) 24

Figure 2.7 - Dispersion and deagglomeration of nano particles 25

Figure 2.8 - Typical result of ultrasonic dispersion of fumed silica in water 25

Chapter 3

Figure 3.1 - Particle size distribution of cement, slag, and fly ash 38

Figure 3.2 - Grading curves of fine and coarse aggregates..... 38

Figure 3.3 - Ultrasonic mixer..... 39

Figure 3.4 - Automax 5 compression test machine..... 39

Figure 3.5 - Denison-Mayes compression test machine 40

Figure 3.6 - Thermometric TAM Air 3115 isothermal calorimeter..... 40

Figure 3.7 - Micromeritics Autopore WIN9400 Series mercury porosimeter..... 41

Figure 3.8 - Rapid chloride permeability test setup..... 41

Figure 3.9 - Schematic diagram of the rapid chloride permeability test according to ASTM C 1202 (2005)..... 42

Chapter 4

Figure 4.1 - Effect of the Type 1 nano-silica dosage of on the compressive strength development of slag mortars 65

Figure 4.2 - Effect of the particle size of nano-silica on the compressive strength development of slag mortar 65

Figure 4.3 - Effect of mixing and dispersing method on the compressive strength development of slag mortar with 1% Type 1 nano-silica 66

Figure 4.4 – Compressive strength development of slag concrete with 2% nano-silica in comparison to that of the reference concrete and concrete with the same amount of silica fume 66

Figure 4.5 – Setting time of slag concrete with 2% nano-silica in comparison to that of the reference concrete and concrete with the same amount of silica fume 67

Figure 4.6 - Effect of the Type 1 nano-silica dosage of on the rate of heat development in slag cement pastes 67

Figure 4.7 - Effect of the particle size of nano-silica on the rate of heat development in slag cement paste 68

Figure 4.8 - Effect of mixing and dispersing method on the rate of heat development in slag cement paste with 1% Type 1 nano-silica 68

Figure 4.9 - Effect of the Type 1 nano-silica dosage of on the porosity and pore size distribution in slag cement pastes 69

Figure 4.10 - Effect of the particle size of nano-silica on the porosity and pore size distribution in slag cement paste 69

Figure 4.11 - Effect of mixing and dispersing method on the porosity and pore size distribution in slag cement paste with 1% Type 1 nano-silica 70

Figure 4.12 - Effect of the particle size of nano-silica on charge passed in slag concrete at 28 days 70

Figure 4.13 - Effect of the Type 1 nano-silica dosage of on the compressive strength development of fly ash mortars 71

Figure 4.14 - Effect of the particle size of nano-silica on the compressive strength development of fly ash mortar 71

Figure 4.15 - Effect of mixing and dispersing method on the compressive strength development of fly ash mortar with 1% Type 1 nano-silica 72

Figure 4.16 – Compressive strength development of fly ash concrete with 2% nano-silica in comparison to that of the reference concrete and concrete with the same amount of silica fume....72

Figure 4.17 –Setting time of fly ash concrete with 2% nano-silica in comparison to that of the reference concrete and concrete with the same amount of silica fume 73

Figure 4.18 - Effect of the Type 1 nano-silica dosage of on the rate of heat development in fly ash cement pastes....73

Figure 4.19 - Effect of the particle size of nano-silica on the rate of heat development in fly ash cement paste....74

Figure 4.20 - Effect of mixing and dispersing method on the rate of heat development in fly ash cement paste with 1% Type 1 nano-silica....74

Figure 4.21 - Effect of the particle size of nano-silica on charge passed in fly ash concrete at 28 days....75

Figure 4.22 - Effect of the particle size of nano-silica on the compressive strength development of slag and fly ash mortars 75

Figure 4.23 – Compressive strength development of slag or fly ash concrete with 2% nano-silica in comparison to those of the reference concrete and concrete with the same amount of silica fume 76

Figure 4.24 – Crack pattern in slag concrete with 2% NS under compressive load. Crack goes through coarse aggregate particles....76

Appendix

Figure A.1 - Determination of setting times of slag concretes 111

Figure A.2 - Determination of setting times of fly ash concretes....111

Chapter 1 Introduction

1.1 Background

In modern concrete technology, replacing cement by mineral admixtures is a well-established practice. Mineral admixtures are added to concrete for various purposes such as:

- Replacing cement for economical consideration,
- Increasing durability of hardened concrete,
- Enhancing some mechanical properties of concrete,
- Reducing heat generation and temperature rise of concrete for hot weather concreting,
- Producing greener concrete for environmental sustainability.

Ground granulated blast furnace slag (will be referred to as slag from this point) and fly ash are the most commonly used mineral admixtures for many years and they have been used to replace Portland cement either in batching plants or in the production of blended cements. Concretes with high percentages of slag (>50%) have been used for applications in marine environments and situations where ground water has high sulphate contents (Mehta 1991; ACI 233R 2003).

As fly-ash has pozzolanic nature, using this mineral admixture at high percentages as a cement replacement in concrete is beneficial. Not only it can achieve desired mechanical properties and durability of concrete over time, but also it decreases the

cost of concrete production (Langley et al. 1989; Bilodeau and Malhotra 2000; Mindess et al. 2003).

Concretes with high volumes of slag or fly ash can develop good strengths over time if cured properly, exceeding those of similar concretes without slag or fly ash. However, early strengths of such concretes are often lower than those of concretes without slag or fly ash because of the slow hydration and reaction of these minerals.

Over the years, silica fume has often been used together with these mineral admixtures for improvement of early strengths of concretes with high volumes of slag or fly ash. Reaction mechanism of silica fume with slag or fly ash along with cement may be explained considering the interaction of each of these mineral admixtures with cement alone, and will be discussed in Chapter 2.

Recent developments in nano-technology and availability of nano-silica have made the use of such materials in concrete possible. Nano-silica (NS) is a nano-sized, highly reactive amorphous material. Spherical NS has diameters less than 100 nm (Sobolev and Gutierrez 2005; Campillo et al. 2007; Sanchez and Sobolev 2010), smaller than the mean size of silica fume (typically about 100 nm). Due to their small particle sizes and high surface areas compared to those of silica fume, NS may enhance the early compressive strengths of concrete with high volumes of slag or fly ash more effectively than silica fume. While numerous publications have been found on the use of silica fume in concrete, there are limited papers on the use of NS in this context.

In recent years several researches showed that early-age and 28-day strengths of cement pastes (Qing et al. 2007), and mortars (Li et al. 2004; Jo et al. 2007) are increased by using small amounts of NS. Nano-silica has also been used to increase

early strength of concrete with fly ash (Li 2004; Said and Zeidan 2009). Higher strengths of cement mortars (Li et al. 2004; Jo et al. 2007) and fly ash concretes (Schoepfer and Maji 2009) with NS are also reported in comparison to those with silica fume. However, no information is available on whether NS can be used to increase early strength of concrete with high-volumes of slag. As NS particles are very fine and they tend to agglomerate due to high surface interaction, uniform dispersion of NS is an important issue to get its beneficial effects.

This research project is carried out with the objectives and scopes given in the following section using a systematic approach.

1.2 Objectives

The objectives of this research project are to study,

1. Effects of NS dosages, particle sizes, and dispersion methods on rate of heat development in cement pastes at early age, porosity and pore size distribution of cement pastes and compressive strength development of mortars.
2. Effect of NS on setting time, compressive strength development and chloride-ion penetrability of concretes in comparison to those of silica fume.

Most cement pastes, mortars, and concretes contained high volumes of slag or fly ash of about 50%. Control Portland cement paste and Mortar without any mineral admixture were also included for comparison.

1.3 Scope

Two types of NS with specific surfaces of 200.1 and 321.6 m^2/g (mean particle size 12 and 7 nm, respectively) were included in the study in comparison to silica fume with a specific surface of 21.3 m^2/g.

A constant water-to-cementitious materials ratio (w/cm) 0.45 was used for all mixtures. A superplasticizer was used to achieve targeted workability. Dosages of the NS varied from 0.5, 1.0 to 2% of the total cementitious material.

The NS were dispersed by two different methods. In one method, NS was premixed with water using ultrasonic mixer before being mixed with other materials. In the second method, NS was dispersed using conventional mechanical mixing.

Properties of cement pastes, mortars and concretes and test methods are as follows:

- Compressive strengths of mortars at 1, 3, 7, 28, and 91 days (according to ASTM C 109/C 109M (2002)) and concrete strengths at 3, 7, 28, and 91 days (according to BS EN 12390-3 (2002)),
- Heat development of cement pastes up to 30 hrs (using isothermal calorimeter following ASTM C 1679 (2008)),
- Concrete setting times (according to ASTM C 403/C 403M (2008)),
- Porosity and pore size distribution (mercury intrusion porosimetry),
- Resistance to chloride-ion penetration (according to ASTM C 1202 (2005)).

1.4 Organization of the Thesis

This thesis consists of 5 chapters. Chapter 1 presents a general introduction of the research background together with the objective and scope of the study.

Chapter 2 covers a comprehensive literature review on Portland cement hydration and hydration and reaction of slag and fly ash. Strength development of high-volume slag or fly ash concrete at early age, early strength improvement of high-volume slag or fly ash concretes using silica fume and their mechanisms were reviewed as well. Limited information available in literature on effect of NS on strength development of mortars and concretes were also reviewed.

In Chapter 3, the details of the experimental program including materials used, mix proportions, specimen preparation, curing conditions, and test methods are presented.

Chapter 4 presents experimental results and relevant discussion. Effects of NS on properties of high-volume slag concrete and high-volume fly ash concrete are presented in Sections 4.1 and 4.2, respectively. In Section 4.3, a comparison of the NS effect on slag and fly ash concrete is presented and discussed.

Finally, Chapter 5 summarizes results and conclusions drawn based on the findings. Recommendations for further research are also presented.

Chapter 2 Literature Review

2.1 Hydration of Portland Cement

When water is added to cement, cement undergoes a series of chemical reactions, for which the setting and hardening of cement take place. A typical chemical composition and physical properties of ordinary Portland cement (OPC) has been given in Table 2.1. Portland cement is mainly composed of four types of chemical compounds or minerals: alite (C_3S), belite (C_2S), aluminate (C_3A) and ferrite (C_4AF) phase. In order to describe the chemical reaction of these four components, they are assumed to react independently (Mindess et al. 2003). The reaction of these components with water is well known as hydration reaction of cement. Hydration reactions of cement are exothermic i.e. these reactions produce heat.

Tricalcium silicate (C_3S) and Dicalcium silicate (C_2S) are the main compounds of Portland cement (75-80% of Portland cement) (Ramachandran and Beaudoin 2001). Hydration reactions of these two compounds produce calcium silicate hydrate (C-S-H or $C_3S_2H_8$) and calcium hydroxide (CH) as follows:

$$2C_3S + 11H \rightarrow C_3S_2H_8 + 3CH$$

$$2C_2S + 9H \rightarrow C_3S_2H_8 + CH$$

Hydration reaction can be followed by an iso-thermal calorimeter by monitoring the heat released from cement hydration at constant temperatures. Five stages can be identified generally by a typical isothermal calorimeter curve (Fig. 2.1) (Mindess et

al. 2003). In the first stage, C_3S comes into contact with water, and there is a rapid dissolution of Ca^{2+} and OH^- ion from the surface of C_3S which comprises a rapid evolution of heat (peak 1 in Fig. 2.1). The pH of the solution reaches about 12 which indicate a high alkaline solution. This is known as pre-induction period and is followed by the induction period (or dormant period) (stage 2) where hydrolysis of C_3S continues slowly. The induction period may continue for a few hours. At the end of the induction period, CH and C-S-H begin to precipitate from the solution and the C_3S reaction accelerates reaching a maximum rate at the end of the third stage (acceleration stage). End of the induction period is considered when the Ca^{2+} and OH^- concentrations have reached critical values required for the formation of crystal nuclei from which hydration products precipitate (nucleation control reaction). It is generally accepted that rapid growth of CH crystals from the solution and fall of the Ca^{2+} concentration in the solution introduce the start of the accelerating period as more Ca^{2+} and OH^- ion can come into solution from the C_3S surface now. Initial setting of cement paste typically occurs at the end of the dormant period and beginning of the acceleration period when the rate of reaction accelerates. Final setting time usually occurs at the middle of the accelerating period. At the end of accelerating period maximum rate of heat evolution occurs (peak 2). The hydration product C-S-H precipitates on the surface of the C_3S grains and with time the layer thickens. As water has to pass through this barrier in order to react with residue C_3S grain and ion has to pass through this grain to come into solution, the hydration reaction is slowed after the acceleration stage. As C-S-H layer thickness increases, mass transport becomes slower and the hydration reactions become diffusion controlled. After the acceleration stage, hydration reaction approaches deceleration period (stage 4) followed by the steady state condition (stage 5). Hydration reaction of C_2S proceeds

in the same way as C_3S but a slower speed and heat liberated from C_2S hydration reaction is lower compared to C_3S.

Tricalcium Aluminate (C_3A) which makes almost 4-11% of cement compounds is very reactive with water (Ramachandran and Beaudoin 2001). With water this compound reacts vigorously and sets rapidly. In order to have sufficient workable time, a small amount of gypsum is added to the Portland cement. The C_3A reacts with gypsum ($C\bar{S}H_2$) and water within a few minutes to form ettringite (AF_t, $C_6A\bar{S}_3H_{32}$) as follows:

$$C_3A + 3C\bar{S}H_2 + 26H \rightarrow C_6A\bar{S}_3H_{32}$$

When all gypsum is consumed, remaining C_3A reacts with already formed ettringite to form monosulfoaluminate (AF_m, $C_4A\bar{S}H_{12}$) as follows:

$$2C_3A + C_6A\bar{S}_3H_{32} + 4H \rightarrow 3C_4A\bar{S}H_{12}$$

Conversion from ettringite to monosulfoaluminate generally occurs within 12-36 hours in normal Portland cement with an exothermic peak (peak 3) (Ramachandran and Beaudoin 2001).

Tetracalcium aluminoferrite (C_4AF) forms about 8-13% of cement compounds (Ramachandran and Beaudoin 2001). The hydration reaction products of C_4AF are similar to those of C_3A but its reaction rate is slower than C_3A and involves less heat. The hydration reaction becomes slower with the increasing amount of iron in ferrite phase. Gypsum retards hydration of C_4AF more drastically than that of C_3A.

2.2 Hydration and Reaction of Slag and Early Strength Development of Concrete with High Volume of Slag

Ground granulated blast-furnace slag is a by-product in production of iron, and is accepted as a mineral admixture because of its glassy nature and chemical composition. The slag is a latent cementitious material with some pozzolanic property. ASTM C 989 (2006) classifies slag to be used in concrete and mortar as Grades 80, 100, and 120 depending on slag-activity index (SIA).

When the slag is mixed with water, it hydrates more slowly than that of Portland cement. The slow hydration of slag is due to the protective layer of amorphous silica and alumina around the surface of slag particles formed at an early stage of hydration (Mindess et al. 2003). Thus, the rate of slag hydration depends largely on the breakdown and dissolution of glassy slag structures. To increase the rate of slag hydration and reaction, activators such as soluble sodium salts, calcium hydroxide and calcium sulfates may be used (Mindess et al. 2003).

The hydration of slag forms a mixture of C-S-H (having lower C/S ratio than C-S-H formed during OPC hydration) and AF_m phases. Generally, slag is used in combination with OPC, where CH formed during cement hydration acts as a main activator and alkali hydroxide plays a minor role (Mindess et al. 2003). According to ACI 233R (2003), hydration of slag and OPC mixture is generally a two stage reaction. Rate of heat development curve of slag-cement blends shows these two stage reactions with two hydration peaks after the dormant period. The first peak corresponds to Portland cement hydration and the second peak corresponds to slag hydration activated by CH. In the slag-cement blends, slag also shows pozzolanic activity (Mindess et al. 2003).

Concretes with a high-volume (> 50%) of slag have been used extensively in situations where durability is of prime concern. For example, William Preston Memorial Bridge in Maryland and Hap Cremeans water treatment plant in Columbus used concrete with a high amount slag for protection against sulfate attack (SCA 15 2003). However, because the slag is a latent cementitious material, high-volume slag concrete generally has lower strength at an early age compared with Portland cement concrete (Hogan and Meusel 1981; Brooks and Al-Kaisi 1990; Swamy and Bouikni 1990; Elahi et al. 2010; Shariq et al. 2010). The extent of the early strength reduction depends on the amount and grade of slag used in the mixture (ACI 233R 2003).

Shariq et al. (2010) found that a 60% cement replacement by slag with w/cm ratio 0.45 reduced the 3- and 7-day compressive strengths of concrete by 57% and 41%, respectively, compared with control concrete with 100% Portland cement. In another study, Hogan and Meusel (1981) reported that with 50% cement replacement by slag, the 3- and 7-day strengths of concrete were reduced by 30% and 12%, respectively, compared with control concrete at w/cm ratio of 0.4.

2.3 Pozzolanic Reaction of Fly Ash and Early Strength Development of Concrete with High Volume of Fly Ash

Fly ash is a by-product of coal-fired electric power stations. There are two major classes of fly ash (class F and class C) specified in ASTM C 618 (2008a) on the basis of their chemical composition resulting from the type of coal burned. Table 2.1 shows typical chemical compositions of class F and class C fly ash. Among the two classes, class F fly ash does not have any cementitious property when mixed with water. Due

to the pozzolanic property, the glassy silica in Class F fly ash reacts with CH, formed during cement hydration, to generate additional C-S-H as follows:

$$CH + S + H \rightarrow C\text{-}S\text{-}H$$

As fly ash is of a pozzolanic nature, using fly ash as a cement replacement in concrete is beneficial. Not only can it achieve desired mechanical properties and durability of concrete if cured properly, it also reduces environmental pollution. However, calorimeter studies show significant reduction of rate of heat evolution in such cement blends due to cement replacement by fly ash (Hwang and Shen 1991; Ma et al. 1994; Poon et al. 2000; Langan et al. 2002; Mounanga et al. 2010) which in turn affects early strength development. Poon et al. (2000) found that with the increasing amount of fly ash as cement replacement, both the maximum rate of heat evolution and the cumulative heat evolution during the first 72 hrs are decreased, and the time of reaching the maximum rate of heat evolution was delayed. As fly ash has limited reactivity, it behaves almost like an inert material denies the early stage of cement hydration. Moreover, it is reported that fly ash acts like a Calcium sink which removes Ca^{2+} and reduces the Ca^{2+} concentration in the solution. This results in delayed nucleation and precipitation of cement hydration products. Mehta (1985) reported that in addition to calcium content, particle size distribution is an important parameter for the reactivity of a fly ash. They reported that for low calcium fly ash the reactivity of fly ash was directly proportional to the amount of particles < 10 μm and inversely proportional to the amount of particles > 45 μm.

Fly ash can improve the mechanical properties and durability of concrete by playing various roles. It reacts with CH, formed during cement hydration, to provide extra C-S-H binder as well as densifies the matrix through space filling (filler effect).

Though fly ash is a pozzolanic material, it is generally agreed that early strengths of concretes with high-volumes of fly ash as cement replacement are reduced (Mehta and Gjørv 1982; Langley et al. 1989; Jiang and Guan 1999; Papadakis 1999; Poon et al. 2000; Li and Zhao 2003; Siddique 2004; Baert et al. 2008). The extent of the early strength reduction depends on the amount of fly ash used for replacing cement and the characteristics of the fly ash used. For example, Poon et al. (2000) revealed that with 45% fly ash replacement, the 3-days compressive strengths of concrete were 61% and 53% of the control concrete for w/cm ratio 0.24 and 0.19, respectively. In another study, Li and Zhao (2003) found that for a 40% fly ash replacement, the 3 and 7-days compressive strength of concrete were 63% and 64% of control concrete, respectively.

Tangpagasit et al. (Tangpagasit et al. 2005) reported that up to 28 days the strength activity index of fly ash is affected mainly by filler effect as the pozzolanic reaction only comes into effect at a later stage. As most fly ashes have particle sizes in the same order as those of cements and the contribution of the filler effect to early strength is limited, strength of fly ash concrete at early age may be assessed from the consideration of cement alone in the concretes (Ganesh Babu and Siva Nageswara Rao 1994).

2.4 Effect of Silica Fume on Early Strength of Concrete Made with Slag or Fly Ash

2.4.1 Characteristics of Silica Fume

Silica fume is fine noncrystalline silica produced in electric arc furnaces as a by-product of the production of elemental silicon or alloys containing silicon (ACI 116R

(2000)). Silica fume consists of spherical particles with mean size of about 100 nm which is about 100 times finer than Portland cement. It typically contains 85% or more silica (Fidjestøl and Lewis 2003).

2.4.2 Mechanisms by which Silica Fume Improve Concrete Strength

From literature review it is clear that silica fume increases the compressive strength and durability of concrete (Grutzeck et al. 1982; Huang and Feldman 1985; Bentur et al. 1988; Mindess 1988; Godman and Bentur 1989; Gutteridge and Dalziel 1990; Goldman and Bentur 1994; Toutanji and El-Korchi 1995; Poon et al. 1999; Poon et al. 2000; Zelic et al. 2000; ACI 234R 2006; Kadri and Duval 2009) because of its physical and chemical effects together with microstructural modifications as follows:

From the physical point of view, fine particles of silica fume,

- Fill the spaces between cement grains and reduce bleeding to improve the packing of solid materials
- Provide heterogeneous nucleation sites to accelerate cement hydration.

From the chemical perspective, silica fume is a highly reactive pozzolanic material with high surface area and high amount of amorphous SiO_2 (shown in Table 2.1). It reacts chemically with CH from cement hydration at faster rates to form extra C-S-H compared with fly ash and slag.

From microstructural modification perspective, silica fume,

- Reduces the porosity of interfacial transition zone (ITZ) and accumulation of water under aggregate particles by its physical effect
- Reduces amount of CH in the ITZ by its chemical effect
- Induces a composite behavior of aggregate and paste where aggregate acts as reinforcing filler due to the modification of ITZ.

Pozzolanic reaction of silica fume may start before 1 day for high amounts of silica fume addition (Huang and Feldman 1985; Zhang and Gjørv 1991). However, it is also reported that at early ages (before 3 days) pozzolanic activity of silica fume may not advance and compressive strength is attributed by physical contribution of silica fume. According to (Sellevold and Radjy 1983; Detwiler and Mehta 1989; Chandra and Berntsson 1996), the pozzolanic activity of silica fume may contribute to compressive strengths after 3 days.

2.4.3 Effect of Silica Fume on Early Strength of Concrete Containing Slag

Researchers have investigated the use of silica fume in slag concretes to compensate for their low early strengths. It is reported that silica fume enhances the early strength of slag concrete (Malhotra et al. 1985).

Malhotra et al. (1985) investigated the effects of silica fume on high-volume (50% by weight) slag concrete with the addition of silica fume ranging from 5 to 20% by weight of (cement + slag) cementitious material. They found that the compressive strength of the slag concrete can be increased by the addition of silica fume, and the gain in strength was directly proportional to the percentage of silica fume as shown in Fig. 2.2. At 3 days, the increase in strength was marginal. However, at 14 days and beyond the loss of concrete compressive strength due to cement replacement by slag was fully compensated for by adding a small amount of silica fume.

2.4.4 Effect of Silica Fume on Early Strength of Concrete Containing Fly Ash

Literature review indicates that decreased compressive strength at early age due to the use of fly ash can be compensated by using a small amount of silica fume (Mehta and Gjørv 1982; Carette and Malhotra 1983; Popovics 1993; Thomas et al. 1999; Erdem and Kirca 2008).

Mehta and Gjørv (1982) investigated compressive strength of concrete using fly ash (15% by volume of cementitious material) and condensed silica fume (15% by volume of cementitious material), and compared with concrete containing only fly ash (30% by volume of cementitious material). They found that 3- and 7-day compressive strengths were 17 and 13 % higher, respectively, for fly ash concretes with silica fume than those of without silica fume.

In another study, Carette and Malhotra (1983) investigated effects of silica fume on fly ash concrete (30% fly ash by weight), and silica fume content ranged from 5 to 20% by weight of (cement + fly ash). They found that early age strength of fly ash concrete was increased by incorporation of silica fume and gain in strength was directly proportional to the amount of silica fume used as shown in Fig. 2.3. At 1 day, the increased in strength was marginal, and at 7 days and beyond, the loss of concrete strength due to replacement of cement by fly ash can be fully compensated and even exceed the strength of concrete without silica fume.

Popovics (1993) found that the use of 5% silica fume (slurry with 38.2% by weight solid content) in concrete with 25% fly ash gave higher compressive strengths both at early ages (1 and 7 days) and later ages compared with those of the concrete without silica fume.

Thomas et al. (1999) reported that fly ash reduced concrete strength at early ages, but significantly enhanced strength at later ages. On the other hand, concrete strength was significantly increased by using silica fume, especially at early ages, and the rate of strength development at later ages for silica fume concrete and plain Portland cement concrete was similar. Thus, the authors pointed out that silica fume and fly ash

combination resulted in improved early age and long-term strength development of concrete.

2.5 Nano-Silica to Improve Compressive Strength

2.5.1 Characteristics of Nano-Silica

Nano-silica is an amorphous material with particle size smaller than 100 nm (Sobolev and Gutierrez 2005; Campillo et al. 2007; Sanchez and Sobolev 2010), which is smaller than the mean size of silica fume as shown in Fig. 2.4. Literature reviewed in this section deals with NS with mean particle sizes ranged from 7 to 40 nm with about 99% SiO_2.

2.5.2 Effect of Nano-Silica on Cement Paste, Mortar and Concrete

In recent years effects of NS on the properties cement based materials have been investigated. Literature review indicates that NS can increase the strengths of cement pastes, mortars, and concretes more effectively than silica fume (Li 2004; Jo et al. 2007; Qing et al. 2007; Belkowitz and Armentrout 2009; Schoepfer and Maji 2009).

In a comparative study, Qing et al. (2007) showed that compressive strengths of hardened cement pastes were increased with increasing amounts of the NS, and the pastes with NS had higher strengths than those with the same amount of silica fume, especially at early ages (Fig. 2.5). For example, with the incorporation of 2% NS (mean particle size 15 nm) 3- and 28-day compressive strengths of cement pastes increased by 19 and 21%, respectively, whereas the same amount of silica fume (mean size 180 nm) did not increase the strengths significantly compared with those of control cement paste.

In another study, Belkowitz and Armentrout (2009) showed that NS increased the compressive strength of cement paste more effectively than silica fume, especially at early ages.

Li et al. (2004) showed that with 5% replacement of cement by NS (mean size 15±5 nm), 7- and 28-day compressive strength of mortars were increased by 20% and 17%, respectively, whereas 15% silica fume replacement increased mortar strengths by 7% and 10% compared with those of control Portland cement mortar. Similar results were reported by Jo et al. (2007).

Schoepfer and Maji (2009) investigated the effect of silica of various particle sizes (150, 100, 40, 12, 7 nm) on the compressive strength development of concrete with small amounts (about 18%) of fly ash. They found that compressive strength of concrete was increased with decreasing size of silica except for mixture with 7-nm nano-silica. No clear explanation was given for the decreased compressive strength of concrete with 7-nm silica.

In the above papers, it is concluded that NS increased C-S-H by providing nucleation sites for cement hydration product and by pozzolanic reactivity. The use of NS also decreased the quantity, orientation and crystal size of CH at paste-aggregate interface by pozzolanic reaction. Apart from acting as filler, NS showed higher pozzolanic reactivity and more effective microstructure modification than silica fume which resulted in increased compressive strengths of the former than latter.

2.5.3 Effect of Nano-Silica on Early Strength of Concrete Containing Fly Ash

It is mentioned earlier that compressive strength of concrete can be significantly increased by NS. These findings may be used to increase the early compressive

strength of fly ash concrete. A few papers were published on the use of NS in fly ash concrete in recent years (Li 2004; Said and Zeidan 2009).

Li (2004) reported that both the short term and long term strength of high-volume fly ash concrete can be increased by adding small amount of NS (mean particle size 10±5 nm). As shown in Fig. 2.6, compressive strength of high-volume fly ash concrete (50% fly ash by mass of cementitious material) with 4% NS (SHFAC) was 81% and 59% higher at 1 and 3 days, respectively, compared with reference fly ash concrete without NS (HFAC).

Said and Zeidan (2009) investigated effect of colloidal NS (mean particle size 35 nm) addition on the strength development of concrete with 30% fly ash. They found that with the addition 3% NS, the 3- and 7-day compressive strengths of concretes were increased by 3.7% and 2.6%, respectively, whereas those with 6% NS were increased by 14.8% and 15.4%, respectively, compared to fly ash concrete without colloidal NS.

The above papers showed that the rate of hydration and pozzolanic reactivity of fly ash concrete are increased by incorporating small amounts of NS. However, the extent of the improvement is different.

As mentioned earlier silica fume increases the compressive strength of slag and fly ash concrete at an early age. However, addition of a small amount of silica fume may not significantly increase the early strength of slag and fly ash concrete. Nano-silica may play a more favorable role than silica fume.

2.6 Nano-Particle Dispersion

A challenge for the application of NS in concrete is dispersion of the nano-particle. Well dispersed individual nano-particles are beneficial allowing NS to be used to their full potential. However, reducing the size of particles leads to increased surface area, and can cause particle agglomeration (Masuo Hosokawa et al. 2007). Agglomeration decreases effective surface area of the nano-particles and may lead to reduced efficiency of the NS.

Nano-particles (e.g. nano-silica) are usually produced as dry powder. Different mixing equipments such as disk mills, high-shear mixer, and high-pressure homogenizer have been used to disperse NS powder in liquid. For applications of nano-particles in cement pastes, mortars, and concretes, special mixing procedures have been reported (Li 2004; Qing et al. 2007; Jayapalan et al. 2009), and some of them used ultrasonic mixer (Metaxa et al. 2009) for the dispersion of nano-particles.

According to (Wang et al. 2001), ultrasonic cavitation from ultrasonic mixer can break nano-particle agglomerates more effectively than conventional stirring. At the time of ultrasonication, alternating high and low pressures are created in the suspension. This results in high speed liquid jets and mechanical stresses between particles which break the attracting force of nano-particles (Fig. 2.7), thus dispersing and deagglomarating the nano-particles effectively. Figure 2.8 shows a typical result of ultrasonic dispersion of fumed silica in water which illustrates the particle deagglomeration and increase in volume of small particles due to the ultrasonic treatment.

No publication has been found which examines and compares the effect of different mixing and dispersion methods of nano-silica on the strength development of mortars or concretes.

Table 2.1 - Comparison of chemical and physical characteristics of Portland cement, fly ash, slag cement, and silica fume (Holland 2005)

Property	Portland cement	Slag	Class F Fly Ash	Class C Fly Ash	Silica fume
SiO_2, %	21	35	52	35	85 to 97
Al_2O_3, %	5	12	23	18	----
Fe_2O_3, %	3	1	11	6	----
CaO, %	62	40	5	21	< 1
Fineness as surface area, m^2/kg *	370	400	420	420	15,000 to 30,000
General use in concrete	Primary binder	Cement replacement	Cement replacement	Cement replacement	Property enhancer

*Surface area measurements for silica fume by nitrogen adsorption method. Others by air permeability method (Blaine)

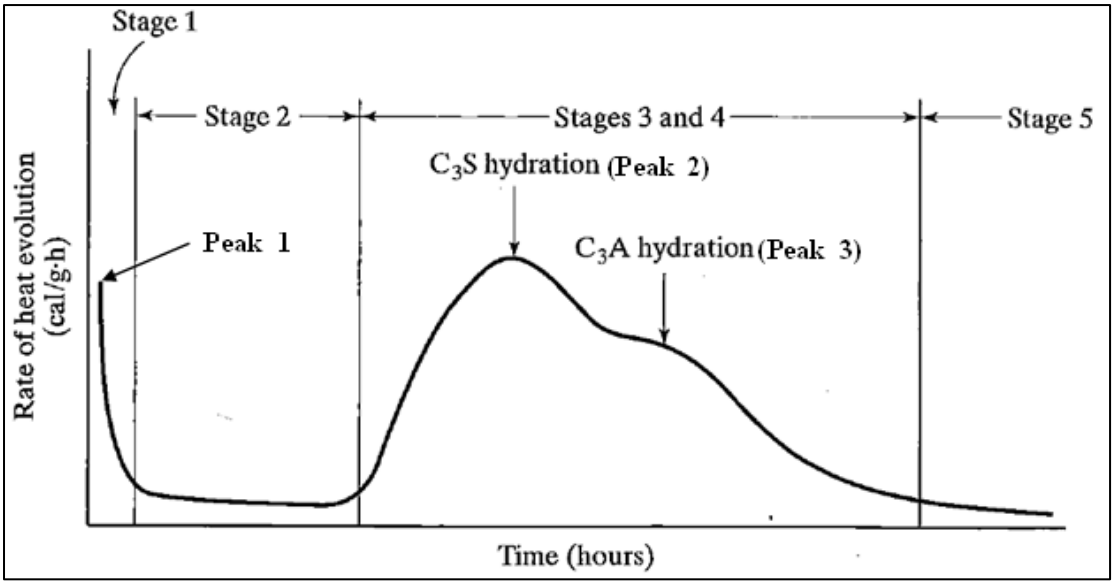

Figure 2.1 - Rate of heat evolution during hydration of Portland cement (Mindess et al. 2003).

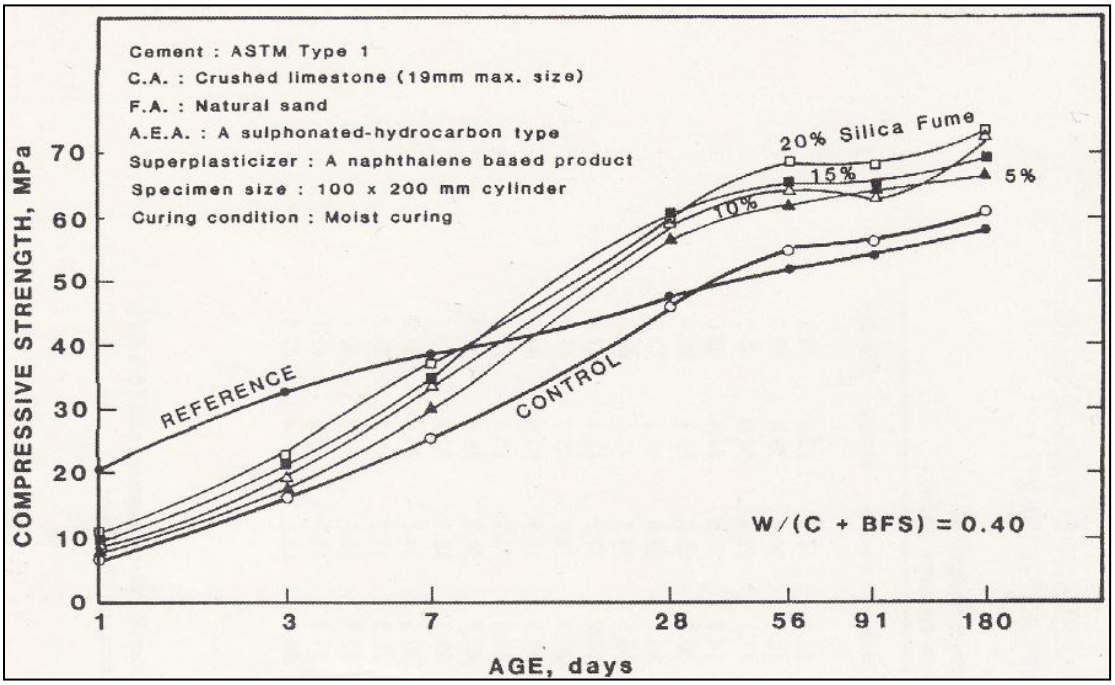

Figure 2.2 - Compressive strength development in blast furnace slag replaced concrete and effect of silica fume (Malhotra et al. 1985). Reference mixture: 100% normal Portland cement, control mixture: 50% normal Portland cement plus 50% BFS, silica fume mixtures: 50% normal Portland cement plus 50% BFS plus additions of silica fume.

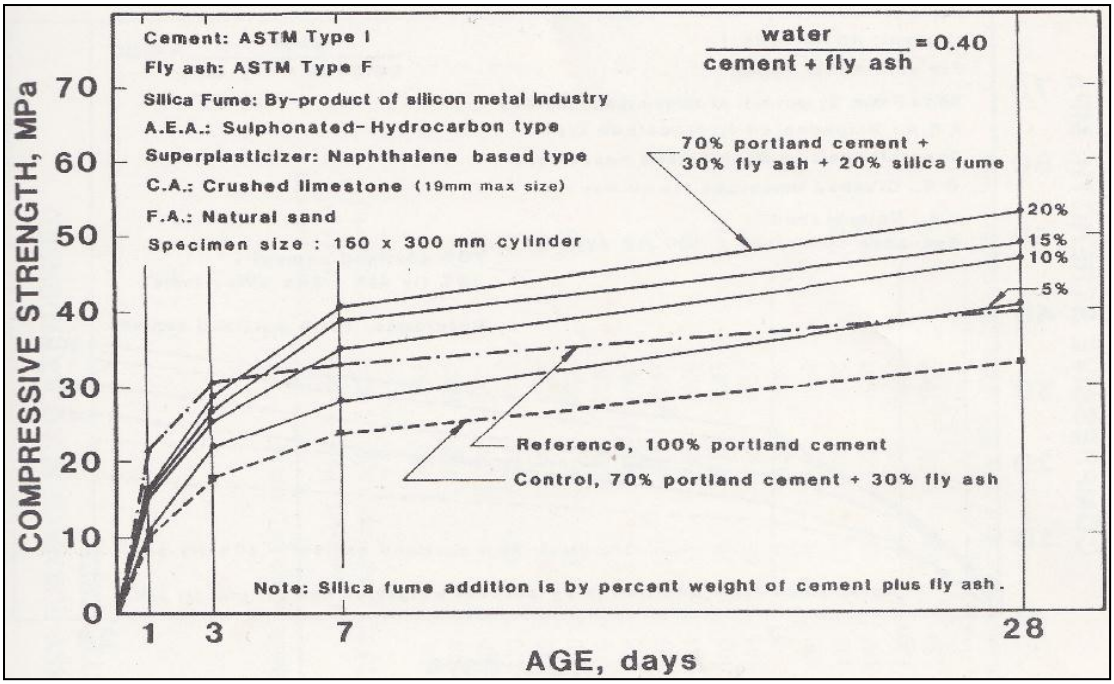

Figure 2.3 - Compressive strength development in fly ash replaced concrete and effect of silica fume (Carette and Malhotra 1983). Reference mixture: 100% normal Portland cement, control mixture: 70% normal Portland cement plus 30% fly ash, silica fume mixtures: 70% normal Portland cement plus 30% fly ash plus additions of condensed silica fume.

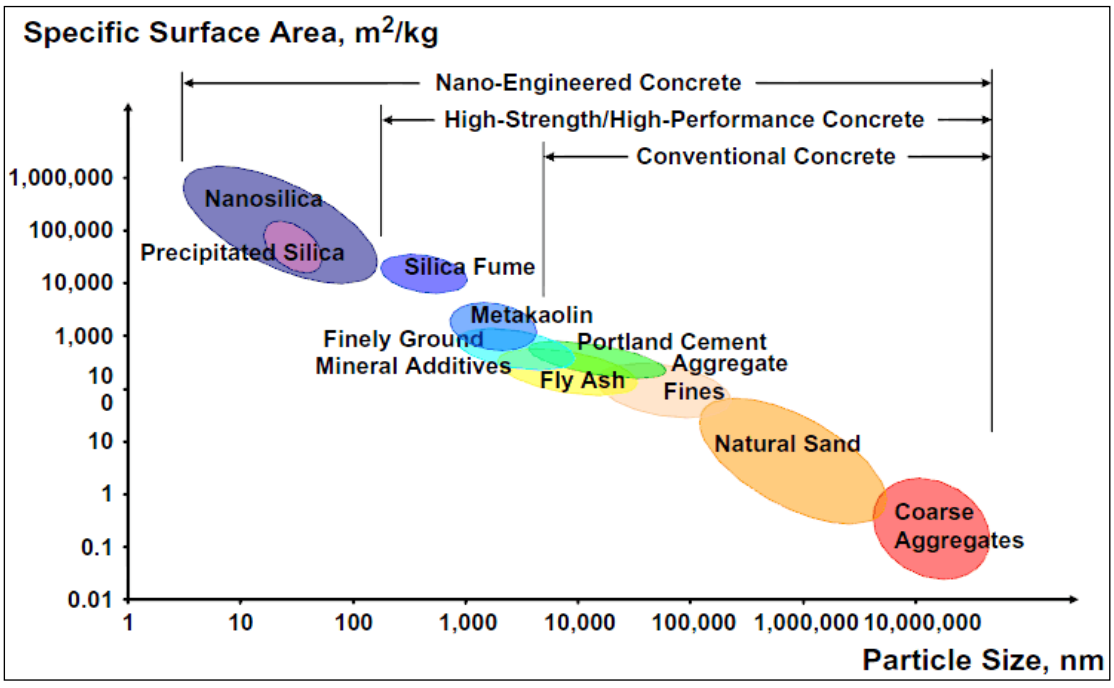

Figure 2.4 - Particle size and specific surface area related to concrete materials (Sobolev and Gutierrez 2005; Sanchez and Sobolev 2010)

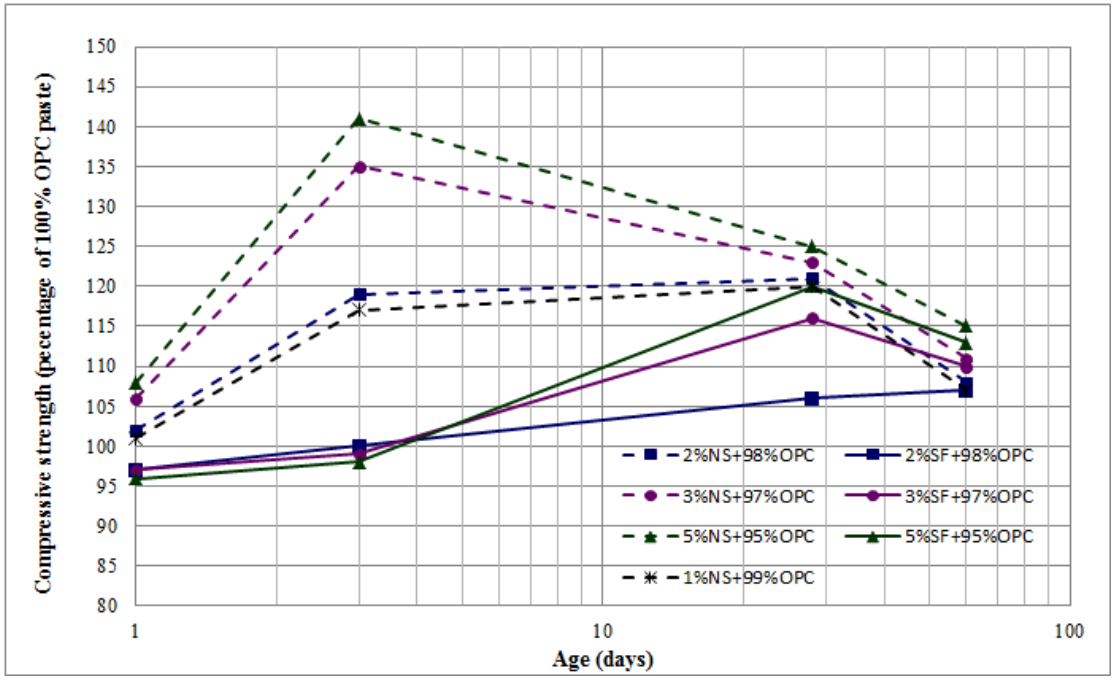

Figure 2.5 - Development of compressive strength for cement pastes with NS or silica fume (SF) as cement replacement (Data taken from Qing et al. 2007) (Average particle diameters of silica fume and NS are 180 nm and 15 nm respectively, w/cm= 0.22)

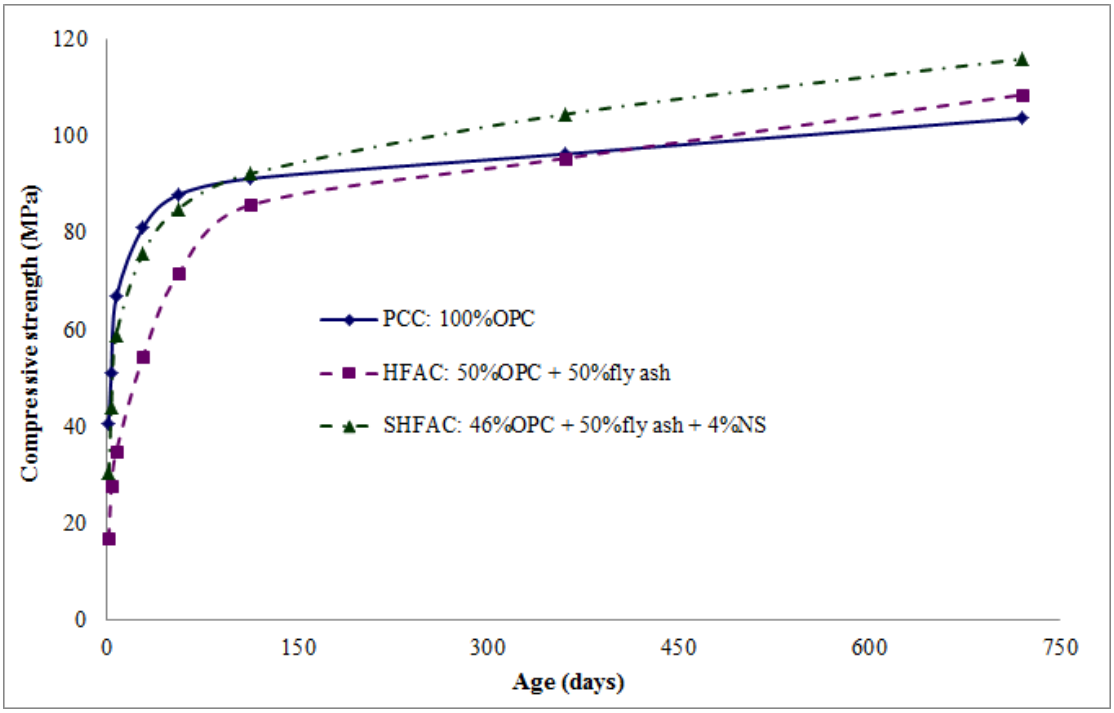

Figure 2.6 - Development of compressive strength of fly ash concrete with a small dosage of NS as cement replacement (Li 2004) (Average NS particle size 10±5 nm, w/cm= 0.28)

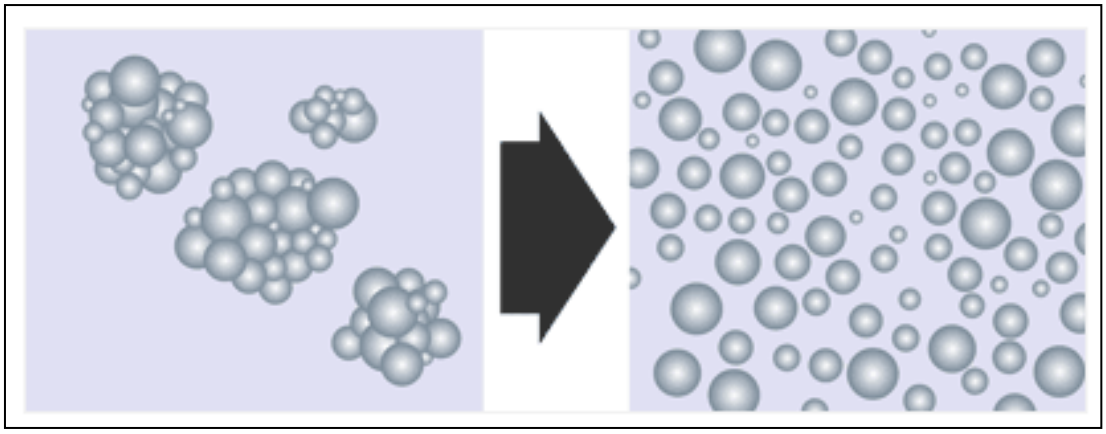

(a) (b)

Figure 2.7 - Dispersion and deagglomeration of nano particles (a) before sonication, (b) after sonication
(Hielscher ultrasound technology, http://www.hielscher.com/ultrasonics/disperse.htm)

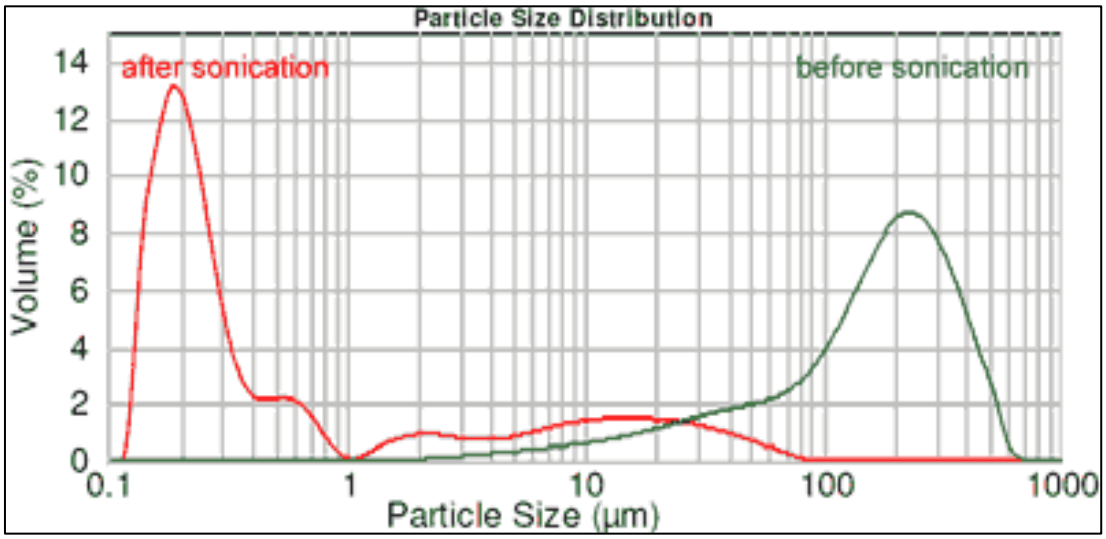

Figure 2.8 - Typical result of ultrasonic dispersion of fumed silica in water
(Hielscher ultrasound technology, http://www.hielscher.com/ultrasonics/size_reduction_silica_01.htm)

Chapter 3 Experimental Details

3.1 Introduction

In this study specimens were prepared to determine effect of dosage, particle size, and dispersion method of NS on compressive strength development of mortars with about 50% GGBFS or ASTM class F fly ash (ASTM C 618 2008a) from 1 to 91 days. The 50% slag or fly ash was selected with the considerations that (1) this content of slag and fly ash has been used in practice; (2) more than 50% fly ash is not common in practice; (3) early strength of concrete with less than 30% slag may not be significantly affected; and (4) relative comparison of slag and fly ash. A superplasticizer was used to achieve target flow from 104 to 112% of the mortars. Cement pastes with the same water-to-cementitious materials ratio (w/cm) and mix proportion as the mortars (except for the sand) were prepared to determine the rate of heat development and cement hydration in the first 30 hrs, and pore structure (slag pastes only) at 28 days. Selected concrete mixtures were prepared to determine the effect of NS on setting time, compressive strength development from 3 to 91 days and resistance to chloride-ion penetration at 28 days in comparison to the reference slag or fly ash concrete and the concrete with silica fume. If the w/cm ratio is below the value

of which complete cement hydration can be achieved, the effect of the NS may not be seen clearly due to the lack of sufficient space and water for hydration and reaction. For concrete with high volumes of slag and fly ash, early strengths are generally compromised. In order to compensate for the reduced strengths, w/cm ratio should be reduced compared with Portland cement concrete. The w/cm ratio of 0.45 was thus selected to take the above two factors into consideration

3.2 Materials

Characteristics of materials used in this research project including cement, slag, fly ash, nano-silica, silica fume, sand, coarse aggregate, superplasticizer, and water are described in this section.

3.2.1 Cement

Normal Portland Cement meeting the requirements of ASTM C 150 (2004) was used. Physical properties, chemical and mineralogical compositions of the cement are presented in Table 3.1. The Chemical composition was determined by X-ray fluorescence spectroscopy (XRF), and the mineralogical composition was calculated using Bogue equations. Figure 3.1 shows particle size distribution of the cement determined by laser diffraction particle size analyzer.

3.2.2 Ground Granulated Blast Furnace Slag and Fly Ash

Ground granulated blast furnace slag meeting the requirements of ASTM C 989 (2006) and fly ash conforming to Class F of ASTM C 618 (2008a) were used. Physical properties and chemical composition of the slag and fly ash are also given in

Table 3.1. Particle size distributions of the slag and fly ash are shown in Fig. 3.1 in comparison to that of the cement.

3.2.3 Nano-Silica and Silica Fume

Two samples of NS with different specific surface areas were used to determine their effect on early strength development of mortars in comparison to that of silica fume. Characteristics of these materials are given in Table 3.1 as well. The two NS were labelled as Type 1[1] and Type 2[2] with specific surface areas of 200 and 321 m^2/g, and average primary particle sizes of 12 and 7 nm, respectively. The silica fume used was undensified with specific surface area of 21.3 m^2/g and average particle size of 150 nm.

3.2.4 Water

Tap water was used for mortar and concrete mixing, whereas deionized water was used for cement pastes.

3.2.5 Superplasticizer

A polycarboxylate based superplastisizer[3] was used in mortar, paste, and concrete mixtures for workability purposes.

3.2.6 Fine and Coarse Aggregates

Natural sand with a fineness modulus of 2.97 was used for mortar and concrete mixtures. Crushed granite coarse aggregate with a maximum size of 20 mm was used for concrete mixtures. Both of them met the requirements of ASTM C 33 (2003). The sieve analyses of the aggregates were conducted according to the procedure described in ASTM C 136 (2006). The grading curves of the sand and coarse aggregate are

[1] AEROSIL 200, Evonik Industries
[2] AEROSIL 380, Evonik Industries
[3] ADVA 181N, W.R. Grace (Singapore) Pte. Ltd.

shown in Fig. 3.2. Specific gravity of the sand and coarse aggregate was 2.62 and absorption of the aggregates was negligible. The aggregates were oven dried for 24 hours and cooled to ambient temperature for use in mortars and concretes.

3.3 Mix Proportions of Mortars, Concretes, and Cement Pastes

3.3.1 Mix Proportions of Mortars

Fifteen mortar mixtures were prepared in the study (Tables 3.2 to 3.4). All the mortars had a w/cm of 0.45 and a sand-to-cementitious materials ratio of 2.75. Dosages of the Type 1 NS varied from 0 to 0.5, 1.0 and 2.0 % by mass of the cementitious materials (Table 3.2). Mortars with 1% Type 1 or Type 2 NS were compared with that with the same amount of silica fume to evaluate the effect of specific surface area and particle size of silica (Table 3.3). As the NS particles were extremely fine, influences of mixing and dispersion methods on properties of the mortars were also evaluated (Table 3.4). Dosage of the superplasticizer was determined to achieve a flow value of about 104-112 %.

3.3.2 Mix Proportions of Concretes

In addition to the mortars, effect of NS on concrete properties was studied in comparison to that of silica fume. Mix proportions of the concretes are given in Table 3.5. Dosage of the superplasticizer was determined to achieve a slump of about 100 mm for the concretes.

3.3.3 Mix Proportions of Cement Pastes

Mix proportions of cement pastes were similar to those of the mortars except for the exclusion of sand.

3.4 Mixing and Preparation of Mortar, Concrete, Cement Paste and Specimens

3.4.1 Mixing and Preparation of Mortar Specimens

The mortars were mixed in a Hobart mixer at an ambient temperature of about 30 ^{o}C. For mortar mixtures with mechanical mixing, solid materials were dry mixed first. Water was added and mixed for 1 min followed by addition of superplasticizer and mixed for 1 more min at low speed and 30 seconds at high speed. The superplasticizer was used to achieve the target flow from 104 to 112%. The flow value was determined according to ASTM C 1437 (2001).

For ultrasonic mixing, NS and water were mixed first using ultrasonic mixer[4] (Fig. 3.3) with 90 Watts power input for 5 minutes. The sonicated mixture was then mixed in a Hobart mixer with cement, slag/fly ash, and sand for 1 min. After that, superplasticizer was added and mixed for 1 min at low speed and 30 seconds at high speed.

For each mortar mixture, fifteen 50-mm cube specimens were cast for compressive strength test. The molded specimens were covered with wet burlap for the first 24 hours to prevent moisture loss. After demold, the specimens were cured in a fog room at a temperature of about 28 - 30 ^{o}C until the time of testing.

3.4.2 Mixing and Preparation of Concrete Specimens

Concretes were mixed using a pan mixer at an ambient temperature of about 30 ^{o}C. Before concrete mixing, NS or silica fume were mixed with water using the ultrasonic mixer for adequate dispersion of the particles. The sonicated mixture was then mixed with aggregate, cement and slag or fly ash in the pan mixer for 1 min. The

[4] Model 300 V/T, Biologics, Inc.

superplasticizer was added and mixed for another 1-2 minutes to achieve a target slump of about 100 mm.

Twelve 100-mm cubes and one 100x200-mm cylinders were cast for each concrete mixture for determining compressive strength and chloride-ion penetrability, respectively. Mortar sieved from the concrete was used to cast a 150-mm cube to determine setting time of concrete. Compressive strengths of concretes were determined at 3, 7, 28, and 91 days according to BS EN 12390-3 (2002), setting time of concretes were determined according to ASTM C 403/C 403M (2008), and resistance to chloride-ion penetration was determined at 28 days according to ASTM C 1202 (2005). Curing of the concretes was the same as that of the mortar specimens.

3.4.3 Mixing and Preparation of Cement Paste and Specimens

As mentioned above, mix proportions of cement pastes were similar to those of the mortars except for the exclusion of sand. For ultrasonic mixing, NS and water were premixed in ultrasonic machine for dispersion of fine particles. Before paste mixing, all the materials including sonicated mixtures were pre-conditioned at 30 °C for 24 hours. The mixing procedures for cement pastes were similar to those of the mortars.

For porosity and pore size distribution test, cement paste was cast in small plastic bottles and sealed with preheated wax and capped. The bottles were slowly rotated for the first 24 hours to minimize segregation/bleeding of the cement paste sample. After that, the sample bottles were stored in the sealed condition at about 30 °C for curing.

At specified ages, the cement paste was removed from the bottles. Top and bottom parts of the paste together with that in contact with inner wall of the bottle were removed by a chisel. The samples were broken into small pieces and dried in a vacuum oven at 50 ºC until constant weight was reached.

3.5 Test Methods and Analyses

3.5.1 Compressive Strength of Mortars and Concretes

Compressive strengths of the mortars were determined at 1, 3, 7, 28, and 91 days according to ASTM C 109/C 109M (2002). The strength of the concretes were determined at 3, 7, 28, and 91 days according to BS EN 12390-3 (2002). Automax 5 compression test machine (Fig.3.4) was used for determining the mortar strength, and loading rate was set at 1200N/s according to the standard. A Denison Mayes compression test machine (Fig 3.5) was used for determining the concrete strength, and loading rate was 180 kN/min.

3.5.2 Rate of Heat Generation and Cement Hydration of Cement Pastes

Effect of NS on the rate of heat generation in cement pastes was evaluated according to ASTM C 1679 (2008) by a Thermometric TAM Air 3115 isothermal calorimeter (Fig. 3.6) at a temperature of 30 °C. This temperature was selected to simulate weather conditions in tropical countries. The heat generation in the cement pastes reflects rate of cement hydration. The calorimeter was conditioned at 30 °C for a day before experiments, and amplifier range was set at 600 mW.

After the mixing, cement paste sample of about 10 grams was transferred into a sample ampoule with the sample mass recorded. After capping the ampoule, the sample and reference ampoules were inserted into the calorimeter. The calorimeter started to record heat at about 15 minutes after the cementitious materials were in contact with water, thus the heat generated initially during mixing and preparation was not captured. The heat generated from the cement hydration was monitored continuously for 30 hours. The power output (in mili-watt) from the calorimeter due to the heat generated was recorded every minute. The power output was normalized

based on sample mass. The normalized power output was then converted to heat generated in the sample (in joules/gram). For each mixture, two samples were tested and their mean result was reported

3.5.3 Porosity and Pore Size Distribution of the Cement Pastes

Mercury intrusion porosimetry (MIP) was used to determine porosity and pore-size distribution of the cement pastes cured for 28 days. The test was conducted using Micromeritics Autopore WIN9400 Series mercury porosimeter (Fig. 3.7) with a maximum pressure of 412.5 MPa. Mercury was forced into the pore system of the sample by the application of external pressure, and the relationship between the pore size and the pressure exerted is expressed by Washburn equation (Washburn 1921):

$$r = -\frac{2\gamma \cos\theta}{P}$$

Where: r - Pore radius (m), γ - Surface tension of mercury (N/m), θ - Contact angle (°), P - Pressure exerted (N/m^2)

The minimum pore diameter reached under the maximum pressure was about 3.8 nm assuming a contact angle of 141.3° and a mercury surface tension of 0.485 N/m (Ramachandran and Beaudoin 2001). Approximately 1.5 grams of the hardened cement paste sample (3-5 mm in size) were used for each test.

3.5.4 Resistance to Chloride-Ion Penetration of Concretes

Resistances to chloride-ion penetration of the concretes were determined at 28 days according to ASTM C 1202 (2005). A PROOVE'it rapid chloride permeability test machine[5] (Fig. 3.8) was used for the test. Three specimens with a diameter of 100 mm and a thickness of 50 mm were used for the test and they were cut from the cylinder with the top and bottom 10 mm removed. The specimens were conditioned before the

[5] PROOVE'it rapid chloride permeability test machine, Germann Instruments, Inc.

test according to the standard. For the test, one reservoir was filled with a 3 % NaCl solution and the other with a 0.3N NaOH solution. A potential of 60V direct current was applied across the specimen (Fig. 3.9). The current was measured for 6 hours. The area under the current versus curve time represented the total charge passed through the concrete specimen in Coulombs. The charge passed was used to classify the concrete according to the standard.

Table 3.1 - Physical properties and chemical compositions of materials

		Portland cement	Slag	Fly ash	Silica fume	Type 1 Nano-silica	Type 2 Nano-silica
Chemical composition, %	CaO	63.4	41.8	3.9	0.2	--	--
	SiO_2	20.1	33.1	46.3	95.9	>99.8*	>99.8*
	Al_2O_3	4.1	13.7	28.5	0.3	--	--
	Fe_2O_3	3.3	0.7	18.5	0.3	--	--
	MgO	3.6	4.9	1.8	0.4	--	--
	Na_2O	0.2	0.2	0.2	0.05	--	--
	K_2O	0.4	0.5	0.6	0.6	--	--
	SO_3	2.1	0.7	0.2	0.2	--	--
	LOI	2.4	0.6	2.3	1.5	--	--
Mineral phases, %	C_3S	66.8	--	--	--	--	--
	C_2S	7.3	--	--	--	--	--
	C_3A	5.3	--	--	--	--	--
	C_4AF	10.1	--	--	--	--	--
Physical properties	Blain fineness, m^2/kg	308	--	--	--	--	--
	BET surface area, m^2/g	--	--	--	21.3	200.1	321.6
	Average primary particle size	28.2μm	16.7μm	27.3μm	150nm*	12nm*	7nm*
	Specific gravity	3.15	2.94	2.47	2.2*	2.2*	2.2*

* Information provided by supplier

Table 3.2 - Mix proportions and flow values of mortars with different dosages of Type 1 nano-silica with specific surface area of 200 m^2/g (w/cm = 0.45)

Mix ID	% of nano-silica by mass of cementitious material	Mixing procedure	Mix proportion							Flow, %
			Water	Cement	Slag	Fly ash	Nano-silica	Sand	Super-plasticizer *	
Control	0	Mechanical	0.45	1	0	0	0	2.75	0.54	110
SL0	0	Mechanical	0.45	0.5	0.5	0	0	2.75	0.42	110
SL0.51	0.5	**	0.45	0.5	0.495	0	0.005	2.75	0.62	110
SL11	1.0	**	0.45	0.5	0.490	0	0.010	2.75	0.88	110
SL21	2.0	**	0.45	0.5	0.480	0	0.020	2.75	1.48	105
FA0	0	Mechanical	0.45	0.5	0	0.5	0	2.75	0.21	107
FA0.51	0.5	**	0.45	0.5	0	0.495	0.005	2.75	0.42	112
FA11	1.0	**	0.45	0.5	0	0.490	0.010	2.75	0.71	108
FA21	2.0	**	0.45	0.5	0	0.480	0.020	2.75	1.18	106

* % of (cement + slag or fly ash + nano-silica)

** With ultrasonic premixing of nano-silica + water

Table 3.3 - Mix proportions of mortars for evaluating the effect of nano-silica size in comparison to that of silica fume (w/cm = 0.45)

Mix ID	Type of silica inclusions	Mixing procedure	Mix proportion							Flow, %
			Water	Cement	Slag	Fly ash	Silica inclusion	Sand	Super-plasticizer *	
SL1SF	Silica fume	Mechanical	0.45	0.5	0.49	0	0.01	2.75	0.42	107
SL11	Type 1 NS	**	0.45	0.5	0.49	0	0.01	2.75	0.88	110
SL12	Type 2 NS	**	0.45	0.5	0.49	0	0.01	2.75	1.04	111
FA1SF	Silica fume	Mechanical	0.45	0.5	0	0.49	0.01	2.75	0.28	106
FA11	Type 1 NS	**	0.45	0.5	0	0.49	0.01	2.75	0.71	108
FA12	Type 2 NS	**	0.45	0.5	0	0.49	0.01	2.75	0.75	107

* % of (cement + slag or fly ash + nano-silica)
** With ultrasonic premixing of nano-silica + water

Table 3.4 - Mix proportions of mortars for evaluating mixing and dispersion methods of nano-silica (w/cm = 0.45)

Mix ID	Mixing and dispersing procedure	Mix proportion							Flow, %
		Water	Cement	Slag	Fly ash	Nano-silica	Sand	Super-plasticizer*	
SL11	**	0.45	0.5	0.49	0	0.01	2.75	0.88	110
SL11 (M)	Mechanical	0.45	0.5	0.49	0	0.01	2.75	1.17	104
FA11	**	0.45	0.5	0	0.49	0.01	2.75	0.71	108
FA11 (M)	Mechanical	0.45	0.5	0	0.49	0.01	2.75	0.57	108

* % of (cement + slag or fly ash + nano-silica) by mass
** With ultrasonic premixing of nano-silica + water

Table 3.5 - Mix proportions of concretes for evaluating the effect of nano-silica in comparison to that of silica fume (w/cm = 0.45)

Mix ID	Type of silica inclusion	Mixing procedure	Mix proportion (kg/m^3)							Slump, mm
			Cement	Slag	Fly ash	silica inclusion	Coarse aggregate	Sand	Super-plasticizer	
CSL0	--	Mechanical	200	200	--	0	1014	774	1.4	95
CSL2SF	Silica fume	*	200	192	--	8	1014	771	1.7	85
CSL21	Type 1 NS	*	200	192	--	8	1014	771	4.0	85
CFA0	--	Mechanical	200	--	200	0	1014	740	0.5	110
CFA2SF	Silica fume	*	200	--	192	8	1014	739	0.6	105
CFA21	Type 1 NS	*	200	--	192	8	1014	739	3.4	100

* With ultrasonic premixing of nano-silica + water

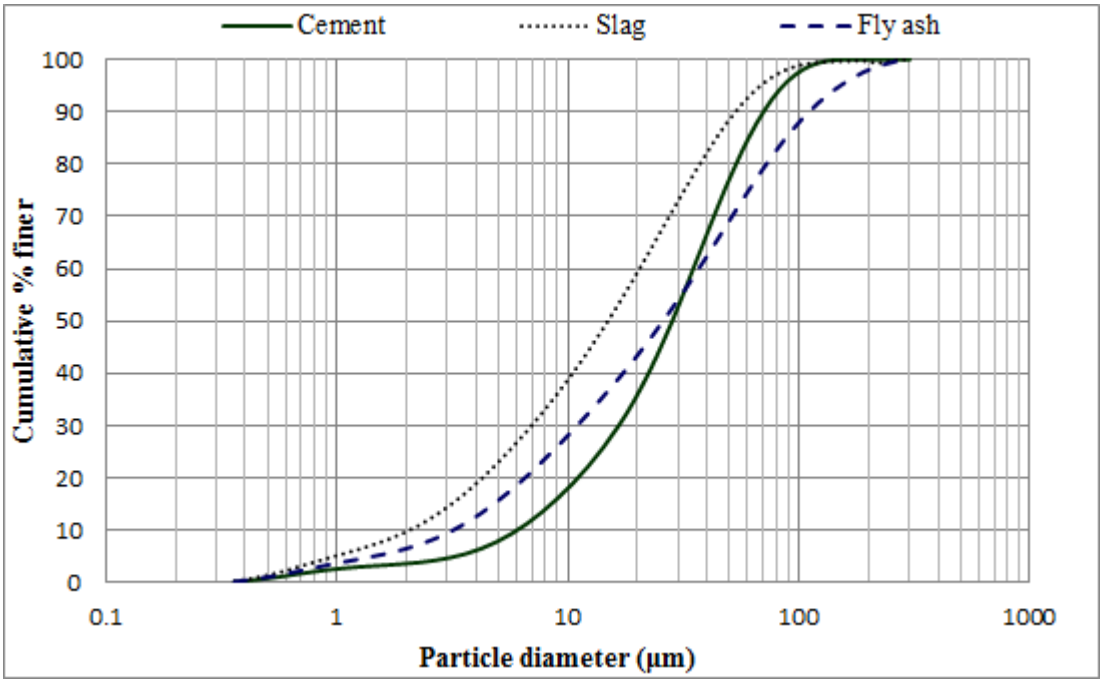

Figure 3.1 - Particle size distribution of cement, slag, and fly ash

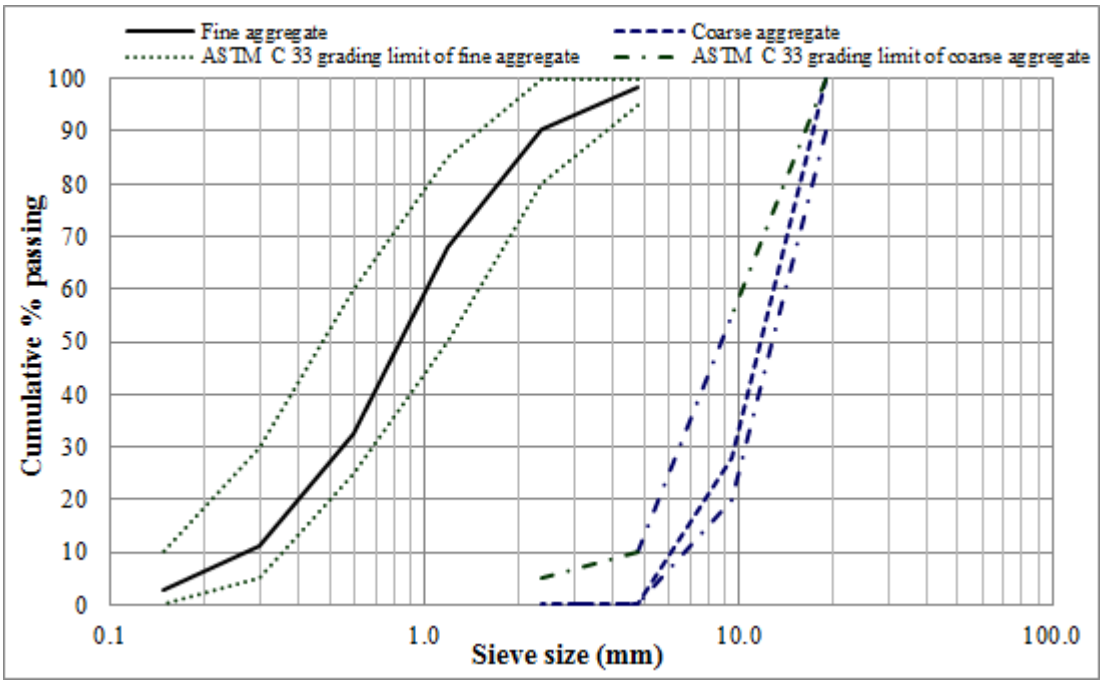

Figure 3.2 - Grading curves of fine and coarse aggregates

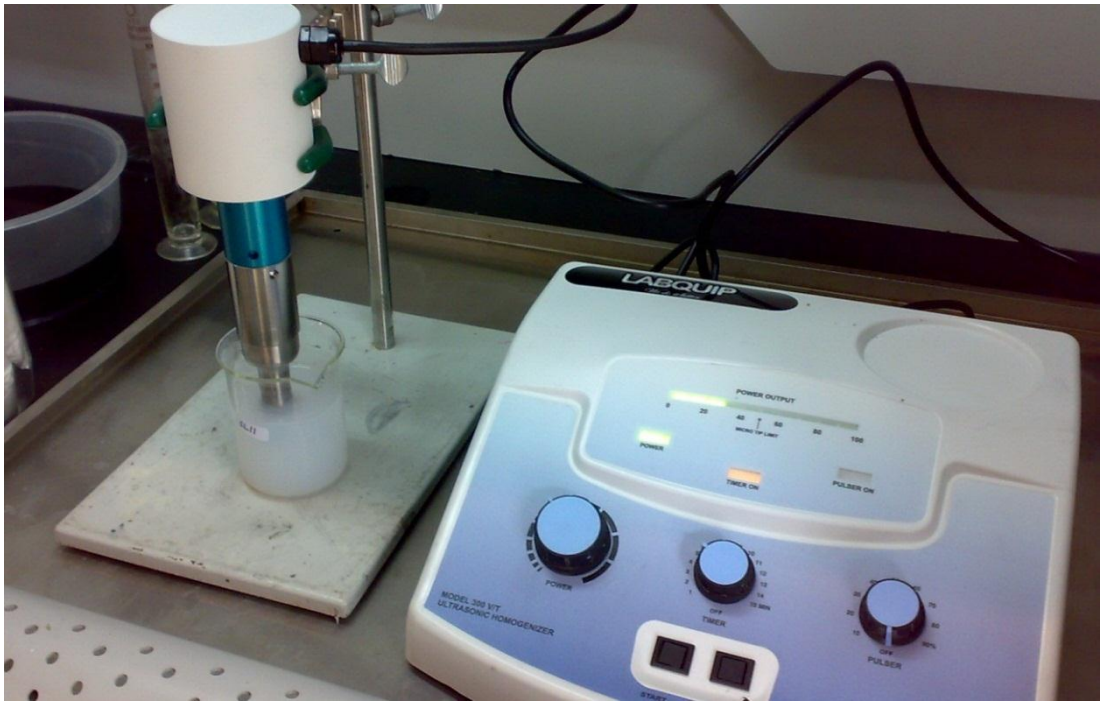

Figure 3.3 - Ultrasonic mixer

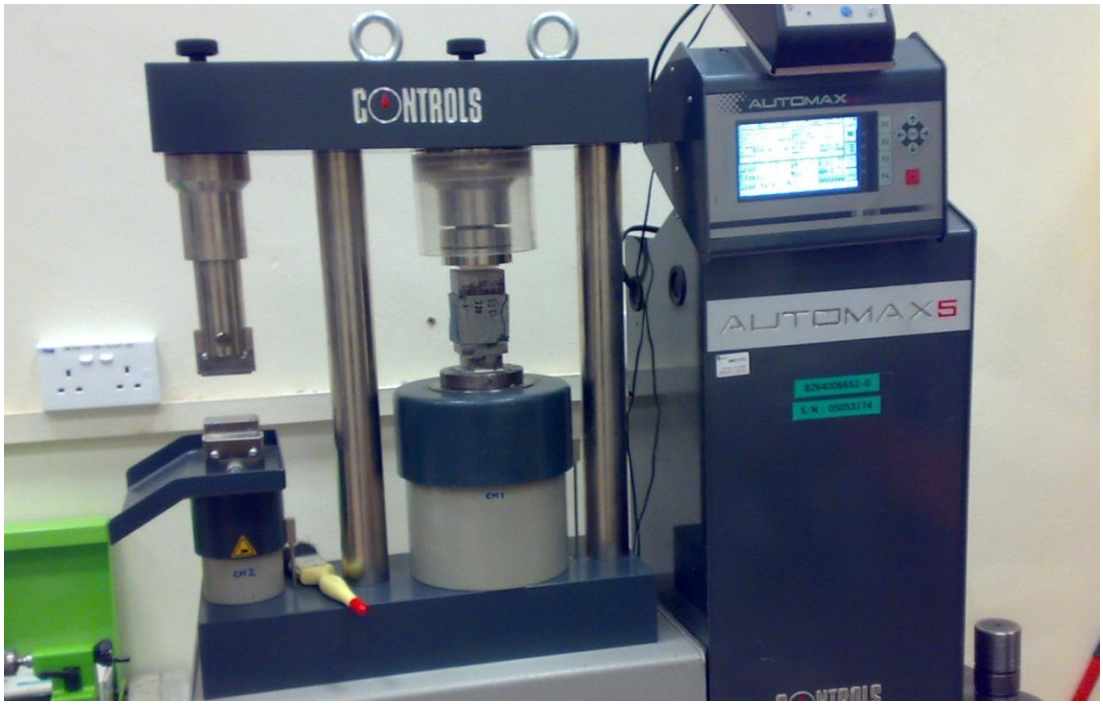

Figure 3.4 - Automax 5 compression test machine

Figure 3.5 - Denison-Mayes compression test machine

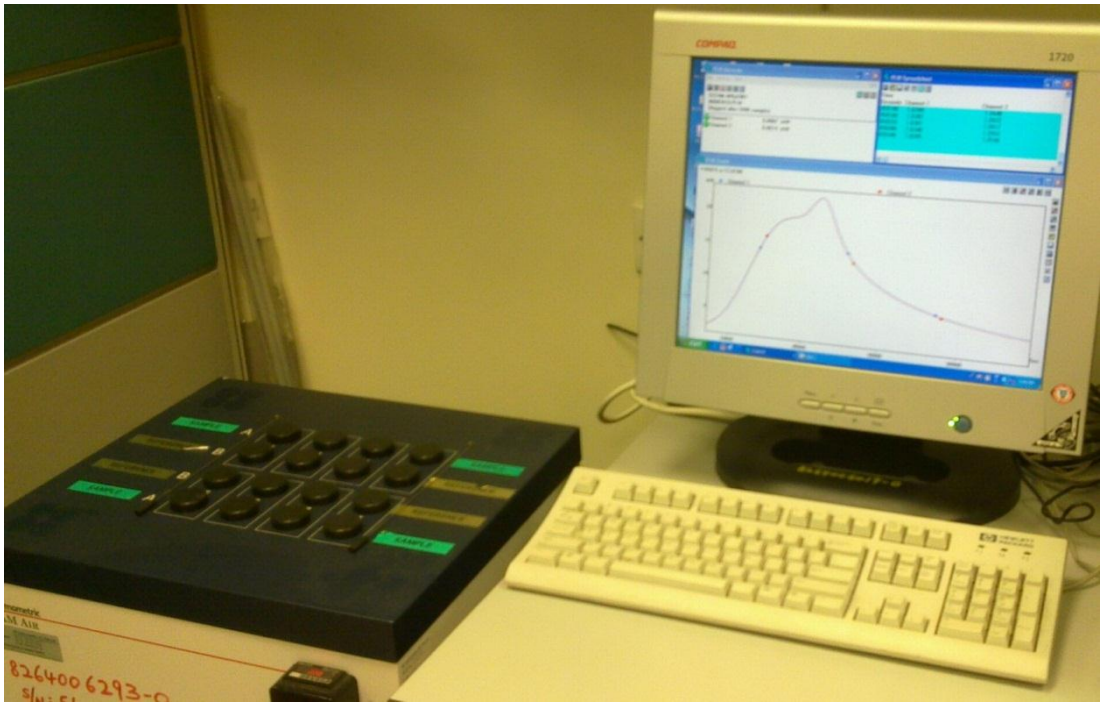

Figure 3.6 - Thermometric TAM Air 3115 isothermal calorimeter

Figure 3.7 - Micromeritics Autopore WIN9400 Series mercury porosimeter

Figure 3.8 - Rapid chloride permeability test setup

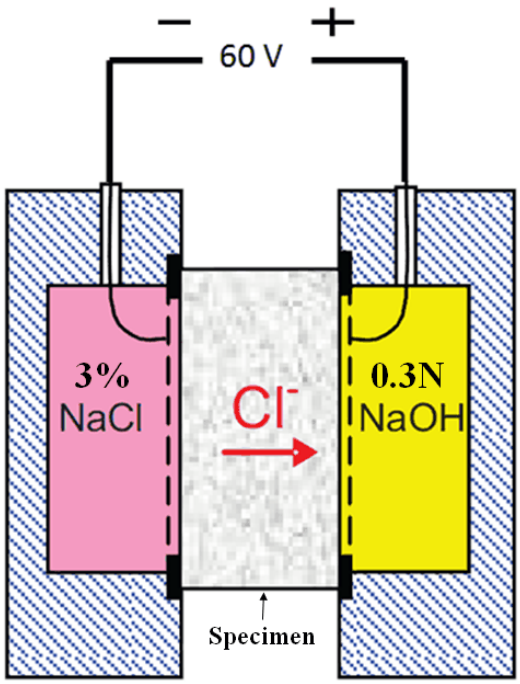

Figure 3.9 - Schematic diagram of the rapid chloride permeability test according to ASTM C 1202 (2005)

Chapter 4 Results and Discussion

In this chapter experimental results are presented and discussed. In the first and second sections, effects of dosage, particle size, and dispersion methods of NS on the compressive strength development mortars, rate of heat development and pore-size distribution of pastes with high-volumes of slag or fly ash are evaluated and discussed, respectively. Effect of NS on compressive strength development, setting time and chloride-ion penetration on high-volume slag or fly ash concretes are also discussed and compared with that of silica fume. In the third section, comparison between high-volume slag and fly ash mortars or concretes with NS is also made and discussed.

4.1 High-Volume Slag Pastes, Mortars, and Concretes

4.1.1 Compressive Strength Development

4.1.1.1 Effect of Nano-Silica Dosage on Strength Development of Mortars

Compressive strength development of the slag mortars incorporating different dosages of Type 1 NS is given in Fig. 4.1 in comparison to that of control Portland cement mortar and reference mortar with 50% slag (SL0). The mortar with 50% slag had lower compressive strengths than the Portland cement mortar from 1 to 91 days as expected. However, the compressive strength of the slag mortars increased with the increase in NS dosages up to 91 days.

Percentage of strength increases of the mortars with the NS compared with the reference mortar with 50% slag is summarized in Table 4.1. With 2% NS, the compressive strength of the slag mortar increased by 39 and 30% at 3 and 7 days, respectively. The slag mortar with 2% NS had almost the same strength as the Portland cement mortar at 7 days, and exceeded strengths of the latter at 28 and 91 days. It is noted that the incorporation of the NS had less significant effect on the 1-day strength of the slag mortars than at 3 and 7 days. This might be related to the higher dosages of the superplasticizer used which had retarding effect in the mortars with NS to achieve a given workability.

4.1.1.2 Effect of Particle Size of Nano-Silica on Strength Development of Mortars

Figure 4.2 shows the effect of NS size on the compressive strengths of the slag mortars compared to that with silica fume. With the incorporation of 1% NS and silica fume, the compressive strengths of the slag mortars were increased. The compressive strengths of the slag mortars were generally increased with the decrease in the particles size of silica inclusions from 1 to 91 days. With 1% NS with particle size of 7 nm, the compressive strengths of the slag mortars were increased by 35 and 21% at 3 and 7 days, respectively (Table 4.1). The increased early strengths with the incorporation of smaller size silica may be related to their high specific surface areas that increased rate of cement hydration and pozzolanic reaction. The results are consistent with findings by Qing et al. (Qing et al. 2007).

4.1.1.3 Effect of Mixing and Dispersion Method on Strength Development of Mortars

Effects of mixing and dispersion methods on the compressive strength development of slag mortars are shown in Fig. 4.3. No significant difference was observed in compressive strength development of mortars prepared by ultrasonicated NS with

water and mechanical mixing method. However, careful examination of the data (Tables A.4 and A.8) shows that the density of the mortar prepared by ultra-sonication of nano-silica (2231kg/m^3) was lower than that prepared by mechanical mixing (2275 kg/m^3). The difference on the density of the mortars might have effect on the strength. This will be discussed further in Sections 4.1.3.3 and 4.3.2.2.

4.1.1.4 Strength Development of Slag Concrete with Nano-Silica

Compressive strength development of the slag concrete with 2% Type 1 NS is shown in Fig. 4.4 in comparison to that of the reference slag concrete and concrete with the same amount of silica fume. Percentage of the strength increase of the slag concrete with 2% NS or silica fume compared with the reference slag concrete is summarized in Table 4.1. The results show that the early strengths of the concrete with the NS were increased by 22 and 18% at 3 and 7 days, respectively, whereas those with silica fume were increased by 4 and 5%, respectively, in comparison to those of the reference slag concrete. However, at the ages of 28 and 91 days, the three concretes had similar strength. This might be related to coarse aggregate used in the concretes which might have reached its strength limit. More detailed discussion will be given in section 4.3.2.3.

4.1.1.5 Discussion on Strength Development

Both the NS and silica fume are nano-sized highly reactive silica, and the average primary particle size of the former is about 10 times smaller than that of the latter. The mechanisms by which silica fume modifies cement paste, mortar, and concrete are summarized in ACI Committee 234 report (2006). These mechanisms are also applicable to NS. As the particle sizes of the NS are much smaller than those of the silica fume, the physical and chemical effect of the former is likely more substantial than the latter.

4.1.1.5.1 Physical Effect

From physical perspective, extremely fine particle size of the NS may have accelerated cement and slag hydration by providing high amount of nucleation sites for precipitation of cement hydration products in the high-volume slag concrete. In the slag concrete, the accelerated cement hydration also results in increased amount of calcium hydroxide in solution which activates and speeds up slag hydration.

In addition to nucleation effect, NS may have acted as reactive filler which reduces bleeding and increases packing density of solid materials by occupying space between cement, slag, and fly ash particles. These physical effects of the NS may have contributed to the increase early strength of the slag concrete observed. However, as both the NS and silica fume are finer than Portland cement and slag the filler effect of the NS and silica fume may be similar.

4.1.1.5.2 Chemical Effect

From chemical point of view, NS is highly reactive pozzolanic material and reacts with CH from cement hydration to form C-S-H. Zhang and Gjørv (1991) reported pozzolanic reaction of silica fume as early as 1-day of cement hydration. Since the NS had specific surface area about 10 times higher than that of silica fume, the pozzolanic reaction of the NS might have started before 24 hrs. The pozzolanic reaction of the NS at very early age might have also contributed to the increase early strength of the slag concrete observed.

4.1.1.5.3 Microstructure Modification

In terms of microstructure modifications, the NS might reduce porosity in cement paste and in ITZ between the cement paste and aggregate due to the physical and chemical effects discussed above. It is also reported that NS can reduce CH crystal

size in the ITZ more effectively than silica fume (Qing et al. 2006). The above effects increased the density of the cement paste and improved bonding between the cement paste and aggregate which might have contributed to the strength development.

4.1.2 Effect of Nano-Silica on Setting Time of Concrete

Figure 4.5 shows the effect of NS on initial and final setting times of the slag concrete in comparison to the reference slag concrete and concrete with silica fume. Results show reduction of initial and final setting times of 95 min and 105 min, respectively, when 2% NS was used in comparison to the reference slag concrete. However, incorporation of 2% silica fume did not affect the initial and final setting time significantly compared to those of the reference slag concrete as expected. The reduction of the setting times of the NS concrete may be related to the finer particle size and higher surface area of the NS compared with those of silica fume which reduced the dormant period and increased cement hydration (will be discussed in the next section).

4.1.3 Rate of Heat Development of Pastes

4.1.3.1 Effect of Nano-Silica Dosage

Figure 4.6 shows effects of Type 1 NS dosage on the rate of heat development of high-volume slag cement pastes for the first 30 hours, and the inset shows the corresponding cumulative heat development. A curve of control cement paste with 100% Portland cement is included for comparison.

The calorimeter curves of the pastes with slag were very different from that of the control Portland cement paste without slag. Hydration of mixtures of Portland cement and slag is generally a two-stage reaction (ACI 233R 2003). During early hydration, predominant reaction is with alkali hydroxide corresponding to Portland cement

hydration (Peak 2). Subsequent reaction is predominantly with calcium hydroxide which represents slag hydration (Peak 3). Figure 4.6 clearly shows this two-stage reaction with slag hydration lag behind Portland cement hydration.

Results show that the length of dormant period was shortened with the incorporation of NS in the slag cement pastes. Peaks 2 and 3 shifted to left with the incorporation of NS in the pastes, suggesting accelerated Portland cement and slag hydration, respectively. The accelerated cement hydration might be due to increased nucleation sites provided by the fine NS particles. Whereas the accelerated slag reaction might be attributed to increased cement hydration and thus increased calcium hydroxide in solution at early age. There was no definite trend with respect to the dosage of NS due to the effect of retardation when higher dosage of superplasticizer was used in paste with increased NS dosage to achieve a given workability.

At 30 hrs cumulative heat generated in the cement paste increased with the increase in NS dosage which suggests increased cement hydration. This seems to be consistent with the slight increase in 1-day strength shown in Fig. 4.1. With the incorporation of 2% NS, the length of dormant period was reduced and cumulative heat development was increased with time compared with reference slag paste. These are consistent with the reduced setting times of concrete with NS observed in Fig. 4.5.

Maximum rate of heat development shown in Fig. 4.6 was reduced substantially with replacing 50% Portland cement by slag as expected. However, the length of the dormant period was reduced with the incorporation of slag. This was contrary to findings by other researchers (Roy and Idorn 1982; Hwang and Shen 1991), and might be due to the higher dosage of superplasticizer in the control mortar with 100% Portland cement than in the reference slag paste with 50% slag.

4.1.3.2 Effect of Particle Size of Nano-Silica

Effect of NS particle size on the heat development of cement pastes compared to that with silica fume is shown in Fig. 4.7. Peak 2 shifted to left and the length of the dormant period was shortened with the decrease in particle size and increase in specific surface area of silica inclusion. The shortened dormant period was probably due to the nucleation effect of finer particle size of silica inclusion. For given amount of NS or silica fume added, the smaller the particle size, the more number of particles are available to act as nucleation sites for precipitation of hydration products. However, the changes of the peak 2, and dormant period were not significant for the different pastes. This was again due to the fact that dosage of superplasticizer was increased with the reduction of NS size in order to achieve a given workability, and the SP used has retarding effect.

With decreasing particle size of silica inclusion, peak 3 of the heat development curve also shifted to the left. This may be explained by the increased amount of calcium hydroxide formed due to the acceleration of cement hydration by finer size of silica which substantially activated the hydration of slag at early age. However, the magnitude of the peak 3 was not significantly increased by finer NS.

Cumulative heat at 30 hrs increased with the reduction in particle size of silica inclusion. This seems to be consistent with the observation of 1-day strength shown in Fig. 4.2. Moreover, the reduced dormant period and increased rate of heat development were consistent with the setting time of the concretes discussed in the previous section.

4.1.3.3 Effect of Mixing and Dispersion Method

Effect of mixing and dispersing method of NS on the rate of heat development of cement paste is shown in Fig. 4.8, and the corresponding cumulative heat development is shown in the inset. For the paste with NS and water premixed with ultrasonic equipment, the dormant period was reduced and both Peaks 2 and 3 occurred before those of the reference slag paste. For the paste prepared by mechanical mixing, however, the length of dormant period increased, and Peaks 2 and 3 appeared later than those of the reference slag paste. The phenomena observed for the paste by mechanical mixing might be related partly to dispersion of NS and partly to the retarding effect due to higher dosage of superplasticizer used. The NS particles are very small and will agglomerate due to high surface interaction. The agglomeration of the NS might have resulted in decreased nucleation effect.

Cumulative heat generated within the first 24 hrs in the cement paste with ultrasonicated NS was higher than that with NS mechanically mixed with other ingredients which suggests that the cement hydration was increased by the sonication of NS and water. However, compressive strength of the mortars prepared by these two methods was not significantly different at the age of 1-day as mentioned in Section 4.1.1.3. The difference between the cement pastes and mortars may be attributed to two possible reasons. First, the lower density of the mortar prepared by the ultrasonication of nano-silica (SL11) might have resulted in lower compressive strength. This suggests that if the density of the two mixtures SL11 and SL11(M) was the same, the former might have higher strength than the latter, consistent with the heat and rate of cement and slag hydration. The lower density of the mortar SL11 might be due to inadequate consolidation. Second, sand in mortar mixtures might have broken down the NS agglomerates, thus the NS particles might have been

dispersed better in mortar than in cement paste. Thus the strength of SL11(M) would be less affected by the agglomeration of NS particles.

4.1.4 Porosity and Pore-Size Distribution of Pastes

4.1.4.1 Effect of Nano-Silica Dosage

Effect of NS on pore size distribution of the various high-volume slag cement pastes at 28 days is shown in Fig. 4.9. The corresponding porosimetry data of various pastes are shown in Table 4.3. According to Mindess et al. (2003) the pores in cement paste are divided into large capillary pores from (10 to 0.05 μm), medium capillary pores (0.05 to 0.01 μm) and gel pores (< 0.01 μm). The gel pores are the intrinsic porosity of C-S-H. The mercury intrusion porosimeter used in this study was able to detect pores with diameter down to 0.0038 μm.

The results show that large capillary porosity of slag paste was decreased, whereas medium capillary porosity was increased with increasing dosage of the NS. The total capillary porosity of the slag pastes, however, was not affected significantly by the incorporation of the NS. Threshold and critical pore diameters were not affected by the incorporation of 1% NS, but were decreased with the inclusion of 2% NS. The threshold pore diameter is a diameter at first inflection point of volume-diameter curve which indicates the minimum diameter of pores that are continuous through the paste (Winslow and Diamond 1970; Mindess et al. 2003). The critical pore diameter is a diameter at which the slope of the volume-diameter curve is the steepest and corresponds to the mean size of pore entryways that allows maximum percolation throughout the pore system (Mindess et al. 2003). Since permeability and penetration of harmful substances into the concrete are affected mainly by the large and medium capillary pores, the incorporation of 1% NS in the slag concrete may not affect such concrete properties significantly. Thus, 2% NS was used for concrete mixtures.

The gel pores of the slag pastes were increased with the increase in the NS dosage, thus the total porosity of the slag pastes was also increased.

Compared with control Portland cement paste, the pastes with high volumes of slag had lower large and total capillary porosities and critical pore diameter, but higher gel porosity. These will contribute to high resistance of slag concretes against penetration of harmful substances and good durability which has been reported in numerous cases (ACI 233R 2003).

Mechanism of reduced large capillary porosity in the slag pastes incorporating NS may be explained by physical and chemical effects attributed by NS (as described in section 4.1.1.5) similar to those with the use of silica fume in cement pastes as described in ACI Committee 234 Report (2006). Nano-silica made the pore structure of paste more homogeneous by decreasing large but increasing medium capillary porosities. The increased gel porosity might have resulted from the increased amount of C-S-H in the paste.

4.1.4.2 Effect of Particle Size of Nano-Silica

Figure 4.10 shows effect of particle size of NS on porosity and pore-size distribution of high-volume slag cement pastes at 28 days in comparison to that of the reference slag paste and paste with the same amount of silica fume. The porosimetry data of the slag pastes are summarized in Table 4.3. The results indicated that the incorporation of the NS with mean sizes of 7 and 12 nm and silica fume did not have significant effect on large, medium, and total capillary porosities and threshold and critical diameters of the slag pastes. However, the gel porosity was increased slightly with the decrease of mean particle sizes of the silica inclusions.

4.1.4.3 Effect of Mixing and Dispersion Method

Effects of mixing and dispersion methods of the NS on porosity and pore-size distribution of the slag cement pastes are shown in Fig. 4.11 with summary of capillary and gel porosity and threshold and critical pore diameters given in Table 4.3. The results indicate that using ultrasonic premixing of NS and water or mechanical mixing of all ingredients did not have significant effect on pore structure of the slag pastes. The result seems to be consistent with the 28 days mortar strength as shown in Fig. 4.3 and Table 4.1.

4.1.5 Resistance to Chloride-Ion Penetration of Concretes

Resistance of concretes to chloride-ion penetrability is shown in Fig 4.12. The concrete with 2% NS had lower charge passed in comparison to that with the same amount of silica fume. However, both of the concretes had charge passed below 1000 coulombs, which is considered “very low” according to ASTM C 1202 (2005). Both of them had lower charge passed in comparison to the reference slag concrete without NS or silica fume. According to Halamickova et al. (1995) the coefficient of chloride-ion diffusion varied linearly with the critical pore diameter. The reduced charge passed through the slag concrete incorporating 2% NS was consistent with the reduced critical and threshold pore diameters discussed in section 4.1.4.1.

4.2 High-Volume Fly Ash Pastes, Mortars, and Concretes

4.2.1 Compressive Strength Development

4.2.1.1 Effect of Nano-Silica Dosage on Strength Development of Mortars

Figure 4.13 shows compressive strength development of mortars containing fly ash with different dosages of Type 1 NS. The strength development of control mortar

containing 100% Portland cement and reference mortar with 50% fly ash are also shown for comparison. The compressive strength of mortars with 50% fly ash were lower than that of 100% Portland cement mortars from 1 to 91 days as expected because of slow pozzolanic activity of fly ash. However, the compressive strength of fly ash mortars increased with increasing NS amount, especially at early ages. For example, with inclusion of 2% NS, the compressive strength of the fly ash mortars increased by 80 and 33% at 1 and 3 days, respectively (Table 4.2).

4.2.1.2 Effect of Particle Size of Nano-Silica on Strength Development of Mortars

Figure 4.14 shows the effect of NS particle size on the compressive strength of fly ash mortars compared to that with silica fume. The compressive strengths of fly ash mortars were increased with the inclusion of NS or silica fume. Generally, fine NS inclusions increased the compressive strengths of fly ash mortars more significantly than the inclusion of silica fume. However, further reduction of NS size from 12 to 7 nm did not further increase the early strengths. The increased early strengths incorporating fine NS may be explained by high specific surface area which increased the rate of cement hydration and pozzolanic reaction. The results agreed with the findings by Qing et al. (Qing et al. 2007).

4.2.1.3 Effect of Mixing and Dispersion Method on Strength Development of Mortars

Effects of mixing and dispersion methods of NS on strength development of fly ash mortars are shown in Fig. 4.15. Compressive strengths of the mortar with ultrasonicated NS and water were higher than those of the mortar prepared by mechanical mixing. For example, with 1% NS inclusion, compressive strengths at 1 and 3 days of the former were 29 and 12% higher than those of the latter, respectively

(Table 4.2). The reduced compressive strength of the latter may be due to less dispersion of the NS by mechanical mixing.

4.2.1.4 Strength Development of Fly Ash Concrete with Nano-Silica

Figure 4.16 shows compressive strength development of the high-volume fly ash concrete with 2% NS in comparison to that of the reference fly ash concrete and concrete with the same amount of silica fume. With the incorporation of 2% NS or SF, the strengths of fly ash concrete were increased. However, the strength increase was more significant for the NS addition from 3 to 91 days as shown in Table 4.2. For example, strengths of concrete incorporating NS were increased by 30 and 25% at 3 and 7 days, respectively, whereas for those with SF addition the strengths were increased by 5 and 6%, respectively, in comparison to those of the reference fly ash concrete.

4.2.2 Effect of Nano-Silica on Setting Time of Concrete

Effects of 2% NS on the initial and final setting times of high-volume fly ash concrete in comparison to reference fly ash concrete and concrete with 2% silica fume are shown in Fig. 4.17. Significant reductions of the initial and final setting times were observed for the fly ash concrete with 2% NS. For example, the incorporation of 2% NS reduced the initial and final setting times of the fly ash concrete by 90 min and 100 min, respectively. However, the incorporation of 2% silica fume did not affect the setting times of the fly ash concretes significantly. The reduction of the setting times of the NS concrete may be related to the finer particle size and higher surface area of the NS compared with those of silica fume which reduced the dormant period and increased cement hydration (will be discussed in the next section).

4.2.3 Rate of Heat Development of Pastes

4.2.3.1 Effect of Nano-Silica Dosage

Figure 4.18 shows effects of NS dosage on the rate of heat development of high-volume fly ash cement pastes for the first 30 hours in comparison to that of reference fly ash paste. The inset shows the corresponding cumulative heat development of the pastes.

As discussed in literature review, Class F fly ash has limited reactivity at early age. Peaks 2 and 3 of the fly ash cement paste are thus likely due to C_3S hydration and conversion of ettringite to monosulfoaluminate, respectively, similar to hydration feature of typical Portland cement (Mindess et al. 2003).

It was observed that with the incorporation of NS, the length of dormant period of the fly ash cement pastes was shortened. Peaks 2 and 3 of the calorimeter curves shifted to left with the incorporation of NS in the fly ash pastes. Shortening of the dormant period and shifting of the peak 2 in the fly ash cement paste to left might be related to accelerated hydration of C_3S due to increased nucleation sites provided by the fine NS. Shifting of the peak 3 to left with the incorporation of the NS might be related to acceleration of C_3A reaction and earlier depletion of SO_3 in the system (Stein and Stevels 1964; Buil et al. 1984). Stein and Stevels (1964) studied NS-cement system and suggest that low calcium ion concentration in the solution at early stage enables more ettringite to precipitate far from the C_3A surface and retards the formation of ettringite coating on the C_3A during the first minute of hydration. This probably enabled accelerated reaction of the C_3A and shifted the Peak 3 to left in the pastes with NS or silica fume. However, no specific trend in heat development with respect to the dosage of NS was observed which might be related to the retardation effect of

higher dosage of superplasticizer used with increased NS dosage to achieve a given workability.

Cumulative heat at 24 hrs of the fly ash cement paste increased with the increasing dosage of NS. This seems to be consistent with the increase 1-day strength shown in Fig. 4.13. With the incorporation of 2% NS, length of the dormant period was shortened and cumulative heat development was increased with time compared with reference fly ash paste. These are consistent with the reduced setting time of fly ash concrete with NS shown in Fig. 4.17.

4.2.3.2 Effect of Particle Size of Nano-Silica

Figure 4.19 shows effect of NS or silica fume on the heat development of high-volume fly ash cement paste in comparison to reference fly ash cement paste. With the incorporation of 1% NS or silica fume, length of dormant period shortened, peak 2 shifted to left and magnitude of peak 2 increased. However, these effects were more significant in the paste incorporating NS than that of silica fume. These may be related to finer particle size of the NS than that of silica fume. For the same amount of NS or silica fume, more numbers of silica particles are available to act as nucleation sites for the precipitation of hydration products.

With the incorporation of the NS, peak 3 of the heat development curve also shifted to left and magnitude of peak 3 increased. However, silica fume did not affect the peak 3 of fly ash cement paste significantly. Shifting of peak in NS-cement paste might be related to low calcium ion concentration in the solution at early age and accelerated hydration of C_3A as discussed in previous section.

Up to 30 hrs, cumulative heat increased with time in the paste with the incorporation of NS or silica fume. However, the increase of the cumulative heat was more

significant for the paste with NS than that of silica fume. This seems to be consistent with the observed 1-day strength of mortar and setting time of concrete shown in Figs. 4.14 and 4.17, respectively.

4.2.3.3 Effect of Mixing and Dispersion Method

Effect of mixing and dispersion methods of NS on the heat development of high-volume fly ash cement paste is shown in Fig. 4.20. With the incorporation of the NS, length of dormant period was reduced, Peaks 2 and 3 shifted to left and increased in magnitude in both fly ash pastes prepared by ultrasonicated NS with water and mechanical mixing method compared with reference fly ash paste (FA0). However, shifting to left and increasing in magnitude of the peaks 2 and 3 were higher for the former than the latter. The reduced effect of the NS using mechanical mixing might be related to less homogeneous dispersion of the NS. The NS particles are very fine and will agglomerate due to high surface interaction. The agglomerated NS might reduce the number of nano-silica particles available as nucleation sites for precipitation of hydration products.

At 24 hrs cumulative heat generated in the cement paste prepared by ultrasonicated NS with water was higher compared to that prepared by mechanical mixing. This suggests that cement hydration was increased by NS dispersed using ultrasonic mixer. The observed cumulative heats at 24 hrs are consistent with the higher 1-day strength of mortar shown in Fig. 4.15.

4.2.4 Resistance to Chloride-Ion Penetration of Concretes

Figure 4.21 shows chloride-ion penetrability of the high-volume fly ash concretes with 2% NS or SF in comparison to that of the reference fly ash concrete. The results show that the total charge passed through the concrete with the NS or silica fume was

lower than that of the reference fly ash concrete. However, difference on the charge passed through the concretes with NS and SF were not significant.

4.3 Comparison between High-Volume Slag and Fly Ash Pastes, Mortars, and Concretes with Nano-Silica

4.3.1 Effect of Nano-Silica on Rate of Heat Development at Early Age

According to Figures 4.7 and 4.19 with the incorporation of 1% NS or silica fume, length of dormant period was reduced and peaks 2 and 3 shifted to left for both slag and fly ash cement pastes.

It was observed that calorimeter curves for the slag and fly ash cement pastes were very different. In the slag cement pastes, Peak 2 occurred at about 10 hrs and Peak 3 occurred at about 19 hrs (Fig. 4.7), which are likely to correspond to Portland cement hydration and slag hydration, respectively, according to ACI Committee 233 Report (2003). For the fly ash pastes, Peak 2 also occurred at about 10 hrs, whereas Peak 3 occurred before 15 hrs (Fig. 4.19). As Class F fly ash generally has limited reactivity at early stage, Peaks 2 and 3 of the fly ash cement pastes (Fig. 2) are likely to correspond to C_3S hydration and C_3A reaction (conversion of ettringite to monosulfoaluminate), respectively, similar to hydration feature observed in typical Portland cement paste (Mindess et al. 2003).

Shifting of the peaks 2 and 3 to the left in the calorimeter curves of the slag pastes (Fig. 4.7) corresponded to accelerated hydration of C_3S in Portland cement and accelerated slag reaction, respectively. In addition to the effect of fine particle size of the NS and silica fume, the accelerated slag hydration (Peak 3) might be attributed to

increased concentration of calcium hydroxide in solution due to increased C_3S reaction.

For the fly ash pastes (Fig. 4.19), shift of the peak 3 to left with the incorporation of the NS or silica fume might be related to acceleration of C_3A reaction and earlier depletion of SO_3 in the system (Stein and Stevels 1964; Buil et al. 1984).

It was observed that compared with reference paste, increase of cumulative heat of the paste with NS was higher for fly ash paste than that of slag paste at 24 hrs. At 24 hrs, increase of total cumulative heat of the fly ash paste was 20% whereas the slag paste was 6.5% in comparison to corresponding reference paste. These results are consistent with 1-day strength increases (will be discussed later) of fly ash and slag mortars shown in Table 4.4.

4.3.2 Compressive Strength Development

4.3.2.1 Effect of Nano-Silica on Strength Development Mortars

The effects of the NS on compressive strength developments of the slag and fly ash mortars compared to those with silica fume are shown in Fig.4.22. The compressive strengths of the slag and fly ash mortars were generally increased with the incorporation of 1% NS or silica fume in comparison to the reference mortars with 50% slag or fly ash. In terms of percentage of strength increase, the NS and silica fume seems to have similar effect on the slag and fly ash mortars at 3 and 7 days, but less effect on fly ash mortars at 28 and 91 days compared with the slag mortars. At the age of 1 day, 1% NS increased the strength of the fly ash mortar by 61% from 7.4 to 12 MPa, whereas 1% NS increased the strength of slag mortar by only 18%. The difference may be attributed to the characteristic difference between slag and fly ash. When mixed with water, slag can hydrate under the activation of cement and lime,

whereas Class F fly ash is pozzolanic material and has limited reactivity at early age. Thus, early strength of slag mortar is higher than that of fly ash mortar with given volume of the slag or fly ash (Table 4.4). Due to accelerated heat development shown in the calorimeter curve and possibility of acceleration of C_3S and C_3A reactions, the NS appears to have more effect on 1-day strength of the fly ash mortar than on the slag mortar.

4.3.2.2 Effect of Mixing and Dispersion Method on Strength Development of Mortars

The effect of mixing and dispersion methods of NS on compressive strength developments of the slag and fly ash mortars are shown in Fig. 4.3 and 4.15, respectively. No significant difference was observed in strength development of the slag mortars prepared by ultrasonicated NS with water and mechanical mixing method (Fig. 4.3). However, compressive strengths were higher for fly ash mortars prepared by the former than the latter (Fig. 4.15). This difference might be attributed to the lower density of the slag mortar SL11 than that of the mortar SL11 (M) discussed in Section 4.1.1.3. The results indicate that ultrasonication of NS with water is probably a better method to disperse the NS particles properly in comparison to the mechanical mixing.

4.3.2.3 Effect of Nano-Silica on Strength Development of Concretes

Figure 4.23 shows compressive strength development of slag and fly ash concretes with 2% NS or silica fume in comparison to that of the reference slag and fly ash concretes. The compressive strengths of the slag and fly ash concretes were increased with the incorporation of the NS in comparison to the corresponding reference concretes, especially at early ages. However, silica fume did not show significant effect on the strengths of the slag and fly ash concretes (Table 4.4).

Comparing the slag and fly ash concretes, the NS and silica fume did not show significant effect on the slag concrete at 28 and 91 days, whereas the NS increased fly ash concrete by 13% and 18% at 28 and 91 days, respectively, in comparison with the reference fly ash concrete. This might be attributed to the coarse aggregate used which appears to have reached its strength limit at about 70 MPa in the slag concretes.

In ordinary concrete, interface transition zone (ITZ) between the coarse aggregate and mortar matrix is usually the weakest link. As a result, cracks generally go through the ITZ around coarse aggregate particles. With reduction of w/c and use of fine mineral admixture such as NS or silica fume, the ITZ and mortar matrix can be improved substantially. Thus, the strength of the concrete can be improved. However, if the strengths of the ITZ and mortar matrix are improved to such extents that coarse aggregate becomes the weakest link in concrete, crack will go through the coarse aggregate particles. In such conditions, reducing w/c and using fine mineral mixtures will no longer increase the concrete strength because coarse aggregate is a limiting factor for the strength of concrete. Figure 4.24 shows that cracks went through coarse aggregate particles in the slag concrete with 2% NS after a compression test. This might explain why the strength of the slag concrete with 2% NS was not higher than that of the reference slag concrete and concrete with 2% silica fume.

Table 4.1 - Strength increases of the high-volume slag mortars and concretes with NS and silica fume compared with reference mortar and concrete with 50% slag

Mix ID	Mortar, % of strength increases compared with reference mortar with 50% slag (SL0)				
	1d	**3d**	**7d**	**28d**	**91d**
SL0.51	8	28	14	7	18
SL11	18	31	16	12	15
SL21	14	39	30	17	23
SL1SF	10	17	14	11	13
SL11	18	31	16	12	15
SL12	29	35	21	17	20
SL11	18	31	16	12	15
SL11(M)	15	31	17	10	14
Mix ID	Concrete, % of strength increases compared with reference concrete with 50% slag (CSL0)				
	1d	**3d**	**7d**	**28d**	**91d**
CSL2SF	--	4	5	1	1
CSL21	--	22	18	3	3

Table 4.2 – Strength increases of the high-volume fly ash mortars and concretes with NS and silica fume compared with reference mortar and concrete with 50% fly ash

Mix ID	Mortar, % of strength increases compared with reference mortar with 50% fly ash (FA0)				
	1d	**3d**	**7d**	**28d**	**91d**
FA0.51	41	14	10	0.3	1
FA11	61	25	17	7	4
FA21	80	33	18	8	12
FA1SF	13	15	10	4	1
FA11	61	25	17	7	4
FA12	65	25	17	7	5
FA11	61	25	17	7	4
FA11(M)	32	13	12	1	2
Mix ID	Concrete, % of strength increases compared with reference concrete with 50% fly ash (CFA0)				
	1d	**3d**	**7d**	**28d**	**91d**
CFA2SF	--	5	6	1	3
CFA21	--	30	25	13	18

Table 4.3 – Porosity of high-volume slag cement pastes with NS or silica fume compared with reference slag paste and control cement paste

Mix ID	Large capillary porosity, %	Medium capillary porosity, %	Total capillary porosity, %	Gel porosity, %	Total porosity, %	Threshold diameter, nm	Critical pore diameter, nm
Control	19.4	10.5	29.9	5.4	35.2	126	98
SL0	11.4	12.7	24.1	8.3	32.4	126	86
SL11	10.9	13.0	23.9	11.1	35.0	126	86
SL21	9.3	14.8	24.1	13.3	37.5	100	75
SL0	11.4	12.7	24.1	8.3	32.4	126	86
SL1SF	11.3	14.8	26.0	9.3	35.3	126	86
SL11	10.9	13.0	23.9	11.1	35.0	126	86
SL12	10.9	12.5	23.4	12.1	35.5	126	87
SL11	10.9	13.0	23.9	11.1	35.0	126	86
SL11(M)	11.2	13.3	24.5	10.5	35.0	126	86

Table 4.4 – Compressive strength increased for different type of nano-inclusions compared to reference slag or fly ash mortar/concrete

Mix ID	Type of specimens	Nano-inclusions		Increased compressive strength compared to reference slag or fly ash mortar/concrete (%)				
		Type	% of cementitious material	**1d**	**3d**	**7d**	**28d**	**91d**
SL11	Slag mortar	Type 1 NS	1	18	31	16	12	15
SL1SF		Silica fume		10	17	14	11	13
FA11	Fly ash mortar	Type 1 NS	1	61	25	17	7	4
FA1SF		Silica fume		13	15	10	4	1
CSL21	Slag concrete	Type 1 NS	2	--	22	18	3	3
CSL2SF		Silica fume		--	4	5	1	1
CFA21	Fly ash concrete	Type 1 NS	2	--	30	25	13	18
CFA2SF		Silica fume		--	5	6	1	3

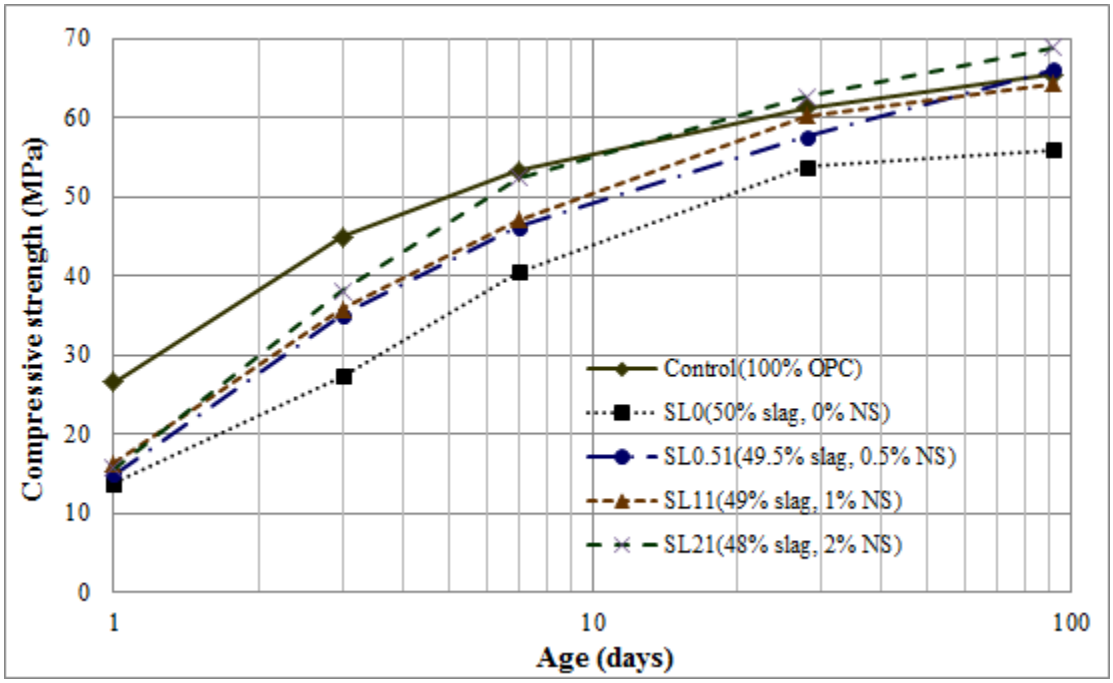

Figure 4.1 - Effect of the Type 1 nano-silica dosage of on the compressive strength development of slag mortars

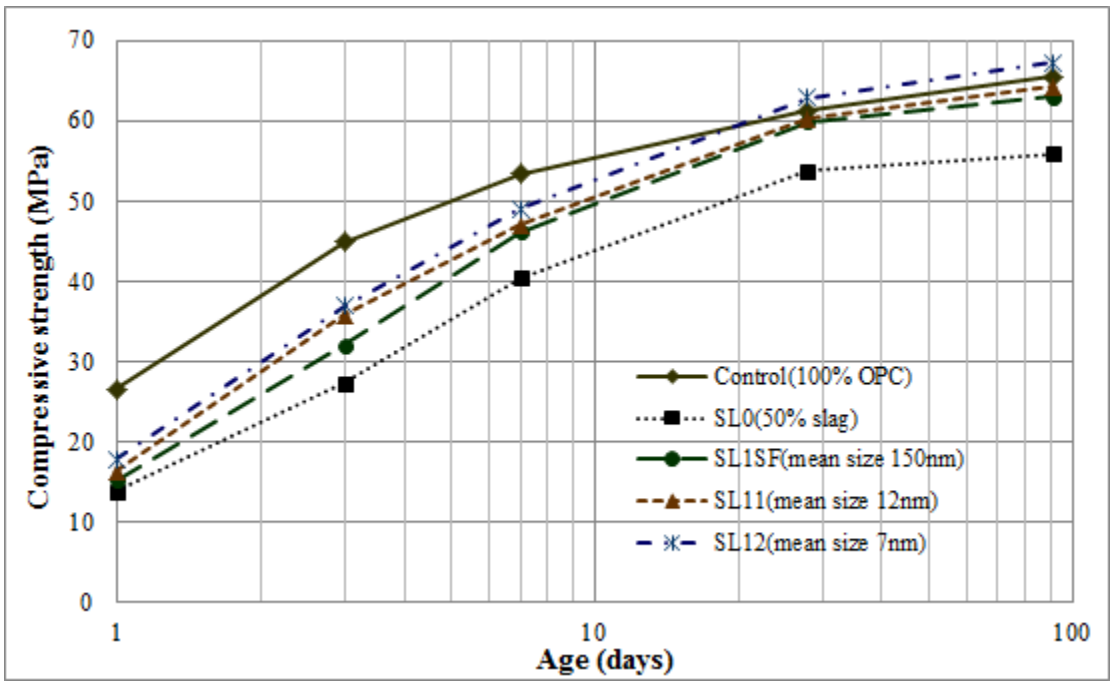

Figure 4.2 - Effect of the particle size of nano-silica on the compressive strength development of slag mortar (nano-silica and silica fume contents are 1% of cementitious materials by mass)

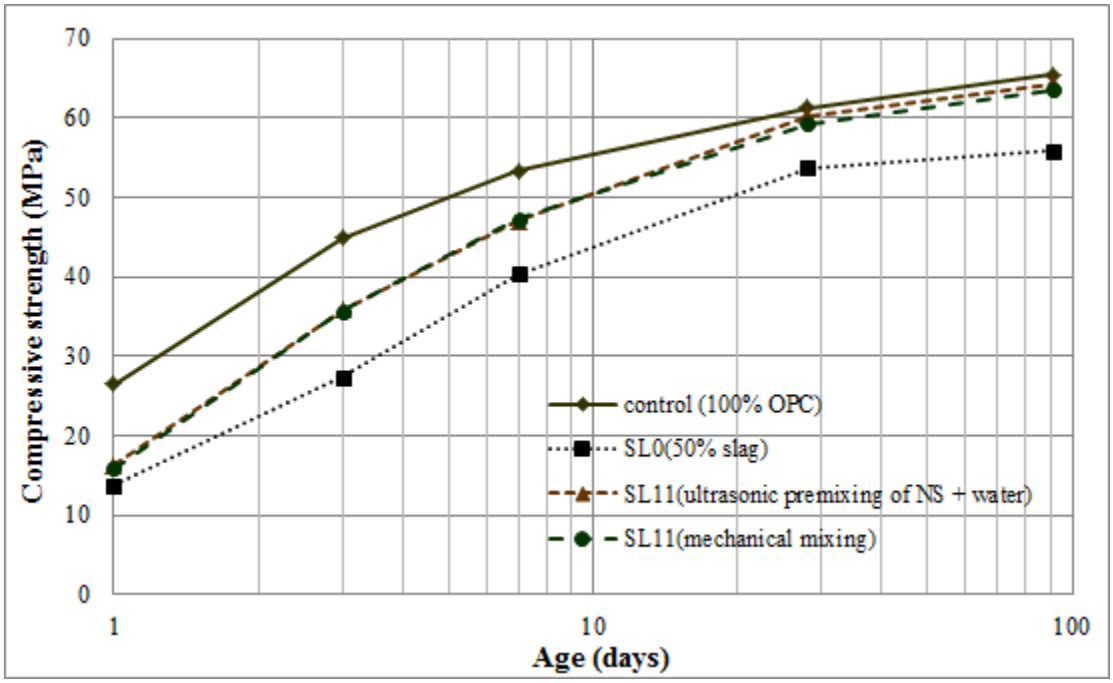

Figure 4.3 - Effect of mixing and dispersing method on the compressive strength development of slag mortar with 1% Type 1 nano-silica

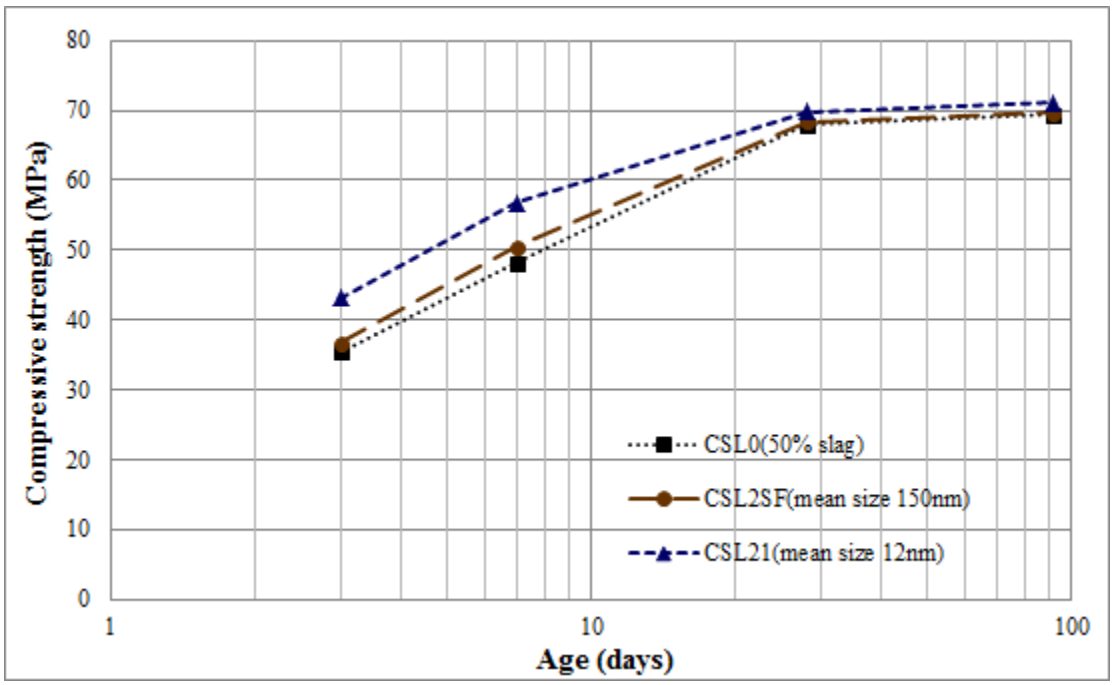

Figure 4.4 – Compressive strength development of slag concrete with 2% nano-silica in comparison to that of the reference concrete and concrete with the same amount of silica fume

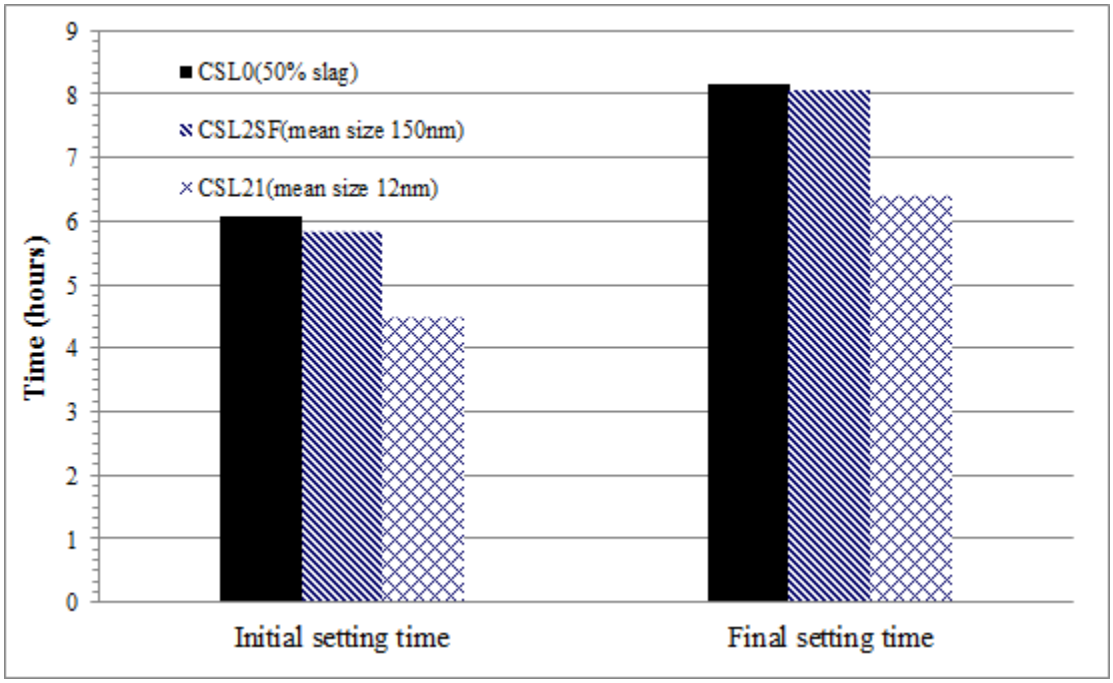

Figure 4.5 – Setting time of slag concrete with 2% nano-silica in comparison to that of the reference concrete and concrete with the same amount of silica fume

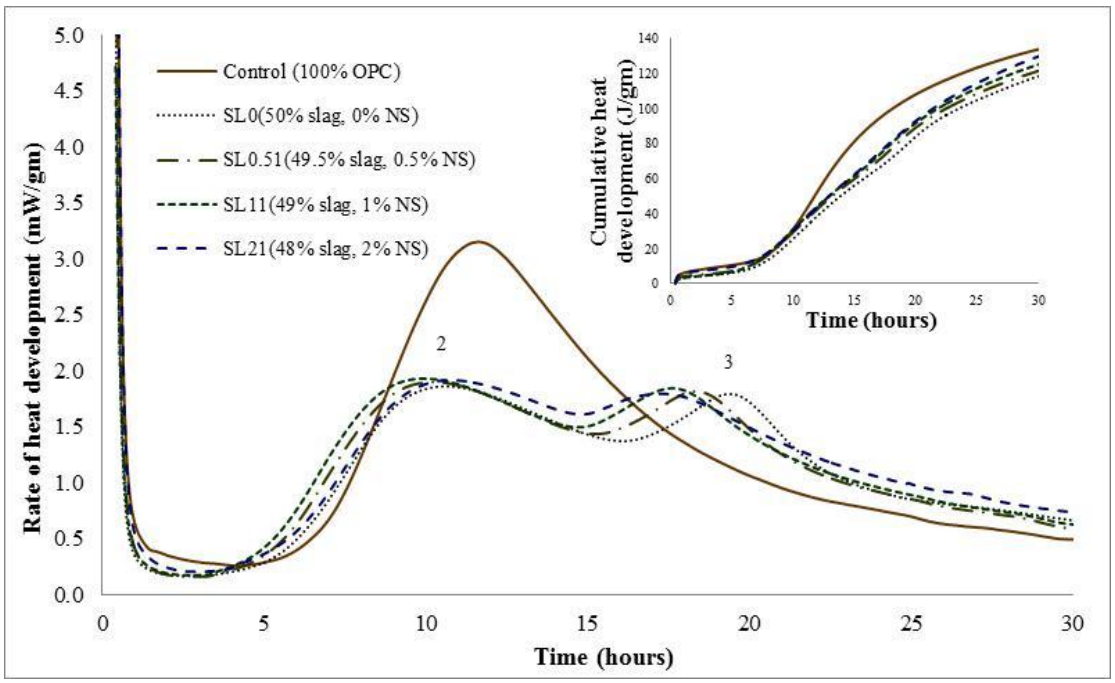

Figure 4.6 - Effect of the Type 1 nano-silica dosage of on the rate of heat development in slag cement pastes

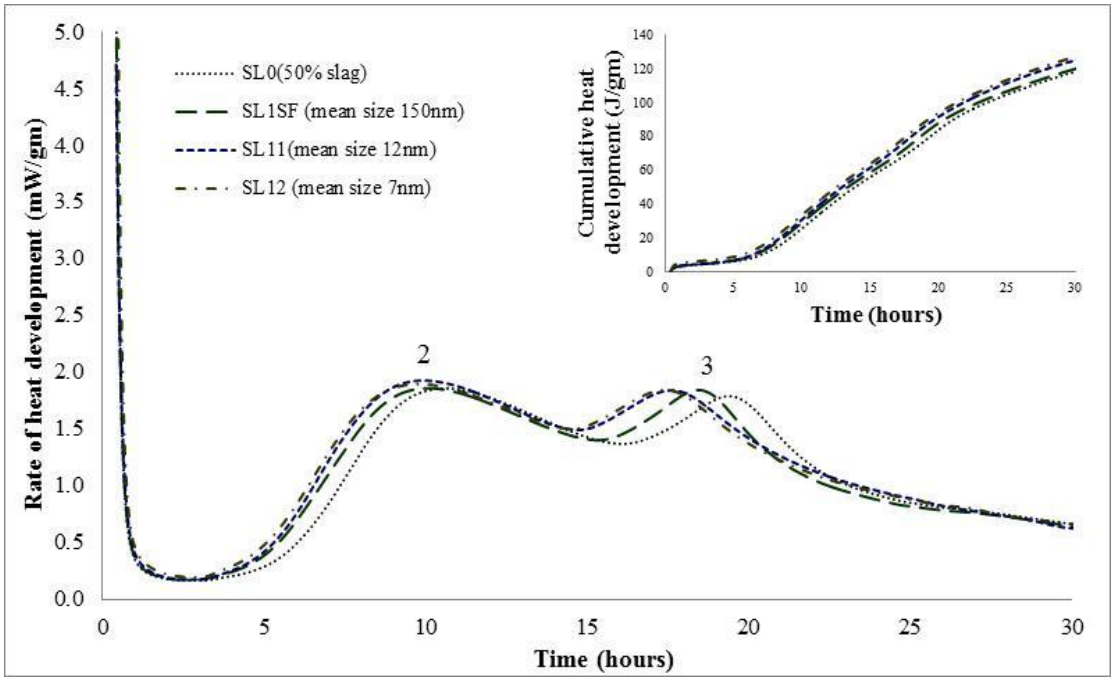

Figure 4.7 - Effect of the particle size of nano-silica on the rate of heat development in slag cement paste (nano-silica and silica fume contents are 1% of cementitious materials by mass)

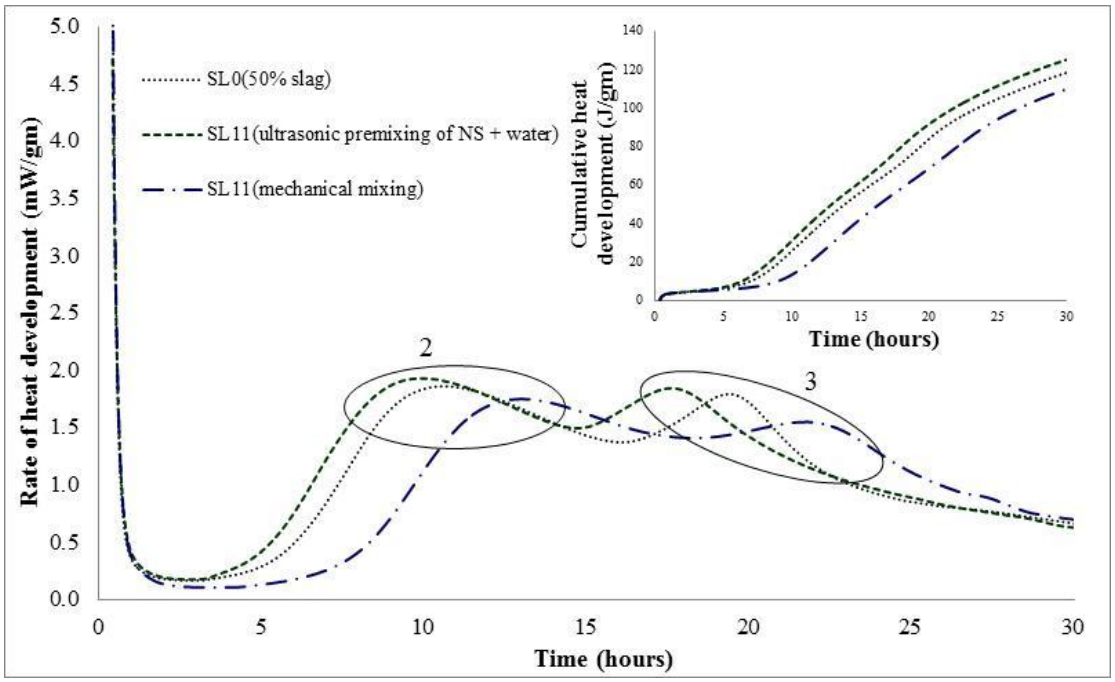

Figure 4.8 - Effect of mixing and dispersing method on the rate of heat development in slag cement paste with 1% Type 1 nano-silica

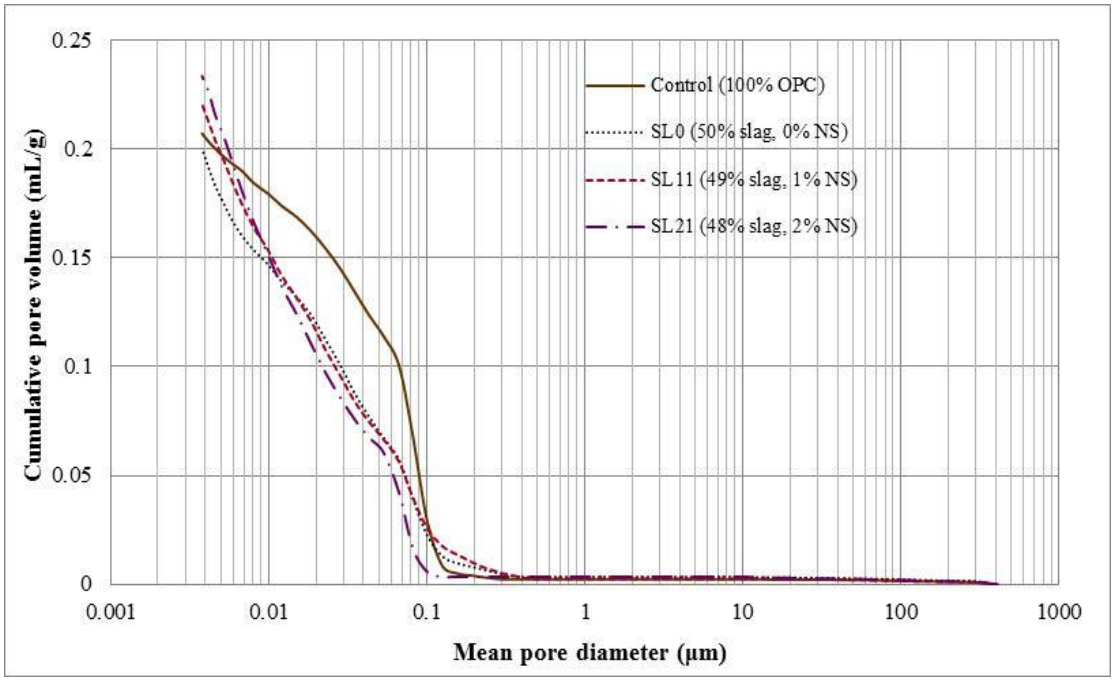

Figure 4.9 - Effect of the Type 1 nano-silica dosage of on the porosity and pore size distribution in slag cement pastes

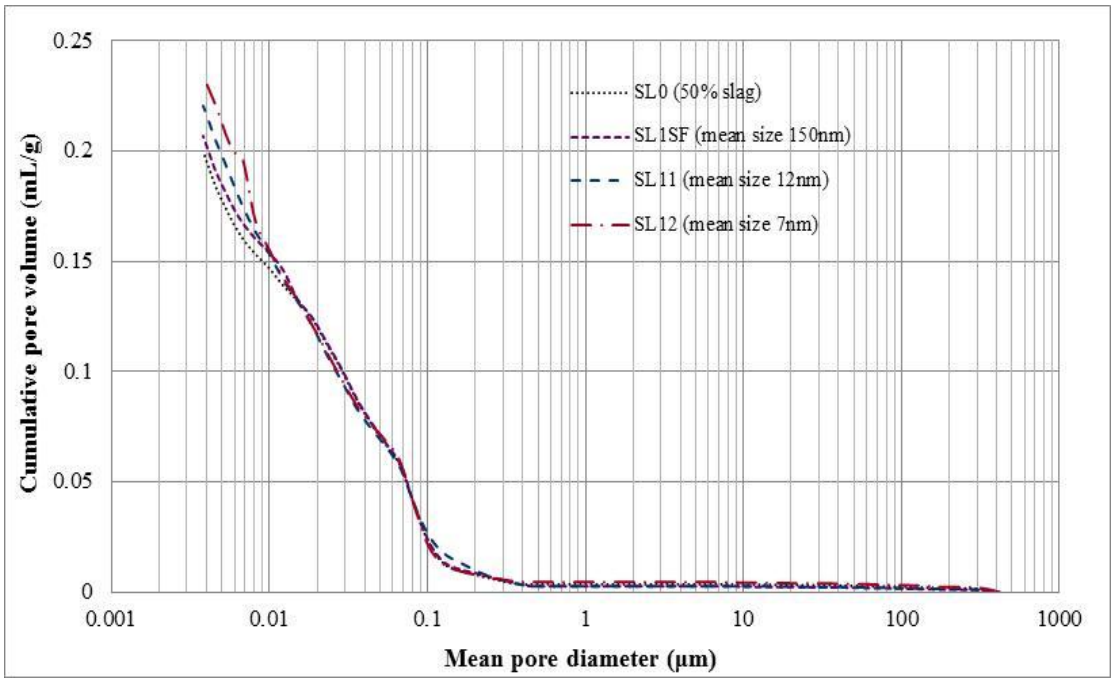

Figure 4.10 - Effect of the particle size of nano-silica on the porosity and pore size distribution in slag cement paste (nano-silica and silica fume contents are 1% of cementitious materials by mass)

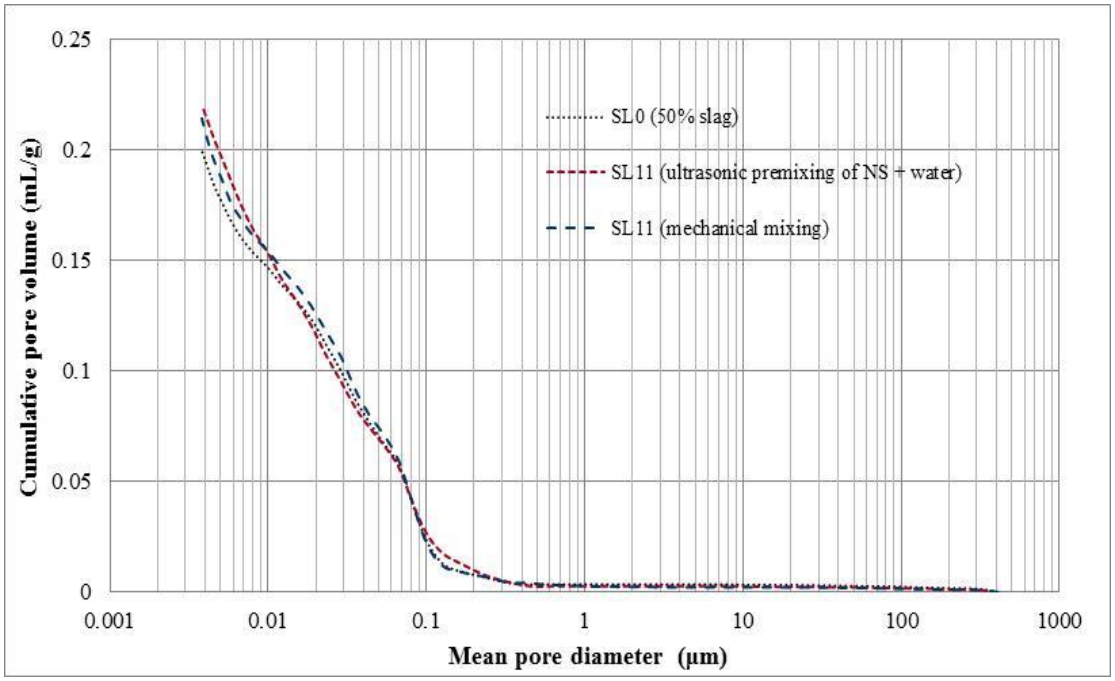

Figure 4.11 - Effect of mixing and dispersing method on the porosity and pore size distribution in slag cement paste with 1% Type 1 nano-silica

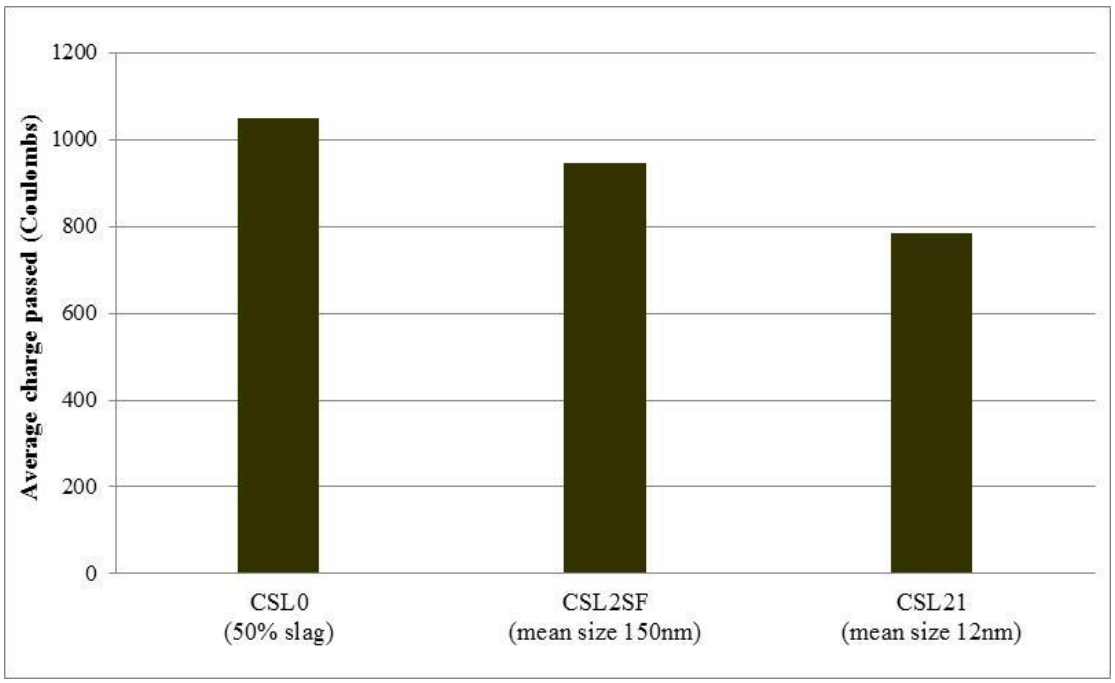

Figure 4.12 - Effect of the particle size of nano-silica on charge passed in slag concrete at 28 days (nano-silica and silica fume contents are 2% of cementitious materials by mass)

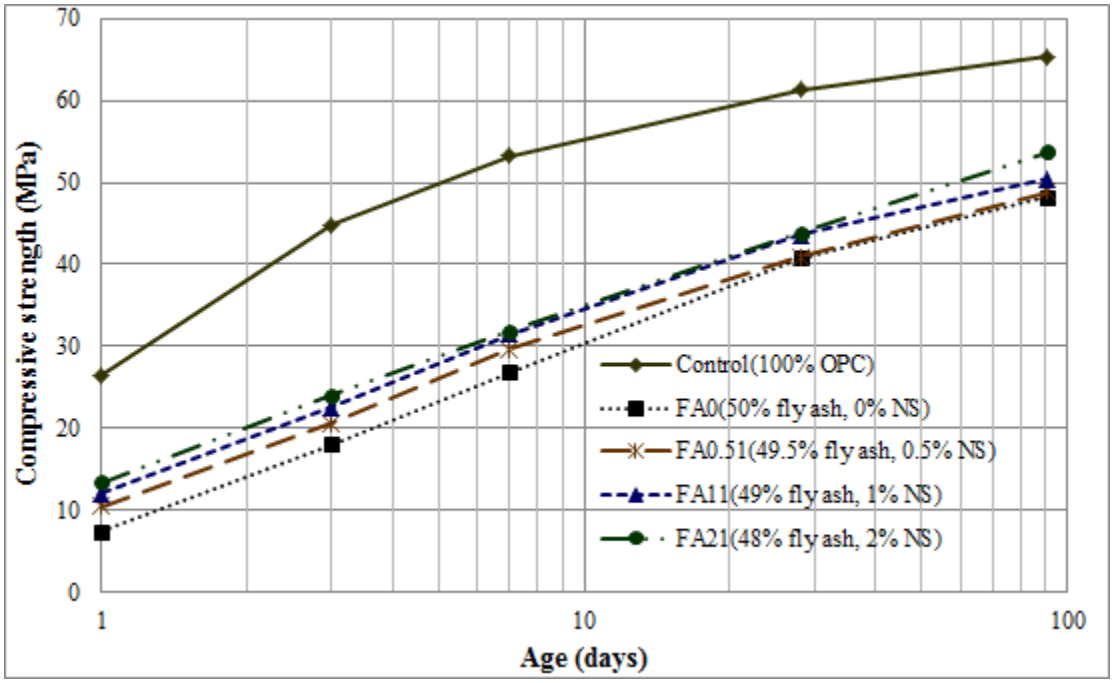

Figure 4.13 - Effect of the Type 1 nano-silica dosage of on the compressive strength development of fly ash mortars

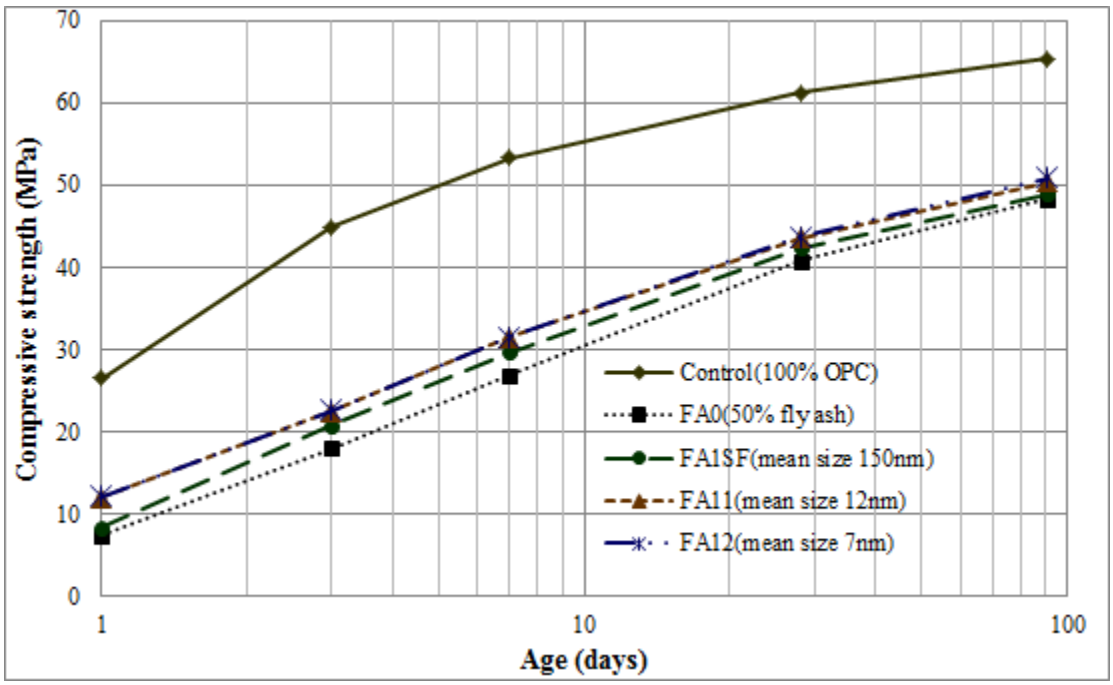

Figure 4.14 - Effect of the particle size of nano-silica on the compressive strength development of fly ash mortar (nano-silica and silica fume contents are 1% of cementitious materials by mass)

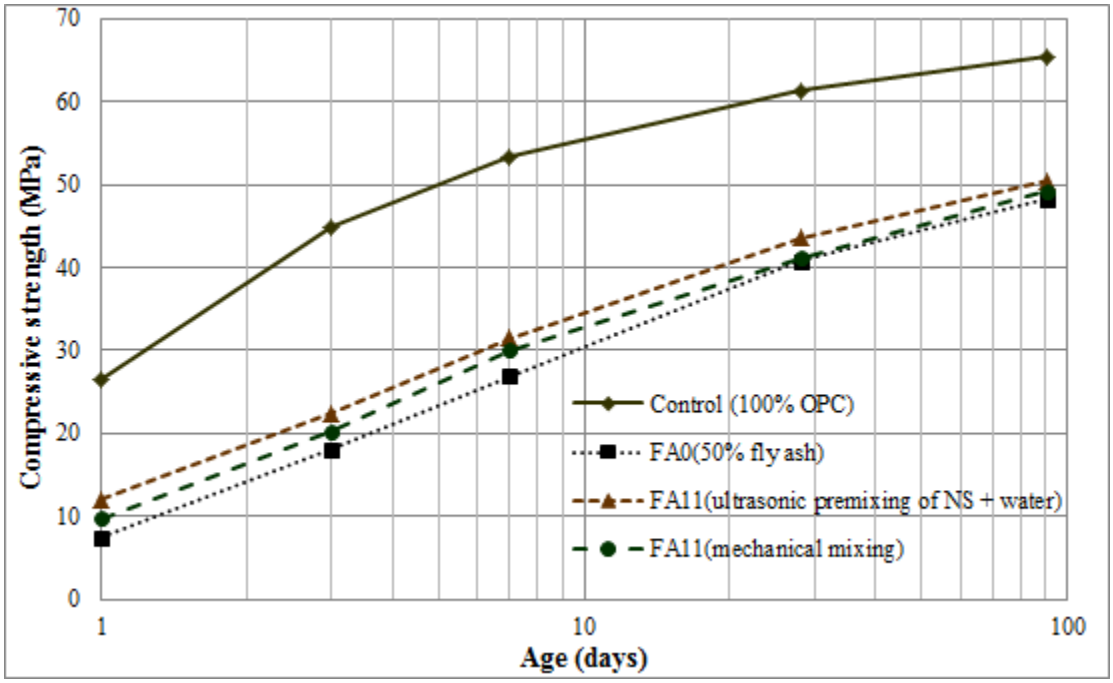

Figure 4.15 - Effect of mixing and dispersing method on the compressive strength development of fly ash mortar with 1% Type 1 nano-silica

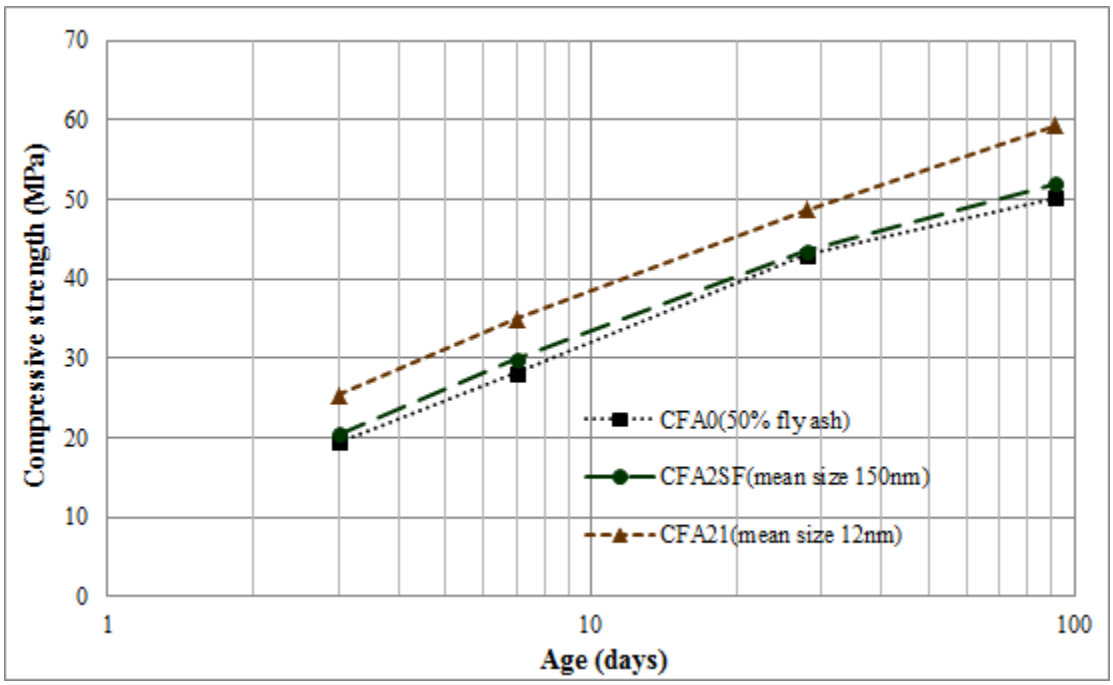

Figure 4.16 – Compressive strength development of fly ash concrete with 2% nano-silica in comparison to that of the reference concrete and concrete with the same amount of silica fume

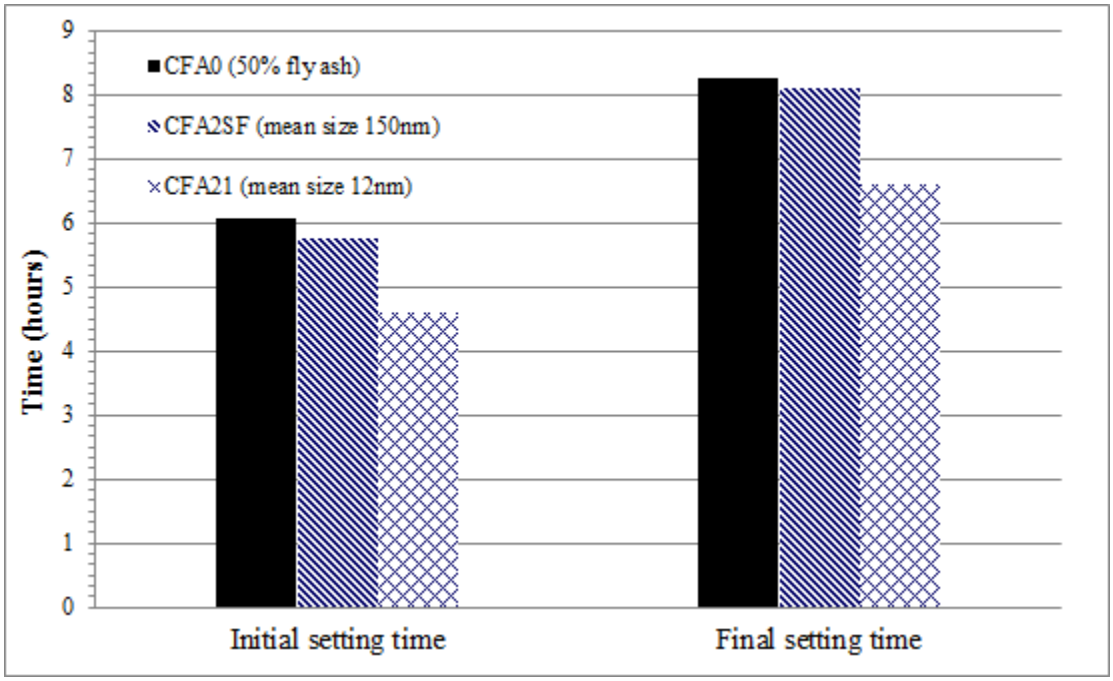

Figure 4.17 –Setting time of fly ash concrete with 2% nano-silica in comparison to that of the reference concrete and concrete with the same amount of silica fume

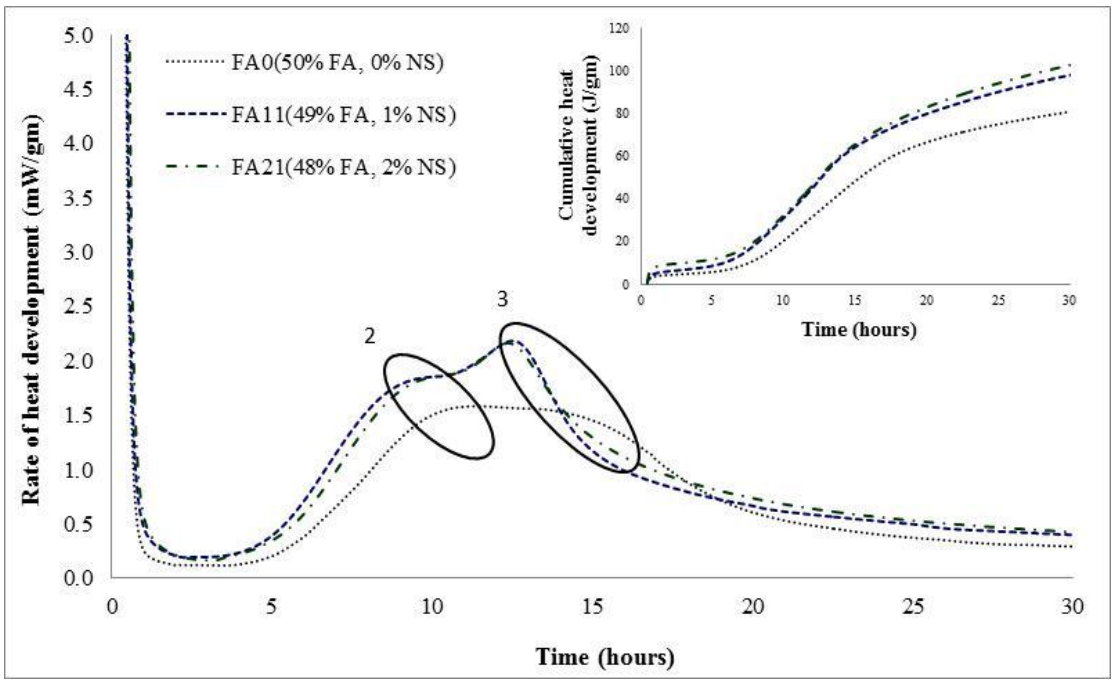

Figure 4.18 - Effect of the Type 1 nano-silica dosage of on the rate of heat development in fly ash cement pastes

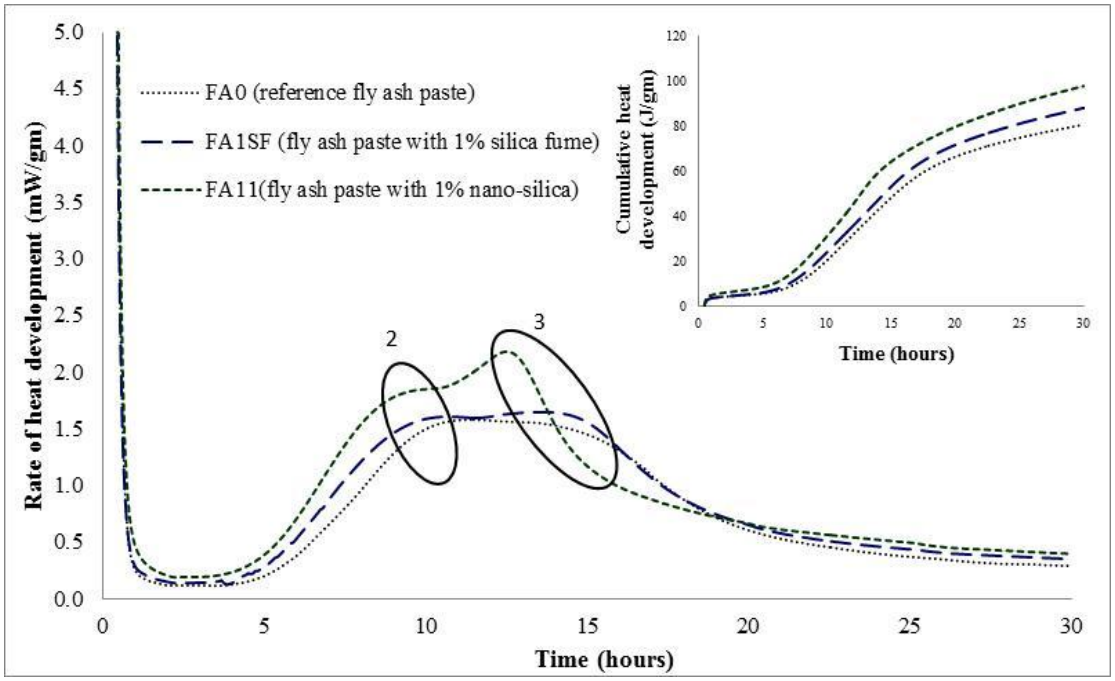

Figure 4.19 - Effect of the particle size of nano-silica on the rate of heat development in fly ash cement paste (nano-silica and silica fume contents are 1% of cementitious materials by mass)

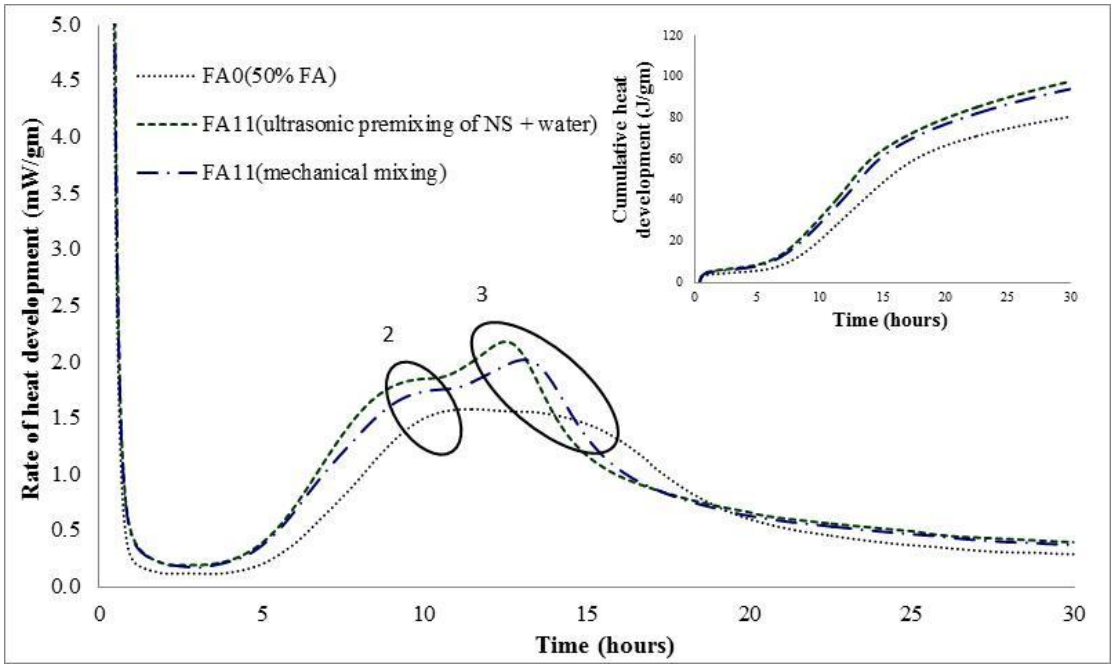

Figure 4.20 - Effect of mixing and dispersing method on the rate of heat development in fly ash cement paste with 1% Type 1 nano-silica

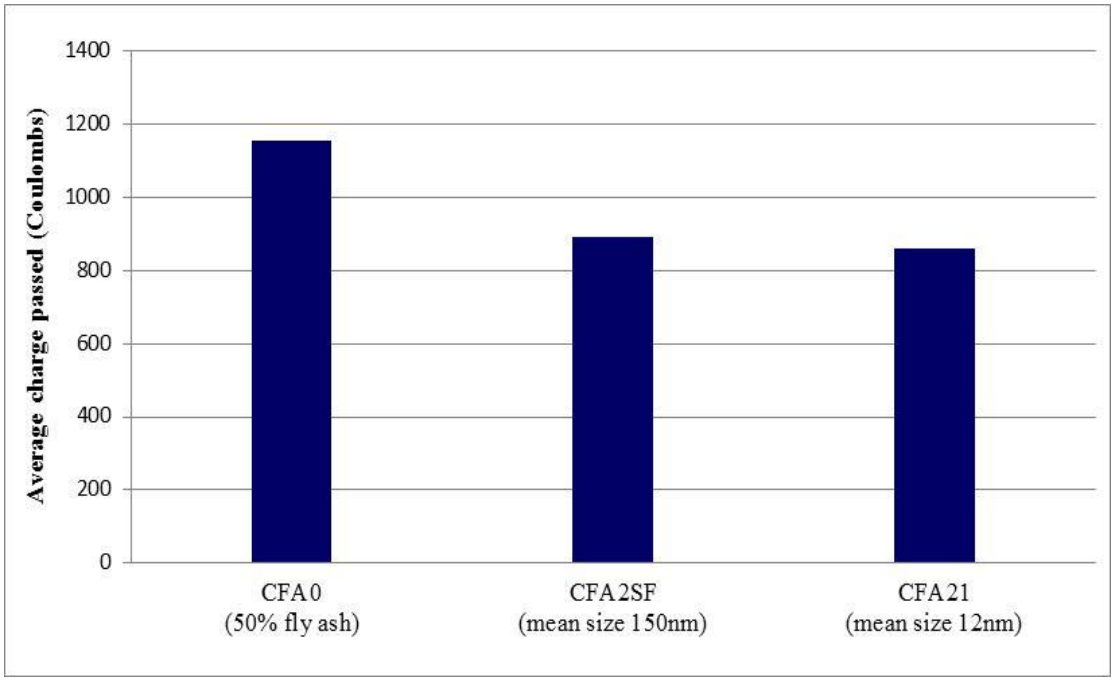

Figure 4.21 - Effect of the particle size of nano-silica on charge passed in fly ash concrete at 28 days (nano-silica and silica fume contents are 2% of cementitious materials by mass)

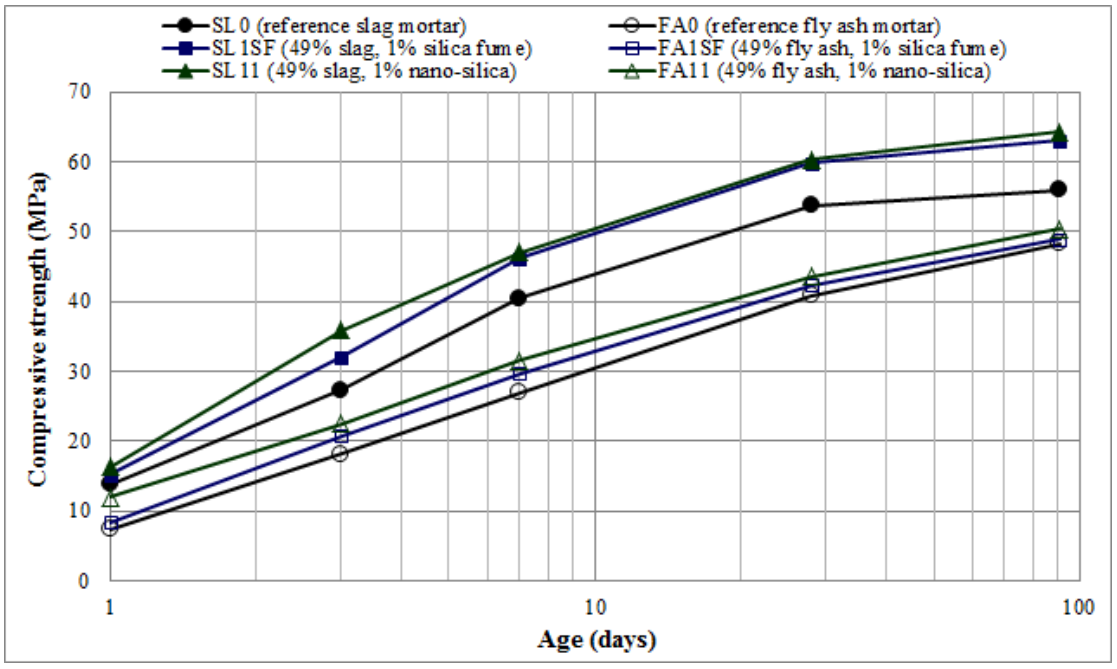

Figure 4.22 - Effect of the particle size of nano-silica on the compressive strength development of slag and fly ash mortars (nano-silica and silica fume contents are 1% of cementitious materials by mass)

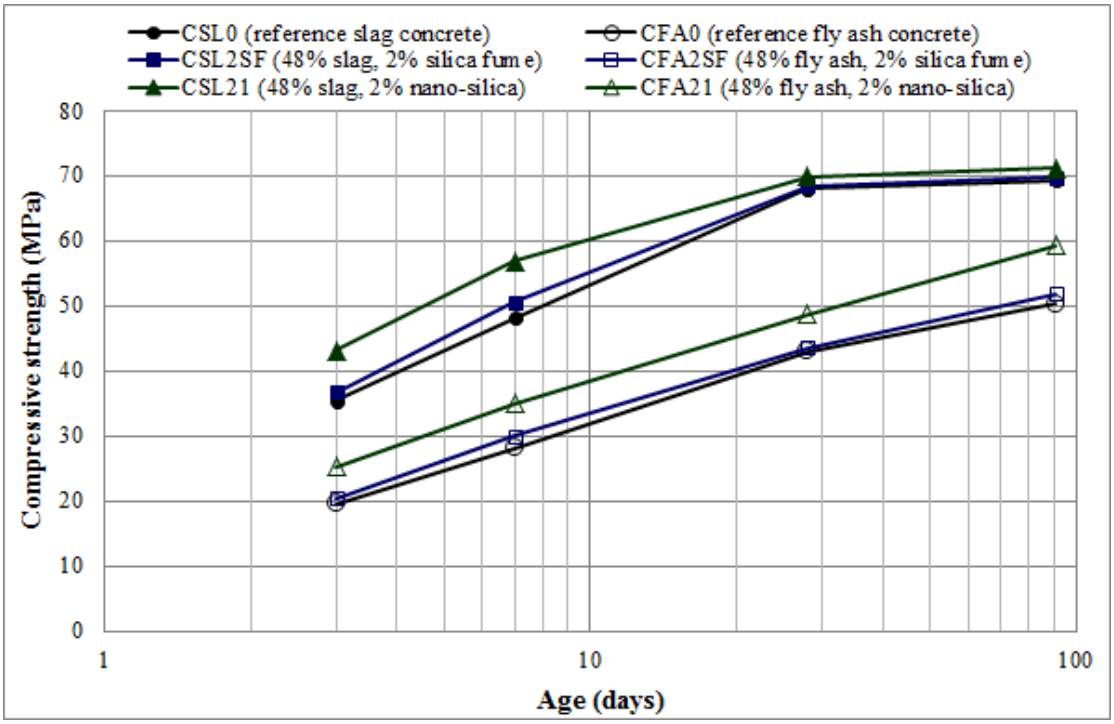

Figure 4.23 – Compressive strength development of slag or fly ash concrete with 2% nano-silica in comparison to those of the reference concrete and concrete with the same amount of silica fume

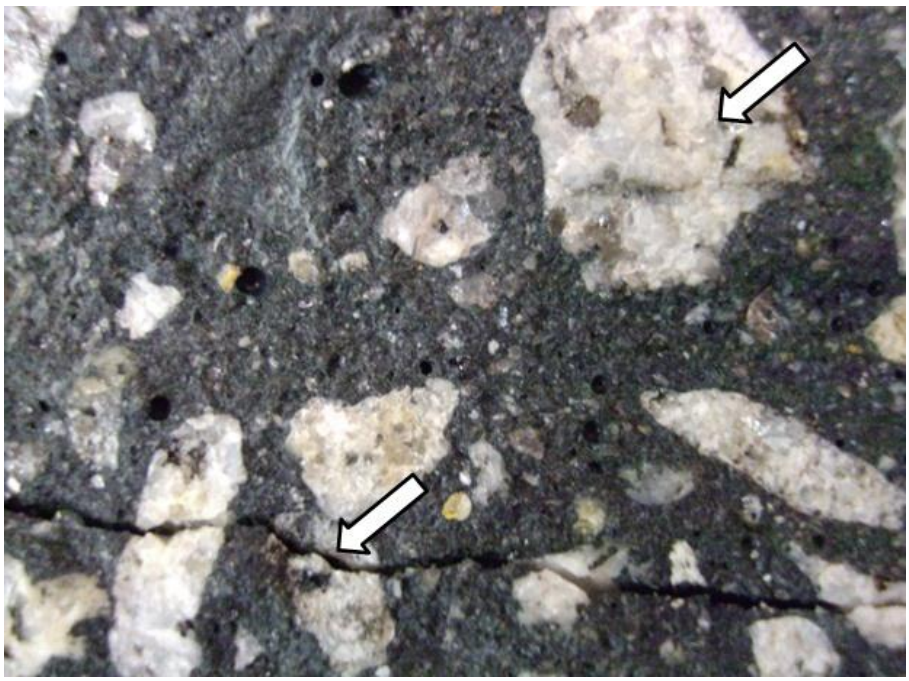

Figure 4.24 – Crack pattern in slag concrete with 2% NS under compressive load. Crack goes through coarse aggregate particles

Chapter 5 Conclusions and Recommendations

5.1 Conclusions

Based on the experimental results using nano-silica with average primary particle size of 7 and 12 nm in high-volume slag or fly ash pastes, mortars and concretes with w/cm of 0.45, following conclusions appear warranted:

1. Length of dormant period was shortened, and rate of cement and slag hydration were accelerated with the incorporation of the NS in the high-volume slag or fly ash cement pastes.

2. The incorporation of a small amount of NS (2% by mass of cementitious materials) reduced initial and final setting time by 95 and 105 min, and increased 3- and 7-day compressive strengths of high-volume slag concrete by 22 and 18%, respectively, in comparison to the reference concrete with 50% slag. Similar trends in reducing the setting times and in increasing the 3- and 7-day strengths were observed in high-volume fly ash concrete incorporating NS compared to reference fly ash concrete.

3. At 28 and 91 days, nano-silica increased strength of fly ash concrete in comparison to the reference fly ash concrete. However, the NS did not show effect on the slag concrete. This might be related to the coarse aggregate used which appears to have reached its strength limit at about 70 MPa in the slag concretes.

4. Compressive strength of the slag or fly ash mortars were increased with the increase in NS dosages from 0.5 to 2.0% by mass of cementitious material at various ages up to 91 days.

5. The strengths of the slag or fly ash mortars were generally increased with the decrease in the particles size of silica inclusions at early age.

6. Ultra-sonication of nano-silica with water is probably a better method for proper dispersion of nano-silica than mechanical mixing method.

7. With the increasing dosage of NS, large capillary porosity was decreased, whereas medium capillary porosity was increased in the slag cement pastes at 28 days. However, the total capillary porosity of the slag pastes was not affected significantly by the incorporation of the NS. Threshold and critical pore diameters in slag cement pastes were not affected by the incorporation of 1% NS, but were decreased with the inclusion of 2% NS. No significant difference in large, medium, and total capillary porosities and threshold and critical diameters was observed among the slag pastes with different particle sizes of silica, and among those prepared by ultrasonicated NS with water and by mechanical mixing method.

8. The 28-day charge passed through the slag or fly ash concrete with NS was lower than that of corresponding reference concrete.

9. Nano-silica with mean particle sizes of 7 and 12 nm appears to be more effective in increasing the rate of cement hydration and reaction compared with silica fume. The NS reduced the setting times and increased early strengths of the high-volume slag or fly ash concrete. However, the setting times and early strength of the high-volume slag or fly ash concrete were not affected by the silica fume significantly. The charge

passed through the high-volume slag or fly ash concrete with NS was similar to that of corresponding concrete with silica fume.

5.2 Recommendations

Further studies are recommended in the following areas:

1. Rate of pozzolanic reaction of NS in slag or fly ash concrete was not determined in current study. Further study for determining the pozzolanic reaction of NS is recommended.

2. In-depth investigation and understanding of effect of NS on microstructure of slag or fly ash cement paste and concrete are important in order to design concrete mixtures with good mechanical properties and durability.

3. In this study, effect of the NS on compressive strength of slag or fly ash concrete at early age was investigated. Effect of the NS on other mechanical properties of concrete should be investigated as well, especially autogeneous shrinkage, drying shrinkage, and creep as the NS increased gel pores in the cement pastes.

4. Further studies could include range of volume of GGBFS and fly ash and other w/cm ratios to cover those used in construction.

References

ACI 116R (2000). Cement and concrete terminology; American Concrete Institute, USA.

ACI 233R (2003). Slag cement in concrete and mortar; American Concrete Institute, USA.

ACI 234R (2006). Guide for the use of silica fume in concrete; American Concrete Institute, USA.

ASTM C 33 (2003). Standard specification for concrete aggregates; American Society for Testing and Materials, West Conshohocken, PA, USA.

ASTM C 109/C 109M (2002). Standard test method for compressive strength of hydraulic cement mortars (using 2-in or [50-mm] cube specimens); American Society for Testing and Materials, West Conshohocken, PA, USA.

ASTM C 136 (2006). Standard test method for sieve analysis of fine and coarse aggregates; American Society for Testing and Materials, West Conshohocken, PA, USA.

ASTM C 150 (2004). Standard specification for Portland cement; American Society for Testing and Materials, West Conshohocken, PA, USA.

ASTM C 403/C 403M (2008). Standard test method for time of setting of concrete mixtures by penetration resistance; American Society for Testing and Materials, West Conshohocken, PA, USA.

ASTM C 618 (2008a). Standard specification for coal fly ash and raw or dalcined natural pozzolan for use in concrete; American Society for Testing and Materials, West Conshohocken, PA, USA.

ASTM C 989 (2006). Standard specification for ground granulated blast-furnace slag for use in concrete and mortars; American Society for Testing and Materials, West Conshohocken, PA, USA.

ASTM C 1202 (2005). Standard test method for electrical indication of concrete's ability to resist chloride ion penetration; American Society for Testing and Materials, West Conshohocken, PA, USA.

ASTM C 1437 (2001). Standard test method for flow of hydraulic cement mortar; American Society for Testing and Materials, West Conshohocken, PA, USA.

ASTM C 1679 (2008). Practice for measuring hydration kinetics of hydraulic cementitious mixtures using isothermal calorimetry; American Society for Testing and Materials, West Conshohocken, PA, USA.

Baert, G., Poppe, A.-M. and De Belie, N. (2008). Strength and durability of high-volume fly ash concrete. Structural Concrete 9(2): 101-108.

Belkowitz, J. and Armentrout, D. L. (2009). The investigation of nano silica in the cement hydration process. ACI Special Publication 267(8): 87-100.

Bentur, A., Goldman, A. and Cohen, M. D. (1988). The contribution of the transition zone to the strength of high quality silica fume concretes. In: Proceedings of the symposium on bonding in cementitious composites, Pittsburgh, Pa., Materials research society.

Bilodeau, A. and Malhotra, V. M. (2000). High-volume fly ash system: concrete solution for sustainable development. ACI Materials Journal 97(1): 41-48.

Brooks, J. J. and Al-Kaisi, A. F. (1990). Early strength development of Portland and slag cement concretes cured at elevated temperatures. ACI Materials Journal 87(5): 503-507.

BS EN 12390-3 (2002). Testing hardened concrete - part 3: compressive strength of test specimens; British Standards Institution, London, UK.

Buil, M., Paillère, A. M. and Roussel, B. (1984). High strength mortars containing condensed silica fume. Cement and Concrete Research 14(5): 693-704.

Campillo, I., Dolado, J. S. and Porro, A. (2007). High-performance nanoestructuerd matrials for construction. In: Hester, R. E. and Harrison, R. M., editors. Nanotechnology: consequences for human health and the environment. Thomas Graham House, Cambridge CB4 0WF, UK: Royal Society of Chemistry: 215-226.

Carette, G. G. and Malhotra, V. M. (1983). Early-age strength development of concrete incorporating fly ash and condensed silica fume. ACI Special Publication 79(41): 765-784.

Chandra, S. and Berntsson, L. (1996). Use of silica fume in concrete. In: Chandra, S., editor. Waste Materials Used in Concrete Manufacturing. Westwood, NJ: William Andrew Publishing: 554-623.

Detwiler, R. J. and Mehta, P. K. (1989). Chemical and physical effects of silica fume on the mechanical behavior of concrete. ACI Materials Journal 86(6): 609-614.

Elahi, A., Basheer, P. A. M., Nanukuttan, S. V., et al. (2010). Mechanical and durability properties of high performance concretes containing supplementary cementitious materials. Construction and Building Materials 24(3): 292-299.

Erdem, T. K. and Kirca, Ö. (2008). Use of binary and ternary blends in high strength concrete. Construction and Building Materials 22(7): 1477-1483.

Fidjestøl, P. and Lewis, R. (2003). Microsilica as an Addition. In: Hewlett, P. C., editor. Lea's Chemistry of Cement and Concrete (Fourth Edition). Oxford: Butterworth-Heinemann: 679-712.

Ganesh Babu, K. and Siva Nageswara Rao, G. (1994). Early strength behaviour of fly ash concretes. Cement and Concrete Research 24(2): 277-284.

Godman, A. and Bentur, A. (1989). Bond effects in high-strength silica fume concretes. ACI Materials Journal 86(5): 440-449.

Goldman, A. and Bentur, A. (1994). Properties of cementitious systems containing silica fume or nonreactive microfillers. Advanced Cement Based Materials 1(5): 209-215.

Grutzeck, M., Roy, D. M. and Wolfe-Confer, D. (1982). Proc. IVth ICMA Conf.: 193.

Gutteridge, W. A. and Dalziel, J. A. (1990). Filler cement. The effect of the secondary component on the hydration of Portland cement. Part 2. Fine hydraulic binders. Cement and Concrete Research 20(6): 853-861.

Halamickova, P., Detwiler, R. J., Bentz, D. P., et al. (1995). Water permeability and chloride ion diffusion in portland cement mortars: Relationship to sand content and critical pore diameter. Cement and Concrete Research 25(4): 790-802.

Hielscher ultrasound technology. Retrieved August 15, 2010, from http://www.hielscher.com/ultrasonics/index.htm.

Hogan, F. J. and Meusel, J. W. (1981). Evaluation for durability and strength development of a ground granulated blast-furnace slag. Cement, Concrete and Aggregates 3(1): 40-52.

Holland, T. C. (2005). Silica fume user's manual. 38860 Sierra lane, Lovettsville, VA 22180, Silica fume association.

Huang, C.-y. and Feldman, R. F. (1985). Influence of silica fume on the microstructural development in cement mortars. Cement and Concrete Research 15(2): 285-294.

Hwang, C.-L. and Shen, D.-H. (1991). The effects of blast-furnace slag and fly ash on the hydration of portland cement. Cement and Concrete Research 21(4): 410-425.

Jayapalan, A. R., Lee, B. Y. and Kurtis, K. E. (2009). Effect of nano-sized titanium dioxide on early age hydration of Portland cement. Nanotechnology in Construction 3: Springer Berlin Heidelberg: 267-273.

Jiang, L. and Guan, Y. (1999). Pore structure and its effect on strength of high-volume fly ash paste. Cement and Concrete Research 29(4): 631-633.

Jo, B.-W., Kim, C.-H., Tae, G.-h., et al. (2007). Characteristics of cement mortar with nano-SiO_2 particles. Construction and Building Materials 21(6): 1351-1355.

Kadri, E.-H. and Duval, R. (2009). Hydration heat kinetics of concrete with silica fume. Construction and Building Materials 23(11): 3388-3392.

Langan, B. W., Weng, K. and Ward, M. A. (2002). Effect of silica fume and fly ash on heat of hydration of Portland cement. Cement and Concrete Research 32(7): 1045-1051.

Langley, W. S., Carette, G. G. and Malhotra, V. M. (1989). Structural concrete incorporating high volumes of ASTM class F fly ash. ACI Materials Journal 86(5): 507-514.

Li, G. (2004). Properties of high-volume fly ash concrete incorporating nano-SiO_2. Cement and Concrete Research 34(6): 1043-1049.

Li, G. and Zhao, X. (2003). Properties of concrete incorporating fly ash and ground granulated blast-furnace slag. Cement and Concrete Composites 25(3): 293-299.

Li, H., Xiao, H.-G., Yuan, J., et al. (2004). Microstructure of cement mortar with nano-particles. Composites Part B: Engineering 35(2): 185-189.

Ma, W., Sample, D., Martin, R., et al. (1994). Calorimetric study of cement blends containing fly ash, silica fume, and slag at elevated temperatures. Cement, Concrete and Aggregates 16(2): 93-99.

Malhotra, V. M., Carette, G. G. and Aitcin, P. C. (1985). Mechanical properties of portland cement concrete incorporating blast-furnace slag and condensed silica fume. In: Proceedings, ACI/RILEM symposium on technology of concrete when pozzolans, slags and chemical admixtures are used, Monterrey, Mexico.

Masuo Hosokawa, Kiyoshi Nogi, Naito, M., et al., Eds. (2007). Nanoparticle Technology Handbook, ElsevierLinacre House, Jordan Hill, Oxford OX2 8DP, UK.

Mehta, P. K. (1985). Influence of fly ash characteristics on the strength of portland-fly ash mixtures. Cement and Concrete Research 15(4): 669-674.

Mehta, P. K. (1991). Concrete in the marine environment, Elsevier Science Publishers Ltd.

Mehta, P. K. and Gjørv, O. E. (1982). Properties of portland cement concrete containing fly ash and condensed silica-fume. Cement and Concrete Research 12(5): 587-595.

Metaxa, Z. S., Konsta-Gdoutos, M. S. and Shah, S. P. (2009). Carbon nanotubes reinforced concrete. ACI Special Publication 267(2): 11-20.

Mindess, S. (1988). Bonding in cementitious composites. In: Bonding in cementitious composites symposium, 2-4 Dec. 1987, Pittsburgh, PA, USA, Mater. Res. Soc.

Mindess, S., Young, J. F. and Darwin, D. (2003). Concrete. Upper Saddle River, NJ, Prentice Hall.

Mounanga, P., Khokhar, M., El Hachem, R., et al. (2010). Improvement of the early-age reactivity of fly ash and blast furnace slag cementitious systems using limestone filler. Materials and Structures: 1-17.

Papadakis, V. G. (1999). Effect of fly ash on Portland cement systems: Part I. Low-calcium fly ash. Cement and Concrete Research 29(11): 1727-1736.

Poon, C. S., Lam, L. and Wong, Y. L. (1999). Effects of fly ash and silica fume on interfacial porosity of concrete. Journal of Materials in Civil Engineering 11(3): 197-205.

Poon, C. S., Lam, L. and Wong, Y. L. (2000). A study on high strength concrete prepared with large volumes of low calcium fly ash. Cement and Concrete Research 30(3): 447-455.

Popovics, S. (1993). Portland cement-fly ash-silica fume systems in concrete. Advanced Cement Based Materials 1(2): 83-91.

Qing, Y., Zenan, Z., Deyu, K., et al. (2007). Influence of nano-SiO_2 addition on properties of hardened cement paste as compared with silica fume. Construction and Building Materials 21(3): 539-545.

Qing, Y., Zenan, Z., Li, S., et al. (2006). A comparative study on the pozzolanic activity between nano-SiO_2 and silica fume. Journal of Wuhan University of Technology--Materials Science Edition 21(3): 153-157.

Ramachandran, V. S. and Beaudoin, J. J. (2001). Handbook of Analytical Techniques in Concrete Science and Technology, William Andrew Publishing/Noyes.

Roy, D. M. and Idorn, G. M. (1982). Hydration, structure, and properties of blast furnace slag cements, mortars, and concrete. ACI Special Publication 79(6): 444-457.

Said, A. M. and Zeidan, M. S. (2009). Enhancing the reactivity of normal and fly ash concrete using colloidal nano-silica. ACI Special Publication 267(7): 75-86.

Sanchez, F. and Sobolev, K. (2010). Nanotechnology in concrete - A review. Construction and Building Materials 24(11): 2060-2071.

SCA 15 (2003). Slag cement in concrete; Slag Cement Association, Woodstock, GA 30189, USA.

Schoepfer, J. and Maji, A. (2009). An investigation into the effect of silicon dioxide particle size on the strength of concrete. ACI Special Publication 267(5): 45-58.

Sellevold, E. J. and Radjy, F. F. (1983). Condensed silica fume (microsilica) in concrete: water demand and strength development. ACI Special Publication 79(35): 677-694.

Shariq, M., Prasad, J. and Masood, A. (2010). Effect of GGBFS on time dependent compressive strength of concrete. Construction and Building Materials 24(8): 1469-1478.

Siddique, R. (2004). Performance characteristics of high-volume Class F fly ash concrete. Cement and Concrete Research 34(3): 487-493.

Sobolev, K. and Gutierrez, M. F. (2005). How nanotechnology can change the concrete world. American Ceramic Society Bulletin 84(10): 14-17.

Stein, H. N. and Stevels, J. M. (1964). Influence of silica on the hydration of $3CaO,SiO_2$. Journal of Applied Chemistry 14(8): 338-346.

Swamy, R. N. and Bouikni, A. (1990). Some engineering properties of slag concrete as influenced by mix proportioning and curing. ACI Materials Journal 87(3): 210-220.

Tangpagasit, J., Cheerarot, R., Jaturapitakkul, C., et al. (2005). Packing effect and pozzolanic reaction of fly ash in mortar. Cement and Concrete Research 35(6): 1145-1151.

Thomas, M. D. A., Shehata, M. H., Shashiprakash, S. G., et al. (1999). Use of ternary cementitious systems containing silica fume and fly ash in concrete. Cement and Concrete Research 29(8): 1207-1214.

Toutanji, H. A. and El-Korchi, T. (1995). The influence of silica fume on the compressive strength of cement paste and mortar. Cement and Concrete Research 25(7): 1591-1602.

Wang, Q., Xia, H. and Zhang, C. (2001). Preparation of polymer/inorganic nanoparticles composites through ultrasonic irradiation. Journal of Applied Polymer Science 80(9): 1478-1488.

Washburn, E. W. (1921). Note on a Method of Determining the Distribution of Pore Sizes in a Porous Material. Proceedings of the National Academy of Sciences of the United States of America 7(4): 115-116.

Winslow, D. N. and Diamond, S. (1970). A mercury porosimetry study of the evolution of porosity in portland cement. Journal of Materials 5(3): 564-585.

Zelic, J., Ruic, D., Veza, D., et al. (2000). Role of silica fume in the kinetics and mechanisms during the early stage of cement hydration. Cement and Concrete Research 30(10): 1655-1662.

Zhang, M.-H. and Gjørv, O. E. (1991). Effect of silica fume on cement hydration in low porosity cement pastes. Cement and Concrete Research 21(5): 800-808.

Appendix – Test Results

Table A.1 - Compressive strength of control Portland cement mortar (Control)

Age (day)	Specimen No.	Density (kg/m^3)	Average density (kg/m^3)	Compressive strength (Mpa)	Average compressive strength (MPa)
1	1	2231	2221 (7)	26.2	26.5 (0.5)
	2	2215		26.2	
	3	2217		27.2	
3	1	2231	2226 (3)	45.9	44.9 (1.7)
	2	2223		46.2	
	3	2226		42.5	
7	1	2239	2240 (1)	55.5	53.3 (1.8)
	2	2242		51.0	
	3	2240		53.5	
28	1	2239	2244 (5)	61.3	61.3 (0)
	2	2251		61.3	
	3	2241		61.3	
91	1	2269	2259 (8)	69.0	65.4 (2.5)
	2	2251		63.1	
	3	2257		64.2	

* Value within () is standard deviation

Table A.2 - Compressive strength of reference slag mortar (SL0)

Age (day)	Specimen No.	Density (kg/m^3)	Average density (kg/m^3)	Compressive strength (Mpa)	Average compressive strength (MPa)
1	1	2116	2124 (9)	13.7	13.8 (0.2)
	2	2136		13.5	
	3	2122		14.1	
3	1	2141	2142 (4)	27.5	27.3 (0.5)
	2	2147		26.7	
	3	2136		27.8	
7	1	2341	2353 (15)	40.6	40.4 (1.8)
	2	2374		38.2	
	3	2345		42.5	
28	1	2140	2154 (10)	52.7	53.8 (0.9)
	2	2157		53.7	
	3	2165		54.9	
91	1	2160	2171 (11)	54.3	55.9 (4.4)
	2	2167		51.5	
	3	2187		61.8	

* Value within () is standard deviation

Table A.3 - Compressive strength of slag mortar with 0.5% type 1 NS (SL0.51)

Age (day)	Specimen No.	Density (kg/m^3)	Average density (kg/m^3)	Compressive strength (Mpa)	Average compressive strength (MPa)
1	1	2248	2238 (7)	14.5	14.9 (0.3)
	2	2234		14.9	
	3	2231		15.3	
3	1	2261	2264 (3)	35.1	35.1 (0.1)
	2	2267		35.1	
	3	2264		34.9	
7	1	2263	2265 (1)	46.6	46.2 (2.5)
	2	2266		49.0	
	3	2266		43.0	
28	1	2280	2274 (4)	48.3	57.6 (6.6)
	2	2271		62.1	
	3	2272		62.5	
91	1	2285	2283 (3)	65.8	66.1 (1.8)
	2	2284		68.4	
	3	2279		64.2	

* Value within () is standard deviation

Table A.4 - Compressive strength of slag mortar with 1% type 1 NS (SL11)

Age (day)	Specimen No.	Density (kg/m^3)	Average density (kg/m^3)	Compressive strength (Mpa)	Average compressive strength (MPa)
1	1	2238	2231 (6)	16.5	16.3 (0.2)
	2	2224		16.0	
	3	2231		16.2	
3	1	2246	2245 (2)	34.3	35.8 (1.0)
	2	2246		36.5	
	3	2242		36.6	
7	1	2269	2255 (10)	48.8	47.0 (1.4)
	2	2250		46.9	
	3	2247		45.4	
28	1	2257	2258 (1)	62.9	60.2 (2.7)
	2	2256		61.2	
	3	2260		56.6	
91	1	2257	2258 (2)	65.9	64.3 (1.4)
	2	2260		64.4	
	3	2255		62.4	

* Value within () is standard deviation

Table A.5 - Compressive strength of slag mortar with 2% type 1 NS (SL21)

Age (day)	Specimen No.	Density (kg/m^3)	Average density (kg/m^3)	Compressive strength (Mpa)	Average compressive strength (MPa)
1	1	2232	2230 (1)	16.5	15.7 (0.6)
	2	2229		15.1	
	3	2228		15.5	
3	1	2223	2233 (7)	36.2	38.1 (1.3)
	2	2236		38.7	
	3	2239		39.3	
7	1	2259	2251 (6)	54.6	52.4 (2.2)
	2	2247		53.2	
	3	2247		49.5	
28	1	2255	2254 (2)	64.7	62.7 (1.8)
	2	2251		60.4	
	3	2255		63.0	
91	1	2253	2252 (3)	70.0	68.9 (0.9)
	2	2248		67.7	
	3	2255		68.8	

* Value within () is standard deviation

Table A.6 - Compressive strength of slag mortar with 1% type 2 NS (SL12)

Age (day)	Specimen No.	Density (kg/m^3)	Average density (kg/m^3)	Compressive strength (Mpa)	Average compressive strength (MPa)
1	1	2224	2227 (3)	17.6	17.8 (0.1)
	2	2227		17.9	
	3	2230		17.9	
3	1	2273	2261 (11)	34.8	36.9 (1.7)
	2	2247		37.0	
	3	2263		39.0	
7	1	2255	2260 (4)	46.9	49.0 (2.6)
	2	2262		47.6	
	3	2262		52.6	
28	1	2263	2264 (1)	59.1	63.8 (3.4)
	2	2264		65.5	
	3	2266		66.9	
91	1	2257	2255 (4)	64.8	67.2 (1.9)
	2	2259		69.5	
	3	2250		67.4	

* Value within () is standard deviation

Table A.7 - Compressive strength of slag mortar with 1% silica fume (SL1SF)

Age (day)	Specimen No.	Density (kg/m^3)	Average density (kg/m^3)	Compressive strength (Mpa)	Average compressive strength (MPa)
1	1	2178	2179 (7)	15.1	15.2 (0.2)
	2	2187		15.5	
	3	2171		15.0	
3	1	2194	2191 (3)	32.7	32.1 (0.7)
	2	2190		32.4	
	3	2188		31.2	
7	1	2211	2214 (2)	46.4	46.1 (0.4)
	2	2216		46.4	
	3	2215		45.5	
28	1	2216	2217 (4)	60.2	59.8 (1.8)
	2	2223		61.8	
	3	2213		57.4	
91	1	2225	2223 (2)	59.9	63.0 (2.4)
	2	2222		65.8	
	3	2222		63.2	

* Value within () is standard deviation

Table A.8 - Compressive strength of slag mortar with 1% type 1 NS and mixed with mechanical mixing method (SL11(M))

Age (day)	Specimen No.	Density (kg/m^3)	Average density (kg/m^3)	Compressive strength (Mpa)	Average compressive strength (MPa)
1	1	2284	2275 (10)	15.0	15.9 (0.8)
	2	2278		17.0	
	3	2262		15.7	
3	1	2276	2272 (3)	35.8	35.7 (0.2)
	2	2269		35.7	
	3	2272		35.4	
7	1	2283	2285 (2)	48.4	47.3 (1.4)
	2	2285		45.3	
	3	2288		48.2	
28	1	2237	2256 (16)	60.9	59.3 (2.2)
	2	2254		60.9	
	3	2276		56.2	
91	1	2296	2296 (3)	62.0	63.5 (1.3)
	2	2292		63.4	
	3	2300		65.2	

* Value within () is standard deviation

Table A.9 - Compressive strength of reference fly ash mortar (FA0)

Age (day)	Specimen No.	Density (kg/m^3)	Average density (kg/m^3)	Compressive strength (Mpa)	Average compressive strength (MPa)
1	1	2200	2199 (3)	7.5	7.4 (0.2)
	2	2201		7.7	
	3	2194		7.2	
3	1	2203	2200 (7)	18.1	18.1 (0.3)
	2	2190		17.7	
	3	2205		18.4	
7	1	2204	2207 (3)	26.2	26.9 (1.0)
	2	2206		26.2	
	3	2211		28.3	
28	1	2220	2214 (5)	41.1	40.8 (1.0)
	2	2215		41.8	
	3	2208		39.4	
91	1	2227	2218 (7)	48.3	48.3 (0.3)
	2	2219		48.6	
	3	2210		47.9	

* Value within () is standard deviation

Table A.10 - Compressive strength of fly ash mortar with 0.5% type 1 NS (FA0.51)

Age (day)	Specimen No.	Density (kg/m^3)	Average density (kg/m^3)	Compressive strength (Mpa)	Average compressive strength (MPa)
1	1	2194	2194 (1)	10.9	10.5 (0.3)
	2	2195		10.4	
	3	2192		10.2	
3	1	2198	2200 (2)	19.11	20.6 (1.1)
	2	2203		20.97	
	3	2199		21.84	
7	1	2216	2211 (8)	29.5	29.6 (0.4)
	2	2216		30.1	
	3	2200		29.1	
28	1	2217	2217 (1)	40.4	40.9 (0.6)
	2	2218		40.6	
	3	2217		41.7	
91	1	2221	2220 (4)	50.0	48.9 (2.2)
	2	2224		45.9	
	3	2216		50.9	

* Value within () is standard deviation

Table A.11 - Compressive strength of fly ash mortar with 1% type 1 NS (FA11)

Age (day)	Specimen No.	Density (kg/m^3)	Average density (kg/m^3)	Compressive strength (Mpa)	Average compressive strength (MPa)
1	1	2211	2210 (1)	12.2	12.0 (0.2)
	2	2212		11.7	
	3	2209		12.0	
3	1	2225	2221 (3)	22.6	22.5 (0.1)
	2	2217		22.3	
	3	2221		22.6	
7	1	2224	2219 (13)	31.4	31.5 (0.6)
	2	2231		30.9	
	3	2201		32.4	
28	1	2229	2230 (1)	43.73	43.6 (0.8)
	2	2231		42.45	
	3	2231		44.5	
91	1	2231	2229 (2)	51.0	50.4 (0.5)
	2	2227		49.8	
	3	2229		50.3	

* Value within () is standard deviation

Table A.12 - Compressive strength of fly ash mortar with 2% type 1 NS (FA21)

Age (day)	Specimen No.	Density (kg/m^3)	Average density (kg/m^3)	Compressive strength (Mpa)	Average compressive strength (MPa)
1	1	2204	2210 (8)	13.5	13.4 (0.2)
	2	2221		13.6	
	3	2206		13.2	
3	1	2214	2216 (2)	23.1	24.0 (0.7)
	2	2219		24.2	
	3	2215		24.8	
7	1	2229	2226 (3)	31.1	31.8 (0.7)
	2	2222		32.7	
	3	2228		31.7	
28	1	2227	2230 (2)	45.0	43.9 (0.8)
	2	2230		43.4	
	3	2233		43.4	
91	1	2243	2242 (5)	54.2	53.8 (1.1)
	2	2247		55.0	
	3	2235		52.4	

* Value within () is standard deviation

Table A.13 - Compressive strength of fly ash mortar with 1% type 2 NS (FA12)

Age (day)	Specimen No.	Density (kg/m^3)	Average density (kg/m^3)	Compressive strength (Mpa)	Average compressive strength (MPa)
1	1	2195	2204 (6)	12.1	12.3 (0.4)
	2	2209		12.0	
	3	2207		12.8	
3	1	2213	2212 (1)	22.9	22.6 (0.2)
	2	2212		22.5	
	3	2212		22.3	
7	1	2212	2211 (3)	31.2	31.5 (0.3)
	2	2216		31.4	
	3	2207		31.8	
28	1	2217	2217 (4)	42.7	43.7 (0.9)
	2	2211		43.6	
	3	2222		44.9	
91	1	2221	2221 (1)	50.9	50.9 (0)
	2	2219		50.9	
	3	2222		51.0	

* Value within () is standard deviation

Table A.14 - Compressive strength of fly ash mortar with 1% silica fume (FA1SF)

Age (day)	Specimen No.	Density (kg/m^3)	Average density (kg/m^3)	Compressive strength (Mpa)	Average compressive strength (MPa)
1	1	2185	2185 (1)	8.2	8.4 (0.2)
	2	2184		8.7	
	3	2187		8.4	
3	1	2197	2198 (2)	21.2	20.8 (0.5)
	2	2200		21.1	
	3	2198		20.2	
7	1	2207	2203 (3)	31.3	29.7 (1.9)
	2	2202		30.8	
	3	2200		27.1	
28	1	2209	2205 (3)	42.4	42.3 (0.8)
	2	2204		41.3	
	3	2201		43.3	
91	1	2213	2213 (3)	46.8	48.9 (2.1)
	2	2210		48.2	
	3	2217		51.8	

* Value within () is standard deviation

Table A.15 - Compressive strength of fly ash mortar with 1% type 1 NS and mixed with mechanical mixing method (FA11(M))

Age (day)	Specimen No.	Density (kg/m^3)	Average density (kg/m^3)	Compressive strength (Mpa)	Average compressive strength (MPa)
1	1	2229	2220 (8)	9.6	9.8 (0.2)
	2	2210		10.1	
	3	2222		9.8	
3	1	2221	2228 (5)	21.0	20.3 (0.5)
	2	2232		20.1	
	3	2231		19.7	
7	1	2238	2230 (9)	31.4	30.0 (1.1)
	2	2218		28.6	
	3	2233		30.1	
28	1	2245	2243 (2)	40.0	41.1 (0.8)
	2	2245		41.5	
	3	2240		41.7	
91	1	2251	2247 (3)	49.7	49.3 (0.7)
	2	2245		50.0	
	3	2245		48.3	

* Value within () is standard deviation

Table A.16 - Compressive strength of reference slag concrete (CSL0)

Age (day)	Specimen No.	Density (kg/m^3)	Average density (kg/m^3)	Compressive strength (Mpa)	Average compressive strength (MPa)
3	1	2370	2371 (4)	35.9	35.4 (1.9)
	2	2377		37.5	
	3	2368		32.9	
7	1	2369	2363 (7)	48.6	48.1 (0.4)
	2	2354		47.7	
	3	2367		47.9	
28	1	2363	2366 (2)	71.3	68.0 (3.0)
	2	2369		64.1	
	3	2366		68.6	
91	1	2368	2368 (3)	70.8	69.3 (1.7)
	2	2365		66.9	
	3	2371		70.2	

* Value within () is standard deviation

Table A.17 - Compressive strength of slag concrete with 2% type 1 NS (CSL21)

Age (day)	Specimen No.	Density (kg/m^3)	Average density (kg/m^3)	Compressive strength (Mpa)	Average compressive strength (MPa)
3	1	2362	2365 (3)	41.6	43.1 (1.0)
	2	2369		43.6	
	3	2364		44.0	
7	1	2362	2361 (8)	55.8	56.8 (2.3)
	2	2370		59.9	
	3	2350		54.7	
28	1	2365	2363 (5)	69.4	69.8 (0.4)
	2	2366		69.7	
	3	2356		70.3	
91	1	2363	2377 (10)	69.9	71.1 (2.7)
	2	2383		68.6	
	3	2385		74.8	

* Value within () is standard deviation

Table A.18 - Compressive strength of slag concrete with 2% silica fume (CSL2SF)

Age (day)	Specimen No.	Density (kg/m^3)	Average density (kg/m^3)	Compressive strength (Mpa)	Average compressive strength (MPa)
3	1	2362	2357 (5)	37.9	36.7 (1.2)
	2	2358		35.0	
	3	2350		37.3	
7	1	2371	2366 (3)	50.6	50.5 (0.5)
	2	2363		49.8	
	3	2364		51.1	
28	1	2363	2365 (3)	71.1	68.4 (2.2)
	2	2361		68.3	
	3	2369		65.8	
91	1	2366	2373 (5)	72.8	69.7 (2.3)
	2	2378		67.3	
	3	2376		68.9	

* Value within () is standard deviation

Table A.19 - Compressive strength of reference fly ash concrete (CFA0)

Age (day)	Specimen No.	Density (kg/m^3)	Average density (kg/m^3)	Compressive strength (Mpa)	Average compressive strength (MPa)
3	1	2357	2351 (5)	19.6	19.5 (0.2)
	2	2352		19.7	
	3	2346		19.2	
7	1	2358	2354 (3)	29.7	28.1 (1.2)
	2	2351		27.6	
	3	2354		27.0	
28	1	2353	2355 (7)	42.8	43.0 (0.3)
	2	2347		42.8	
	3	2364		43.4	
91	1	2351	2358 (6)	49.2	50.2 (1.2)
	2	2356		52.0	
	3	2367		49.5	

* Value within () is standard deviation

Table A.20 - Compressive strength of fly ash concrete with 2% type 1 NS (CFA21)

Age (day)	Specimen No.	Density (kg/m^3)	Average density (kg/m^3)	Compressive strength (Mpa)	Average compressive strength (MPa)
3	1	2344	2345 (2)	24.2	25.3 (0.8)
	2	2343		25.8	
	3	2347		26.0	
7	1	2331	2341 (7)	34.5	35.0 (0.4)
	2	2346		35.0	
	3	2345		35.6	
28	1	2336	2339 (2)	49.3	48.7 (0.4)
	2	2341		48.6	
	3	2340		48.4	
91	1	2352	2346 (12)	63.1	59.3 (3.2)
	2	2355		59.7	
	3	2329		55.1	

* Value within () is standard deviation

Table A.21 - Compressive strength of fly ash concrete with 2% silica fume (CFA2SF)

Age (day)	Specimen No.	Density (kg/m^3)	Average density (kg/m^3)	Compressive strength (Mpa)	Average compressive strength (MPa)
3	1	2341	2343 (1)	20.9	20.4 (0.8)
	2	2344		21.1	
	3	2344		19.2	
7	1	2350	2350 (5)	27.7	29.9 (1.7)
	2	2344		30.1	
	3	2357		31.8	
28	1	2352	2347 (3)	44.0	43.5 (0.4)
	2	2343		43.5	
	3	2347		42.9	
91	1	2349	2349 (1)	52.4	51.9 (0.9)
	2	2350		52.8	
	3	2349		50.6	

* Value within () is standard deviation

Table A.22 - Charge passed in slag concretes at 28 days

Mix ID	Specimens	Charge passed (coulombs)	Average charge passed (coulombs)	Chloride ion penetrability (According to ASTM 1202-05)
CSL0	Top	1149	1049 (104)	Low
	Middle	1093		
	Bottom	905		
CSL2SF	Top	958	946 (20)	Very low
	Middle	963		
	Bottom	918		
CSL21	Top	827	786 (69)	Very low
	Middle	842		
	Bottom	688		

* Value within () is standard deviation

Table A.23 - Charge passed in fly ash concretes at 28 days

Mix ID	Specimens	Charge passed (coulombs)	Average charge passed (coulombs)	Chloride ion penetrability (According to ASTM 1202-05)
CFA0	Top	1322	1154 (125)	Low
	Middle	1115		
	Bottom	1024		
CFA2SF	Top	905	891 (31)	Very low
	Middle	920		
	Bottom	848		
CFA21	Top	909	858 (40)	Very low
	Middle	855		
	Bottom	810		

* Value within () is standard deviation

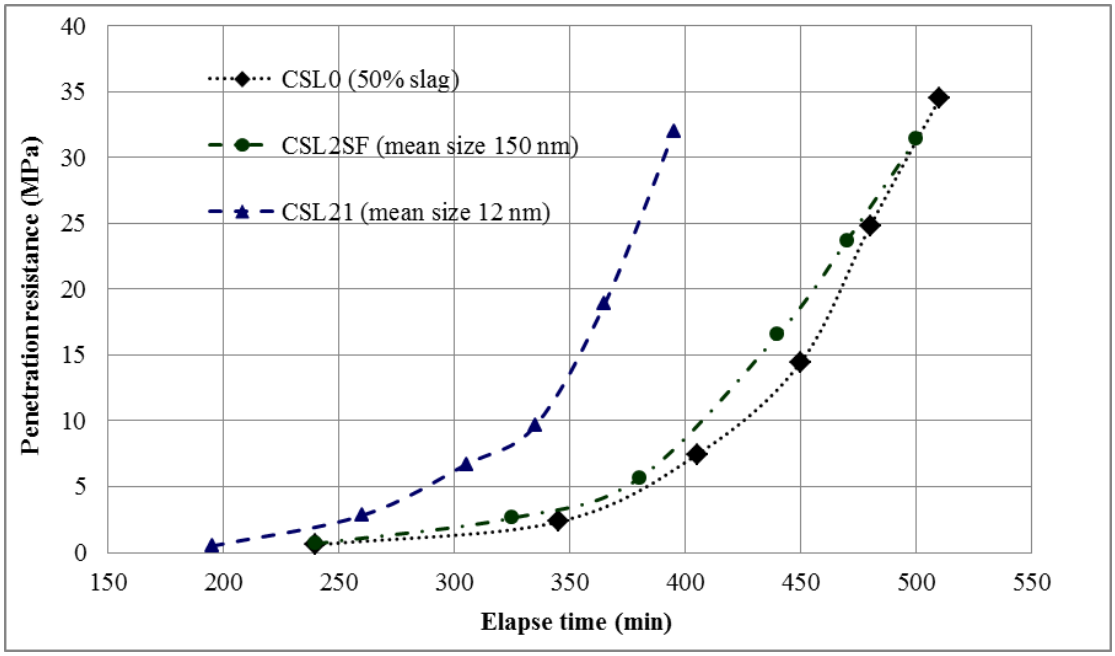

Figure A.1 - Determination of setting times of slag concretes

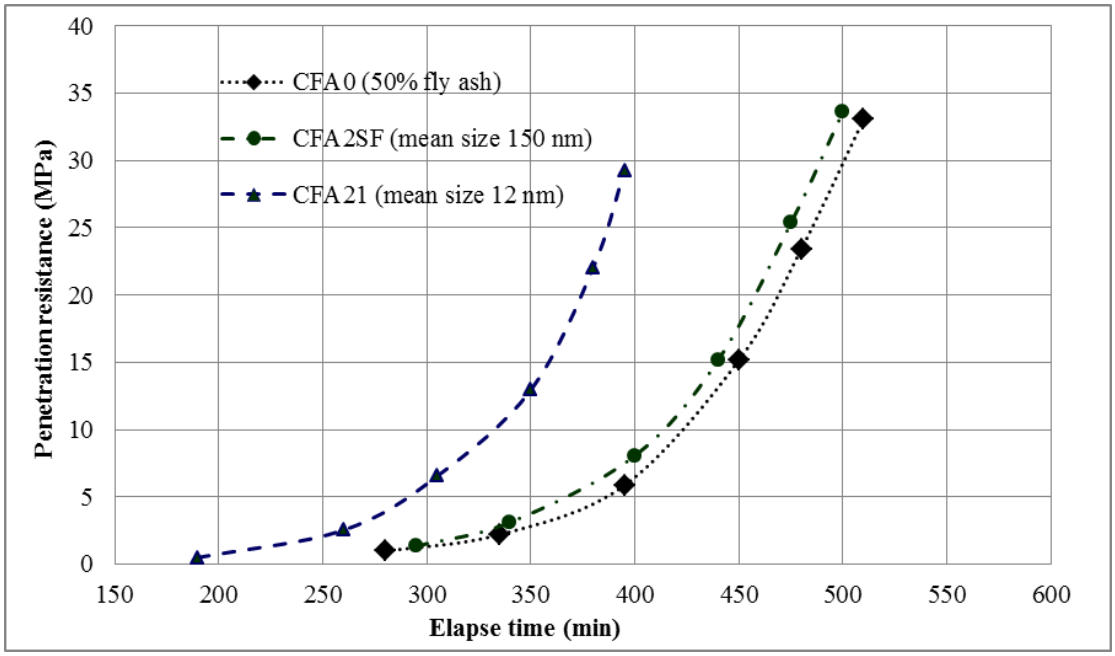

Figure A.2 - Determination of setting times of fly ash concretes